DOE/NASA/0130/80/1
NASA CR-159776

THE PERFORMANCE AND EFFICIENCY OF FOUR MOTOR/CONTROLLER/BATTERY SYSTEMS FOR THE SIMPLER ELECTRIC VEHICLES

Paul R. Shipps
3E Vehicles

(NASA-CR-159776) THE PERFORMANCE AND EFFICIENCY OF FOUR MOTOR/CONTROLLER/BATTERY SYSTEMS FOR THE SIMPLER ELECTRIC VEHICLES Final Report (Three E Vehicles) 88 p HC A05/MF A01 CSCL 09C G3/33 N80-24550 Unclas 20919

May 1980

Prepared for
NATIONAL AERONAUTICS AND SPACE ADMINISTRATION
Lewis Research Center
Under Contract DEN 3-130

for
U.S. DEPARTMENT OF ENERGY
Conservation and Solar Energy
Office of Transportation Programs

DOE/NASA/0130/80/1
NASA CR-159776

THE PERFORMANCE AND EFFICIENCY OF FOUR MOTOR/CONTROLLER/BATTERY SYSTEMS FOR THE SIMPLER ELECTRIC VEHICLES

Paul R. Shipps
3E Vehicles
P.O. Box 19409
San Diego, CA 92119

May 1980

Prepared for
NATIONAL AERONAUTICS AND SPACE ADMINISTRATION
Lewis Research Center
Cleveland, Ohio 44135
Under Contract DEN 3-130

for
U.S. DEPARTMENT OF ENERGY
Conservation and Solar Energy
Office of Transportation Programs
Washington, D.C. 20545
Under Interagency Agreement EC-77-31-1044

PREFACE

3E Vehicles and the author acknowledge the major contribution made to the reported test program by Mr. Paul A. Brock of Sine Engineering, Sunnyvale, California. Mr. Brock and his company designed, built and calibrated the special instrumentation system used to measure current, voltage and power in chopper controlled power circuits.

CONTENTS

1/ SUMMARY

A cost-shared test and analysis program was performed on four complete propulsion systems designed for a small urban electric vehicle (EV). Dynamometer tests of the complete systems were performed, followed by correlation road tests in an operating EV. A conventional DC series motor and a permanent magnet (PM) motor of similar size and rating were each tested throughout the program. Two types of speed and power controllers were tested: first, a system having 4 steps of series/parallel voltage switching (V-switch) plus a series-resistor for start-up; followed by a system using a pulse-width-modulating, 400 Hz transistorized chopper. The V-switch control required a higher level of driver skills to select settings and properly use the start-up resistors; analogous to use of a "stick-shift" transmission. The chopper, although less efficient, provided smooth, stepless control and driving simplicity; analogous to use of an automatic transmission.

The four propulsion systems were sized for a small, 2-person, urban EV. The EV was tested at 725 lb (329 kg) and was geared for top speeds of 38 mph (61 km/h). The motors were each rated at 2.5 hp (1.86 kw) at a constant 36 volts DC and were tested to just over 8 hp (5.97 kw). While this vehicle and propulsion system are lighter and smaller than most EVs, the performance is considered indicative of, or scalable to, that of larger EVs.

1.1 Instrumentation Preparations and Tests

Instrumentation refinement, development and testing was considered necessary to (1) attain more accurate torque and speed data than normal, and (2) measure "true" power over a broad range of chopper controlled operations. For the latter purpose, a new dynamic instrument was designed, built and calibrated by Sine Engineering. For a reference standard a Clarke-Hess volt-ampere-wattmeter, a model previously tested and qualified by NASA, was used. Conventional DC instruments were also used during all chopper tests. Tests to determine adequate and comparative accuracy and precision included tests of the dynamic instrumentation in measuring ripple-free DC, chopped DC dissipated into a pure resistive load, and chopped DC controlling the complete propulsion system. When tested by measuring ripple-free DC, the dynamic instruments each exhibited a 2% or 3% error in power values; the Sine reading was higher and the Clarke-Hess reading was lower than the conventional DC instrumentation. Subsequent system tests using chopper control resulted in a similar spread between the Sine and Clarke-Hess power, with values from the two often bracketing the KVA values of the DC instruments. Measurements were made on both the motor side and the battery side of the chopper controller. Oscilloscope photographs show that the two sides have markedly different current and voltage waveforms.

A conclusion from the instrumentation tests, later collaborated by the dynamometer and road vehicle tests, is that conventional DC shunts and voltmeters — when used on the battery side of choppers of the type tested — provided adequate accuracy for normal EV power and energy consumption measurement purposes (i.e., within a few percent of actual). On the motor side of the chopper, by contrast, power and energy data from the DC instrumentation contained large errors. Oscillographs of current and voltage waveforms illustrate the primary reason: chopped battery circuit currents and voltages start, vary and stop at nearly the same times; while motor circuit current continues to flow long after the voltage is switched "off".

1.2 Dynamometer Test Results

Dynamometer tests of the four motor/controller/battery systems (the same four later used in the road test vehicle) were performed. The three different instrumentation systems continued to be used when under chopper control: the Sine instrument for current, voltage and power values; the Clarke-Hess for confirming power values only; and the conventional DC instruments to explore their road vehicle suitability. Preliminary tests were performed to investigate the effects of different amounts of added motor circuit "choke" inductance in the chopper controlled system. For these tests, measurements continued to be made on both the battery side and the motor side of the chopper. After selecting a choke for use in the system tests, current voltage and power were measured only on the battery side of the chopper. Three motor temperatures were also measured during all full system dynamometer tests and road tests; brush temperature was continuously recorded, field temperatures were displayed and logged, and label-type temperature indicators were used to record the maximum attained temperature of the motor cases.

The efficiency of the series and PM motors, when operating under ripple-free V-switch control, is shown in Figure 1-1. The PM

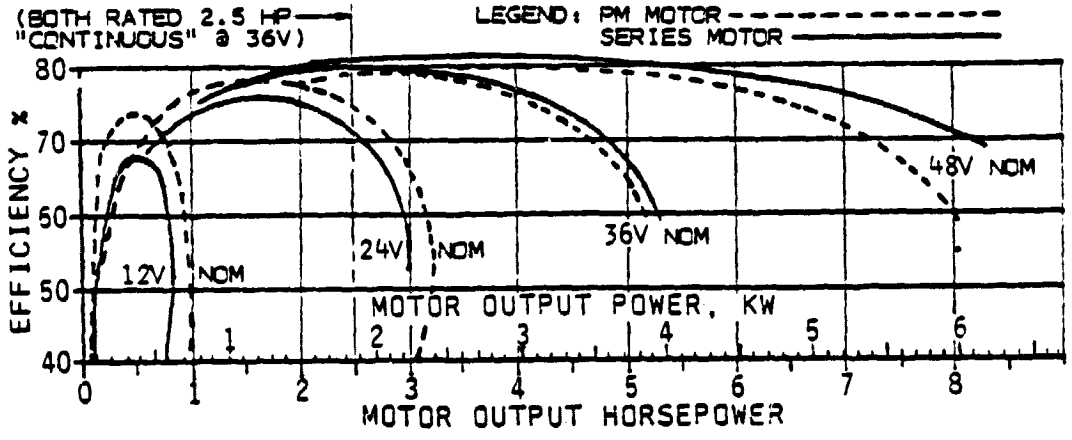

Figure 1-1 Comparative Efficiency of Series and PM Motors on Battery Power with Voltage-Switch Control

motor had higher efficiencies and a broader useful power range at the two lower voltage settings. The series motor had higher efficiencies in the more often used higher voltage settings and exhibits a reduced drop-off at the higher powers. The PM motor, however, since it was designed for relatively constant power applications, approached overheating rapidly at the higher power outputs required for the steeper upgrades. The series motor, by contrast, had been designed for vehicle traction and exhibited no temperature rise problems.

Under chopper control the addition of motor circuit choke inductance appreciably improved system efficiency at low duty cycles. The added inductance also appreciably reduced acoustic noise. The light and compact choke selected caused an 8 to 9% increase in efficiency at a typical low-speed cruise setting. At 100% duty cycle (ripple-free) the selected choke caused about 1% efficiency loss due to added circuit resistance.

Chopper controlled system efficiencies were noticeably lower than those using voltage switch control, as illustrated in Figure 1-2. At the noted 22 mph level road cruising torque the chopper shows a nearly 12% decrease in efficiency at 50% duty cycle compared to a 24 volt setting with ripple-free power. In typical vehicle operation, however, these low duty cycle efficiency losses are less damaging than they first appear, since, with the exception of lower speed cruising EV operations, a driver will rarely dwell in the lower duty cycle settings. At 100% duty cycle and "V-max" torque the chopper efficiency is about 3% below that for V-switch control. About 2% of this is due to the tested controller not having a transister circuit override at 100% duty cycle.

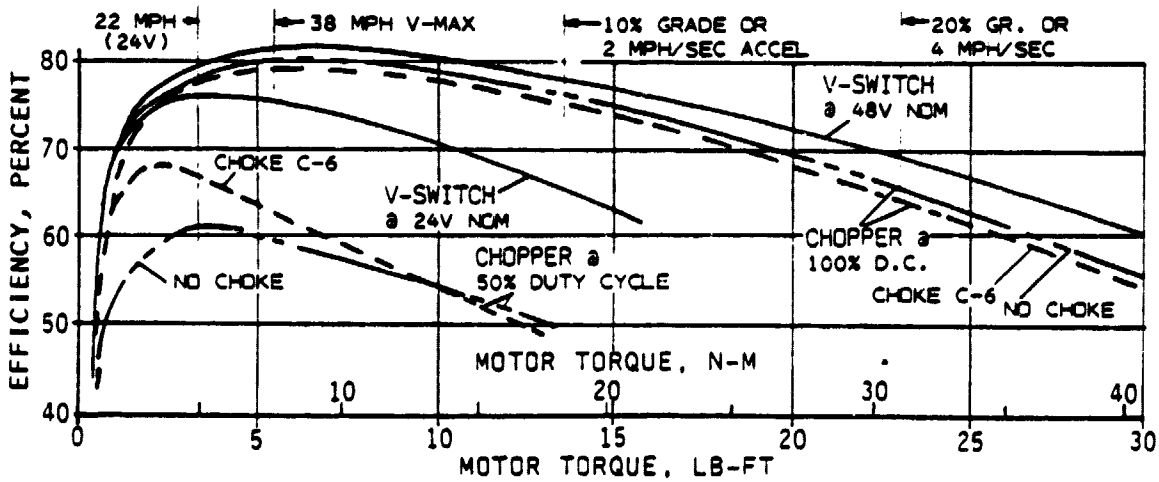

Figure 1-2 Comparative Efficiency of Voltage-Switch Controlled and Chopper Controlled Series Motor, over Road Test Vehicle Torque Range

1.3 Road Test Correlation

The road test program was performed to correlate actual vehicle street operations data with vehicle performance analyses. An analysis was made for each of the four propulsion systems, using the dynamometer test data, and road test instrumentation was much the same as used for the dynamometer tests. The road tests emphasized high torque operations (a variety of defined upgrades) to explore sustained torque effects on propulsion system capabilities and motor heating limits.

The performance analyses, described herein, began with a re-analysis of the test vehicle's torque-vs-speed requirements, at its test weight and over the full spectrum of climbs and accelerations, on typical, "fair" condition urban streets. Torque-vs-speed availability data were then calculated, and a torque required/torque available "performance envelope" was plotted for each propulsion system. The performance envelopes for the PM motor systems included time-at-torque (or current) limitations to prevent motor brush overheating.

The resulting road test data correlated well with the performance analyses; road test data-points fell quite close to the appropriate torque required/torque available intersections. The efficiency differences indicated earlier for the four propulsion systems were also apparent in the road tests, as shown by Table 1-1. The road test emphasis on higher torque grade climbs exaggerated the modest efficiency difference between the series and PM motors, and increased all energy rates compared to typical urban traffic.

Table 1-1 Comparative Energy Use During Road Tests (Mostly Grade Climbs)

TYPE OF MOTOR & CONTROLLER	BATTERY AMP-HR	NOMINAL KWH*	VEHICLE TEST MI	ENERGY RATE KWH/MI	KWH/KM
SERIES MOTOR & V-SWITCH	39.3	1.89	15.7	.120	.075
PM MOTOR & V-SWITCH	51.3	2.46	18.4**	.134	.083
SERIES MOTOR & CHOPPER	47.3	2.27	15.6	.146	.090
PM MOTOR & CHOPPER	54.2	2.60	15.6	.167	.104

*NOMINAL KWH = NOMINAL VOLTAGE (2V/CELL) X AMP-HR/1000
**REGENERATIVE BRAKING TESTS WITH THIS COMBINATION ONLY

The PM motor, since its fixed field strength and voltage-switching made the process relatively simple, was also tested for regenerative braking performance. For a 1-mile descent and reclimb of a 6.8% grade, the regeneratively braked descent replaced 15% of the battery charge required for the climb.

2/ INTRODUCTION

Battery powered electric vehicles are again being seriously considered and numerous firms, from large to very small, are designing and building prototype vehicles. Most of these designs, and especially those of the smaller firms, use brush-commutated DC motors. The basic characteristics of such motors have been known since the beginning of this century, with the series motor version recognized and used — during most of that time span — as a logical choice for vehicle traction applications.

Control of these conventional DC motors in battery powered vehicles, however, has often been inefficient and wasteful, complicated and expensive, or, in some cases, all of these. In addition, permanent magnet (PM) motors are beginning to appear as a possible alternative for powering the simpler electric vehicles. Relatively little technical information, however, has been available from texts or manufacturers to permit engineering comparisons or trade-off studies of motors or controllers. With today's large number of electric car enthusiasts and small shop developers, the manufacturers can afford very little in technical assistance to each of these.

Shipps Engineering, the R&D organization that preceded 3E Vehicles, had made (in July 1975) a long-term commitment of skills and resources to the development of energy-efficient electrics for personal urban transportation. Systems engineering studies were performed which, among other outputs, emphasized the importance of high electrical efficiencies and low energy use rates in battery powered vehicles (references 1 and 2). Many comparative tests were performed to investigate and minimize energy losses — both electrical and mechanical — in small and relatively simple vehicles. Those results were incorporated into several versions of an electric mini-car, which was then instrumented and road-tested in its several versions.

The road test results emphasized the desirability of more closely controlled dynamometer tests, to compare a quite efficient but driver-skill requiring voltage-switching system with a less efficient but smoother and simpler-to-operate chopper controller. An unsolicited, cost-sharing proposal was then made to the NASA Lewis Research Center to cooperate in an expanded-data version of the planned test program.

The resulting contracted test and analysis program, being reported herein, consisted of three major tasks. These were:

(1) The modification of a torque-absorption dynamometer of high accuracy; including the installation of dynamic instrumentation capable of measuring true values of chopper-controlled current, voltage and power.

(2) The conduction of four sets of dynamometer tests of "vehicle-duplicate" battery/controller/motor electrical power systems:

a series motor with V-switch control,

a PM motor with V-switch control,

the series motor with chopper-control, and

the PM motor with chopper control.

The effect of added circuit inductance, for the PM motor with chopper control, was also investigated, and the test vehicle performance with each of the four power systems was predicted.

(3) The conduction of road tests, to correlate with dynamometer results and to verify or correct the analysis methods. These tests were performed with each of the four power systems installed in 3E's model EP-10 test vehicle.

The EP-10 vehicle is a 2-person, 3-wheel, urban mini-car. It was tested at a gross vehicle weight of 725 lb (329 kg) while geared for top speeds of 38 mph (61 km/h). The tested motors were each rated at 2.5 hp (1.86 kw) at a constant 36 volts DC, and were tested to outputs of just over 8 hp (5.97 kw).

3/ THE EV POWER SYSTEMS TESTED

The electric vehicle power systems tested under this program were complete systems as used in a carefully designed but relatively simple electric vehicle. For the laboratory dynamometer tests, all components of the power train were either the same or duplicates of those used in the actual vehicle, including lengths and wire gauges of conductors between the various components and the batteries themselves. The two power circuits each had a distinctive type of speed control and each circuit was tested with two types of motors, making a total of four power systems which underwent similar test programs.

3.1 Two Minicar Complete Power Circuits

The test vehicle to be used for road test correlation and confirmation of the dynamometer test data had been originally designed to be marketed as a labor intensive, do-it-yourself kit. Such a design — which could be expected to be operated primarily by its owner-builder — could feature a speed and power control system requiring more driver knowledge and skill than a system suitable for an average driver trained in an automatic transmission car. The original power circuit, accordingly, used a series/parallel combination voltage switch (V-switch) for speed settings. The V-switch was supplemented by a two-step resistor bank used primarily for motor start-up purposes. Such start-up resistors, since they are intended to momentarily dissipate unwanted power as heat, will cause a serious loss of efficiency if inadvertently used for speed control rather than start-up.

The second power system tested makes use of a commercially available electronic chopper for speed and power control. Similar choppers, which utilize either transistors or silicon controlled rectifiers (SCRs) to provide smooth acceleration and speed control are used in most of today's EV designs. These controllers are more costly and operate with lower system efficiency than the voltage switching type.

Figure 3-1 diagrams the primary elements of the two power circuits. Both use the same four 12-volt batteries and both operate the same DC motor through a typical reversing relay or switch. The voltage switch circuit features four speed settings in addition to reverse. The V-switch provided, by means of series/parallel switching, a choice of 12, 24, 36 or 48 volts DC at the switch outputs leading to the motor. With the exception of the 36 volt setting, each of the four batteries provides a nominally equal amount of energy. Any inequality is due to minor differences in battery parameters, such as internal resistance, or in differences in conductor resistances. When operating in the 36 volt setting only three of the four batteries provides power to the motor. To help equalize the overall power drain the fourth carries the power train

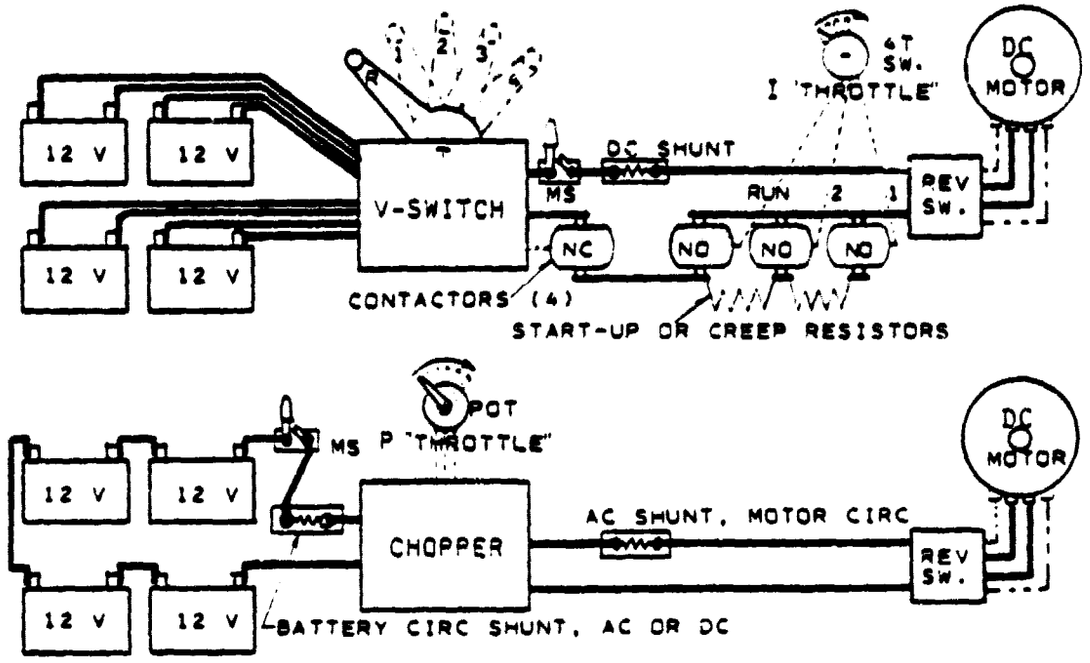

Figure 3-1 The Basic EV Power Circuits Tested

accessory loads (the contactors' 12-volt solenoid coils) as well as the vehicle lighting and accessory loads. This voltage switching system also uses a nominal 12-volt charging mode to approach charge equalization at each recharge; in addition, an occasional special equalizing charge is also used after an appreciable amount of operation involving an unequal discharge.

The motor circuit side of the V-switch power circuit includes four high current relays or "contactors." One of these (marked NC for normally closed) is activated by a limit switch upon initial movement of the V-switch shift lever, when shifting to a different voltage setting. This protects the high current V-switch contacts from potential damage by "break-circuit" arcing. The other three contactors are controlled by a 4-position rotary switch, or equivalent, which acts as a motor current stepping switch or "throttle." In normal operation, the two unshaded NO (normally open) contactors are each closed for only a second or two each during start from a standstill. The shaded contactor remains closed while the motor is under power. Devising a "throttle" switch which discourages use of the resistor activating contactors for other than start-up purposes is an important part of such a control system if it is to be used by average drivers.) The V-switch system, since it requires individual conductors from each battery, will normally have a higher total conductor resistance than will a chopper control system. While power losses in conductors are not negligible, the test data in Sections 5 and 6 will show that these losses are small compared to losses in the chopper system.

The power circuit for the chopper controlled system is appreciably simpler and requires much shorter conductors in the battery circuit. This circuit has the additional advantage of its master switch (MS) interrupting current to all components of the power system. The master switch of the V-switch system, as shown, does not protect the battery circuit from a possible malfunction within the V-switch. Power control or "throttle" action to the chopper is provided by a potentiometer as in most electronic chopper control systems.

3.2 Motor Types

Two quite different types of DC motors were tested during this program. One was the conventional series motor (i.e., field pole windings connected in series with the armature causing the magnetic field strength to increase and decrease with increasing and decreasing current) which has been the most popular choice for electric traction vehicles for almost a century. The other motor tested was a permanent magnet type, which only recently has been produced in sizes adequate for small vehicle propulsion. As the name implies, permanent magnet motors have a fixed magnetic field strength and, therefore, a speed versus torque characteristic curve quite different from the series motor. As a very general statement, a permanent magnet motor may be expected to have somewhat higher efficiencies in its low torque range (no field winding resistance) but lower efficiencies and more limited capability in the high torque regime (no increase in field strength). For a given traction task, a suitable PM motor might be smaller in diameter yet longer and heavier than a comparably performing series motor. Being of simpler construc-

Table 3-1 Specification Data on Motors Tested

TYPE	SERIES FIELD	PERMANENT MAGNET
MANUFACTURER	GENERAL ELECTRIC	OHIO (MAGNETICS INTL)
MODEL NUMBER	5BC48 JB 538A	D56 1228 X 8290
RATED HORSEPOWER " RPM " VOLTAGE " CURRENT	2.5 (1.86 KW) 2800 (293 RAD/S) 36 VOLTS DC 80 AMPERES	2.5 (1.86 KW) 3600 (377 RAD/S) 36 VOLTS DC 65 AMPERES
WEIGHT	42.5 LB (19.3 KG)	43.5 LB (19.7 KG)
DIMENSIONS	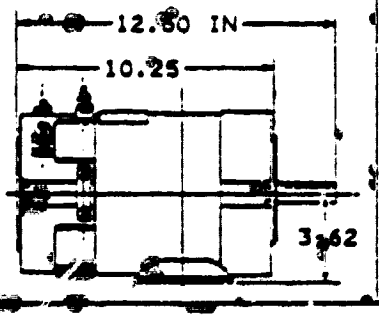	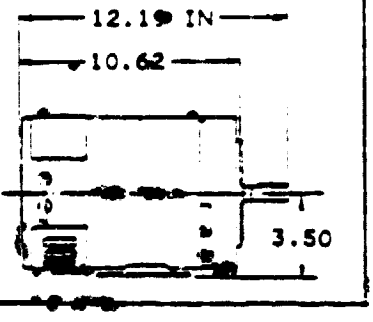

tion, the PM motor has the potential for lower unit cost. The PM motor, due to its fixed magnetic field strength, can also provide regenerative braking with relatively simple switch gear, especially if steps in either voltage selection or motor-to-wheel speed ratios are available.

The specifics of the two motors tested are shown in Table 3-1. It needs to be pointed out that the two types of motors are not comparable designs for vehicle traction purposes. The General Electric motor has been developed specifically for traction applications; this "JB" series has been used and modified over many years to become the most popular golf car motor. The permanent magnet motor tested, by contrast, was designed for applications requiring relatively constant torque. This motor is not recommended, by the manufacturer, for vehicle propulsion use (nor are any known, presently-produced PM motors) since it was not designed for the short duration, high current demands of traction applications. Accordingly, the PM motor was tested to investigate its basic operating characteristics in comparison to the better-known series motor. Allowances need to be made for its time-at-current temperature limitations.

3.3 Controller Types

The general types of controllers used in the two power circuits were discussed in Section 3.1 above. The V-switch controller is a proprietary design by 3E Vehicles while the transistorized chopper controller is a commercial unit produced by EVC, Inc., of Inglewood, California. General specifics of the two units are shown in Table 3-2.

Table 3-2 Specifications of Speed Controllers Tested

TYPE	VOLTAGE SWITCH	TRANSISTOR CHOPPER
MANUFACTURER	3E VEHICLES	EVC INCORPORATED
MODEL NUMBER	(PROTOTYPE)	EVC 300-60-12H
RATED CURRENT " VOLTAGE	300 AMPERES TO 120 VOLTS DC	300 AMPERES TO 60 VOLTS DC
WEIGHT	4.4 LB (2.0 KG)	4.8 LB (2.2 KG)
CONTROL MEANS	5-POSITION VOLTAGE SWITCH PLUS ON-OFF CONTACTORS WITH START-UP RESISTORS	POTENTIOMETER CONTROL OF DUTY CYCLE PLUS ON-OFF CONTACTOR
CURRENT LIMIT	NONE	300 AMP CUTOFF
THERMAL PROTECTION	NONE REQUIRED	CURRENT CUTS BACK @ CHOPPER 150°F (66°C)

4/ TEST INSTRUMENTATION AND EQUIPMENT

For this test program a relatively large effort was spent on developing, modifying and calibrating instrumentation to attain adequate accuracy. Good data-point repeatability and a minimum of data scatter resulted. In general, the least data scatter occurred in the low and medium torque regime typical of normal vehicle operations. Greater scatter occurred in the rarer and transient high torque regime, primarily because of difficulty in logging "simultaneous" data while high currents caused a continuing drop in battery voltage.

4.1 The Need For Accuracy

For this test program there were two primary requirements for greater than conventional data accuracy. The first requirement for high accuracy stems from the need for accurate data in the normal level road cruising regime of motor torque or current – with instruments that must also be capable of obtaining data in the high acceleration and climb regime, which can be a factor of ten greater. Typical instrument accuracy specifications, in terms of the instrument's "full scale" value, are not very meaningful in this situation. The SAE J227A recommended practice for "electric vehicle test procedure" DC power instrumentation states: "The overall error in recording or indicating instruments shall be no more than ±2% of the maximum value of the variable to be measured (not including reading error)." While uncertainties of this magnitude are considered adequate for road vehicle tests, they are much too broad for the types of data comparisons made in this dynamometer test program. For example, a ±2% uncertainty when measuring the maximum torque values of interest translates to ±10% to ±20% in percent-of-reading uncertainty for the more important cruising values (some 1/5 to 1/10 of the maximum required).

The second unusual requirement for accuracy stems from the difficulty in measuring true RMS current, voltage and power when the motor's torque and power are modulated by an electronic chopper. A chopper's rapid off-on switching action creates voltage and current waveforms whose shape and phase relationships change as functions of the power circuit impedance characteristics, as well as changing with the chopper duty cycle. Accordingly, relatively sophisticated electronic instrumentation is needed in comparison to the instruments conventionally used for measuring DC power.

4.2 Motor Output Dynamometer

An electric torque-absorption dynamometer was specially designed and fabricated for testing the smaller sizes of EV motors. This

dynamometer was patterned after the time-proven Sprague electric type and designed around a 28 volt - 300 ampere aircraft surplus motor-generator. The motor-generator is operated as a shunt excited generator with a broad range of field excitation voltage and current control. Its output is dissipated in a variable resistance load-bank having a resistance range of 0.005 to 1.0 ohm. Using a speed limit of 6000 rpm (628 rad/s) and the above field strength and load variables, this small unit can absorb brief period torques exceeding 30 lb-ft (40.7 N-m) and torque-speed products exceeding 10 HP (7.46 kw).

The dynamometer, along with some of the laboratory test data instrumentation, is illustrated in Figure 4-1. An uncertainty analysis (conducted during the design and development of the dynamometer) clearly illustrated that for torque measurements the dynamometer scale accuracy and the instrument reading tolerance or resolution were the two primary factors in percent-of-reading accuracy (minor factors being the torque arm length tolerance and the suspension bearing friction or hysteresis). To maximize the accuracy of torque measurements, therefore, two dynamometer scales were used. The 0 to 10 lb high resolution scale shown in

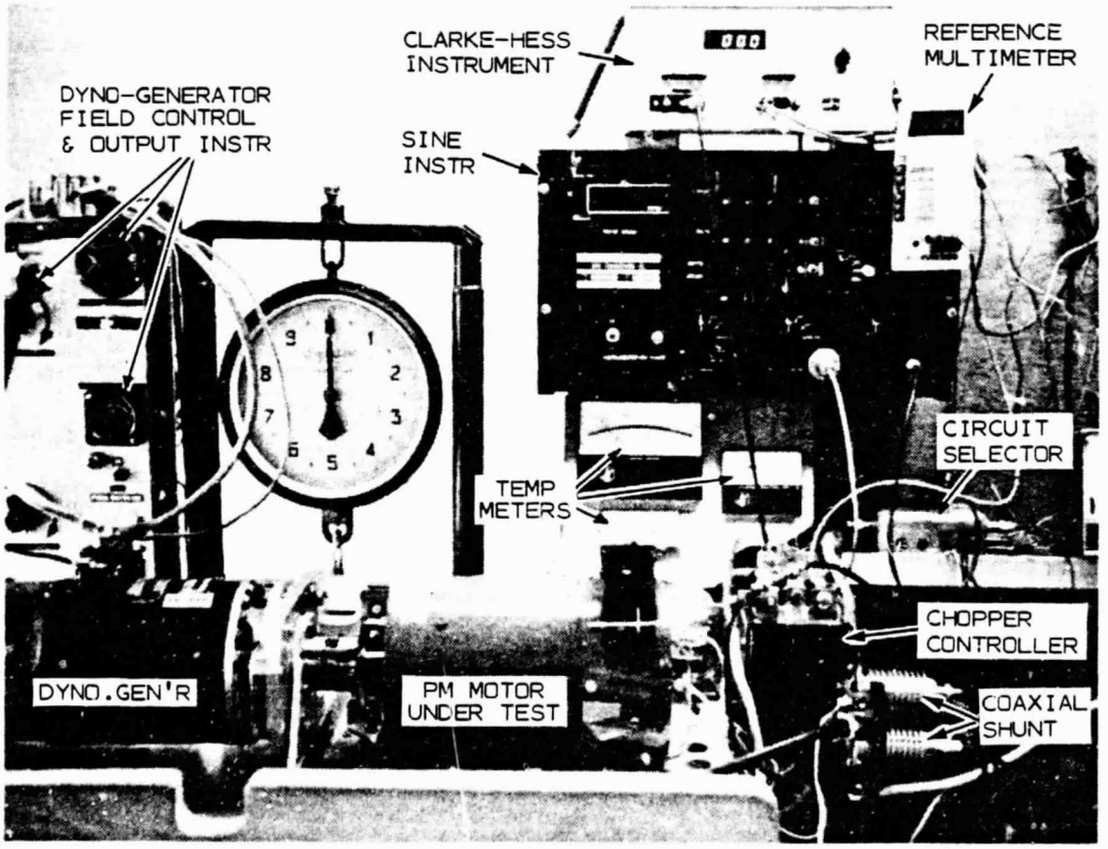

Figure 4-1 The Test Dynamometer and Part of the Instrumentation

Figure 4-1 was used for the lower, cruising range torques with a 0 to 30 lb scale used for the higher readings. In addition, both of these dynamometer force scales were dead weight calibrated, after being subjected to final fine-trim adjustments, and found to be of appreciably higher accuracy than specified. The accuracy specifications and the calibration data for the dynamometer, as well as most of the additional laboratory instrumentation for the program, are listed in Table 4-1.

4.3 Ripple-Free DC Instrumentation

For dynamometer tests using the voltage switching means of control, the accurate measurement of current, voltage and power was relatively simple — requiring only the use of high quality digital meters for readout values of voltages and the use of accurate DC current shunts. High quality shunts were used and, in addition, these DC shunts were calibrated against the still higher accuracy coaxial resistors used as AC shunts. This calibration was performed throughout a range of currents from near 0 to over 200 amperes by discharging a bank of parallel-connected batteries into the previously mentioned resistance load-bank.

A semi-pictorial wiring diagram for the voltage switch dynamometer tests is shown in Figure 4-2. As previously stated, the power circuitry is essentially an exact duplicate of that later used in the road test vehicle — including the length and gauge of conductors between the various power components. As indicated, the reversing switch was installed (shown in the diagram as connected for the series motor) and the resistance losses due to it and its wiring are included in the system performance data, although no reverse data was desired nor obtained. The illustration also shows the small shunt and analog ammeter used to measure the modest current required for the 12-volt contactor circuit. These contactors are used for speed control and current cutoff during voltage switching. (In these semi-pictorial diagrams power circuit conductors appear as heavy lines, control wiring as light lines, and instrumentation circuitry as dashed lines.)

Table 4-1 Instrumentation Specifications and Calibration Data

ITEM	MANUFACTURER, RATING OR MODEL, SERIAL NO.	SPECIFICATION ACCURACY	CALIBRATION SUMMARY
DYNO. FORCE SCALE	CHATILLON 0-10 LB NO. 9693	±0.5% FULL SCALE	±.02 LB
DYNO. FORCE SCALE	DETECTO 0-30 LB, 0.1 GRAD.	UNKNOWN	±0.2 LB
DYNO. LEVER ARM	SHIPPS ENG'G DES. & FAB.	12.002" ± .005" LONG	——
DYNO. TACHOMETER (BASIC)	POWER INSTR. MOD 1709	±1 RPM	FUNC. CHECK
TACH. GENERATOR (SPARE)	SINGER/KEARFOTT MOD 05088	UNKNOWN	323.4 RPM/V
DC CURRENT SHUNT	EMPRO HT, 300A/100MV	0.5% READING	.000332 OHM
DC CURRENT SHUNT	WESTON 300A/50MV	0.5% RDG	.000166 OHM
COAXIAL AC SHUNT	T&M 75W MODEL 1M-20, #7917	0.2% RDG	.001006 OHM
COAXIAL AC SHUNT	T&M 75W MODEL 1M-20, #7925	0.2% RDG	.001009 OHM
DIGITAL DC MILLIVOLTMETER	SIMPSON MODEL 2860, ±200 MV	±(0.1% RDG+1 DIGIT)	FUNC. CHECK
CALIB. & REF. MULTIMETER	FLUKE MODEL 8020A #2190535	±(0.1% RDG+1 DIGIT)	FUNC. CHECK
TEMP. PYROMETERS (2)	MODUTEC 3.5", 0-300°F	±2% SPAN	+5°, -2°
TEMP. PYROMETER	MODUTEC 5.5", 0-500°F	±2% SPAN	+7°, -3°
TEMP. CHART RECORDER	RUSTRAK 2153A, 0-600°F	±2% SPAN	+2°, -8°

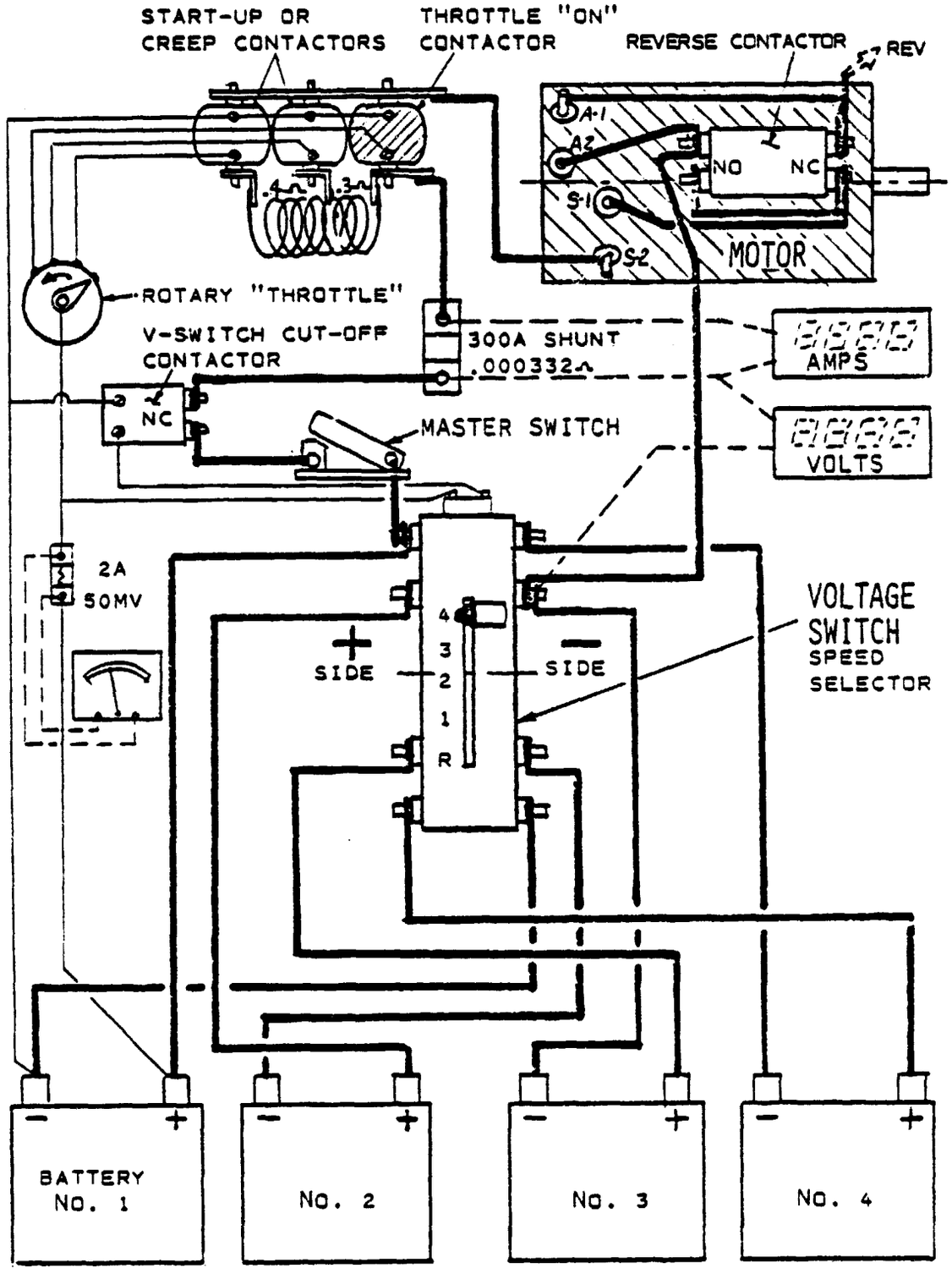

Figure 4-2 Schematic/Pictorial Wiring Diagram for Tests Using Voltage-Switch Control

In addition to the relatively permanent instrumentation shown in the diagram, a highly accurate portable multimeter was used to measure the voltage drop and, therefore, the resistance of all components and conductors within the power circuit shown. The details of these power circuit losses are given in Section 5 of this report, along with the system performance data of the voltage switching motor-controller-battery system.

4.4 Road Test Data Recorders

For road test data to correlate with and/or confirm dynamometer test results, primary reliance was upon two Gulton "Rustrak" portable strip chart recorders. These recorders are relatively simple and rugged units, using damped galvanometer movements which record on pressure sensitive strip chart paper, and both operate on 12V DC power. One three-channel recorder simultaneously recorded on separate channels DC current, DC voltage and test vehicle speed in miles per hour. The other single channel recorder, typically geared to run at the same chart speed, simultaneously recorded temperature in degrees Fahrenheit — with the usual transducer being a thermocouple cemented into the base of one of the motor brushes to record the changing brush temperature. The 3-channel current, voltage and speed recorder has a specification accuracy (for laboratory use) of $\pm 2\%$ of full scale, with a full scale response time of 0.8 to 1.0 seconds. Calibration checks during actual vehicle use on relatively rough neighborhood streets — with the instrument resting on the passenger seat of the vehicle oriented so the galvanometer needles move side to side — show accuracies in current readings of ± 6 amps with an additional correctable zero offset as high as ± 3 amps; a voltage accuracy of ± 1.5 volts or approximately 3% of full scale. The temperature chart recorder, as listed previously in Table 4-1, had a laboratory condition calibration range (after trim-pot settings for thermocouple lead resistance) of $+2^{0}$, -8^{0} over its 250^{0} to 500^{0}F range of data interest. Its in-vehicle accuracy was doubtless degraded somewhat by vehicle motions as was the 3-channel recorder just discussed.

An example of the three-channel recorder's analog output is shown as Figure 7-8 of the section on road testing. The road test data points illustrated in the four data correlation figures of Section 7 were also taken from such strip chart records. Most of the data points for the V-switch controlled tests and all of them for the chopper controlled tests were confirmed (or superceded) by instantaneous data readings as discussed below.

The strip chart temperature recorder made a continuous record of motor brush temperature during all road tests as well as during all dynamometer tests. This approximate half-hour record per test simply confirmed, for most of the testing, that no motor temperature problems occurred. For the higher torque (hence higher current) uses of the PM motor, however, as discussed in Section 7, extended time-at-current dynamometer tests established rather restrictive brush temperature current limits that were later observed and closely temperature-monitored during road tests.

For all data points of particular interest and as a continuous check on the strip chart recorder accuracy, an accurate portable digital multimeter was used to frequently check the steady-state current and voltage readings for the ripple-free DC measurements. Additionally, recorded speed data was frequently checked by stop watch measurements of time required to cover an accurately measured and marked one-tenth mile, level street, segment of the road test route. As a further addition, during these road tests, the normal vehicle instrument panel speed, current and voltage instrumentation was augmented by two panel meter pyrometers to continuously display the temperature of the motor field poles and (when installed) the chopper controller. The field poles (coil wound or permanent magnet) never approached their nominal temperature limit (210°F or 99°C). The maximum logged field temperatures, observed during the more prolonged steep grade climbs, were 130°F (54°C) for the series motor and 150°F (66°C) for the PM motor. The chopper controller, whose heat-sink was not well ventilated, did reach its 150°F (66°C) cut-back temperature several times during the road tests as discussed in Section 7.

For specific test point data confirmation when using the chopper controller, the complete Sine instrumentation system, fitted with a digital meter to record vehicle speed in addition to RMS current, voltage and power, was used. To simultaneously record these four data parameters during vehicle operation, a Polaroid automatic camera (SX-70) was appropriately mounted and sun-shielded so as to record the four digital panel meter readings on film at the press of a remote shutter button (samples of these photo-records can be seen in Figure 7-10.

4.5 Dynamic Instrumentation for Chopper Data

To determine and record current, voltage and power data when using the electronic chopper control system, two relatively advanced state-of-the-art instrument systems were used. The primary instrumentation system used for these data was developed specifically for this test program by Mr. Paul Brock of Sine Engineering. This Sine instrumentation, being designed specifically for electric vehicle power circuits, has a range of 0 to 100 volts DC and a current range of 0 to 400 amperes. The instrument is shown in Figure 4-1. The instrument panel is equipped with 3 digital panel meters (DPMs) to simultaneously display current, voltage and power outputs. Since the NASA Lewis Research Center had previously tested a variety of such dynamic instruments and found a Clarke-Hess unit most acceptable, a Clarke-Hess Model 255 volt-ohm-watt meter was also used, primarily for correlation and confirmation purposes. This standard model Clarke-Hess unit has a voltage measuring range of 0 to 1000 volts, with a 0 to 200 volt range setting used for this program, and is provided with a current range of 0 to 5 amperes. For this test program, the Clarke-Hess current capability was expanded by a factor of 40 by a relatively simple addition and change of two matched resistors.

A semi-pictorial wiring diagram for the chopper controlled system tests is shown in Figure 4-3. The power circuit essentially

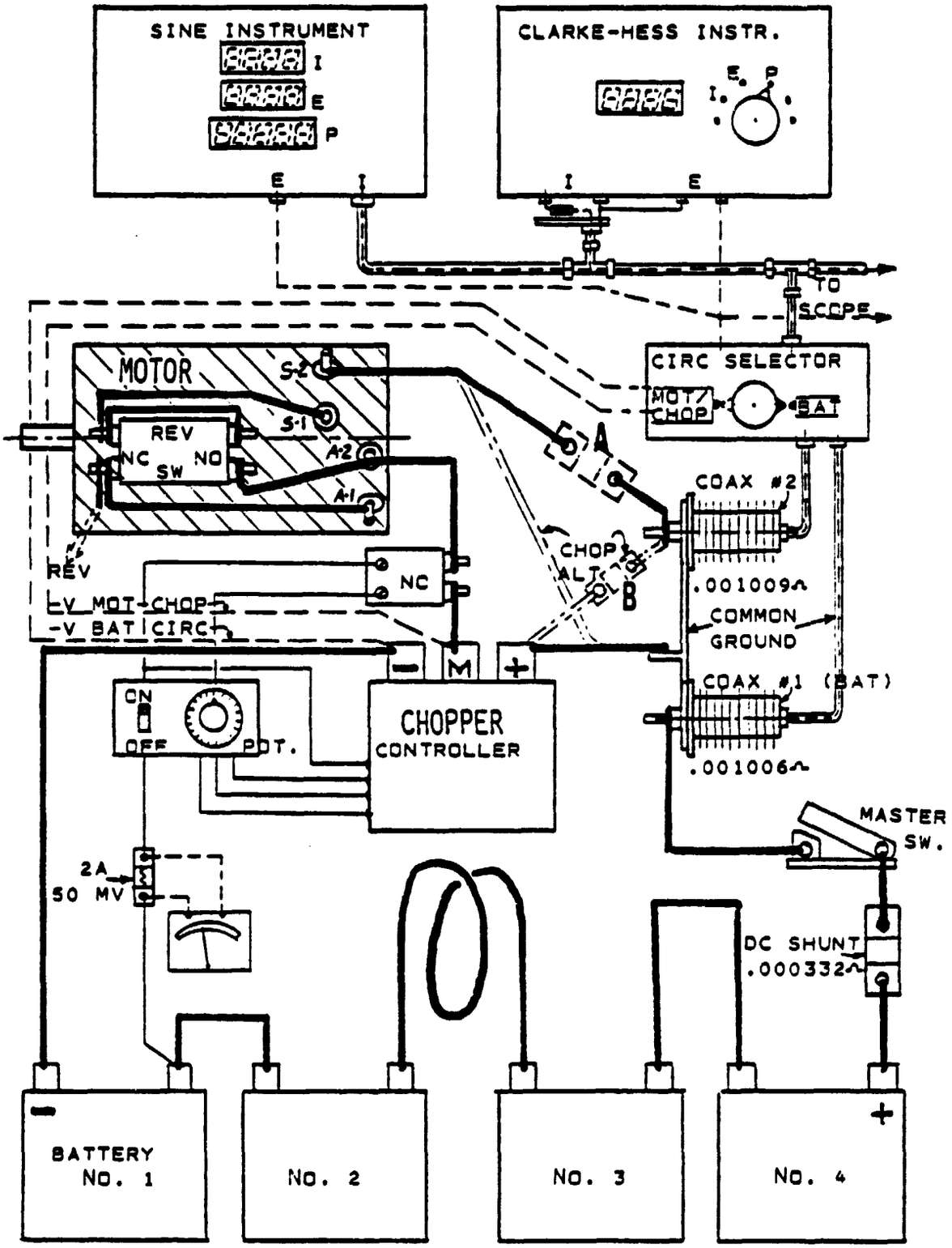

Figure 4-3 Schematic/Pictorial Wiring Diagram for Tests Using Electronic Chopper Control

duplicates the one later used in the road test vehicle, including details such as lengths of cables between the series connected batteries, etc. At the top of the figure, the Sine and Clarke-Hess instruments are shown connected, via shielded coaxial cables, to simultaneously record data from either the battery circuit or motor circuit (or chopper circuit) as determined by the circuit selector switch shown. Two coaxial resistors are shown serving as dynamic current shunts, one in the battery circuit and one in the motor (or chopper) circuit. Also indicated are leads going to an oscilloscope which displayed current and voltage waveforms in the selected power circuit.

The circuit diagram also shows a number of conventional DC shunts. The DC shunt shown between the master switch and battery No. 4 (the same shunt used for current measurements during voltage switching operation) was used to determine the accuracy of readily available and economical DC instrumentation in chopper controlled EV power circuits. For a similar purpose, during the earlier chopper controlled tests, a DC shunt was also used in the motor circuit (shown by dotted lines and labeled "A" in Fig. 4-3). Another much smaller DC shunt was also used temporarily in the revised connections used for directly measuring chopper power (shunt "B" in the diagram changes indicated by phantom lines). These earlier chopper controlled tests revealed that waveform and power factor effects on the motor side of the chopper made DC instrumentation here relatively inaccurate, and highly inaccurate in the chopper circuit. Consequently, these motor and chopper circuit DC shunts were removed for the later tests. The battery circuit DC shunt, however, was retained and used for all tests and provide respectable data as discussed later in this section. Still another small shunt and an associated ammeter were used to measure the modest 12 volt power required by the chopper circuitry.

4.6 Dynamic Instrument Calibration and Comparisons

Following the fabrication, check-out and calibration of the Sine instrument's internal circuits, and modification of the Clarke-Hess instrument to increase its current and power measuring capability, the two dynamic instruments were ready for overall calibration and data comparison tests. Three types of tests were performed. First, the ability of the instruments to accurately measure ripple-free DC voltage, current and power over a broad range of values was checked. Such "use of complex instruments for a simple measuring task" was performed both with completely ripple-free current (knife-switch activated discharge of batteries into a resistor bank) and by nearly-square-wave chopper modulation of power going to the resistor bank. Second, the two instruments were compared to each other and to standard DC instruments, with oscilloscope records of current and voltage waveforms, in the measuring of actual motor/chopper/battery system power flow. In these tests the Clarke-Hess instrument, being a design previously tested and qualified by the Lewis Research Center, was generally considered as a reference standard. Third, and the test considered most demanding of instrument precision, was a "power balance"

experiment. For this test two "quick change" instrumentation set-ups were used with the various test conditions approximately duplicated in each of the two set-ups. One set-up first measured the power (including current and voltage values) in the battery and the motor circuits, for a range of chopper duty cycle settings and a given load. The basic instrument circuitry shown in Figure 4-3 was used. The instrument's current measuring set-up was then changed to the phantom-line "chopper alternate" of Figure 4-3 to measure the much lower chopper power and remeasure battery output power. To the extent that these powers were precisely measured, the battery output power should equal the sum of the motor and chopper input powers. The correlation of these measurements is discussed and illustrated later in this section.

Typical ripple-free DC test results for the Sine and Clarke-Hess instruments are shown in Figure 4-4. As indicated, these data combine the results of two different tests and cover a power range of approximately 1 to 8 kilowatts. The Sine instrument data averaged approximately 2% higher than the nominal DC power reading, while the Clarke-Hess instrument averages some 3% lower than nominal DC. Since these tests were using the relatively complex dynamic instrumentation to measure ripple-free DC power, the deviations can be considered as actual error in the dynamic instruments; with the exception that data scatter effects are also included (which are primarily the result of DPM reading changes that occur during the period of logging data). The several calibration and adjustment functions prescribed in the instrumentation manuals and instructions had little effect upon the patterns of deviation shown. Accordingly, these deviations were considered inherent in the circuitry of the instruments. In the subsequent dynamometer tests the two dynamic instruments continued to be used simultaneously. The three digital panel meters of the Sine instrument were used to measure voltage, current and power; while the single Clarke-Hess panel meter was used to measure confirming power only.

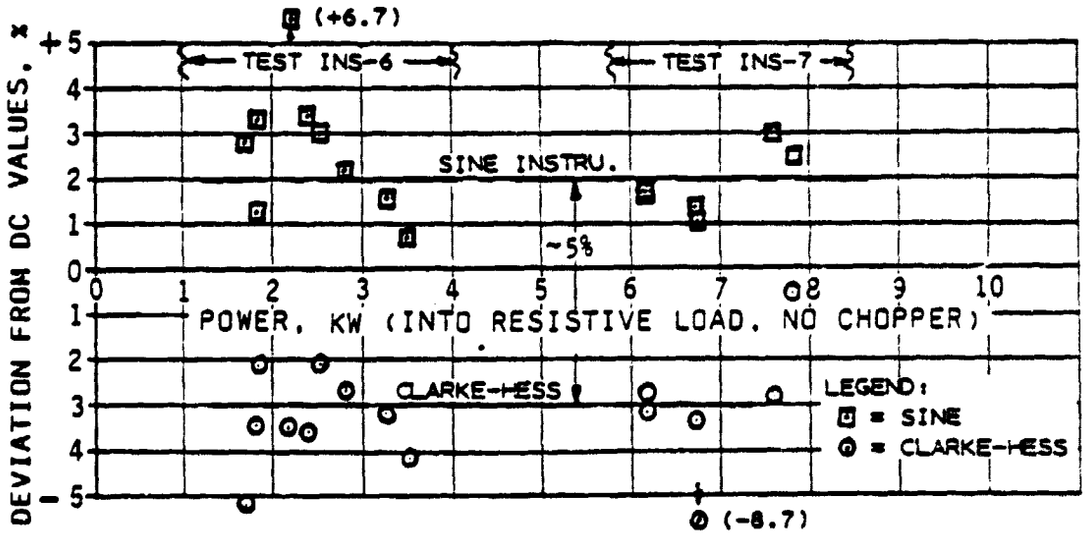

Figure 4-4 Typical Comparison of Dynamic Instruments in Measuring Ripple-Free DC Power

Throughout the chopper control portion of the dynamometer test program, the two dynamic instruments continued to show a 5 or 6 percentage point spread in their measurements of power. This spread is illustrated in Figure 4-5. These data show the two instruments approximately tracking each other but with a 6 percentage point spread. Considerably greater spread is shown at the very low power setting of approximately 150 volt-amperes. This low power is well below the practical range of the instruments, which have capabilities of 10 and 40 kilowatts respectively. Here the deviations from KVA values shown do not, as in the previous figure, imply instrumentation error. While measurements of average current and voltage values in the battery circuit, under chopper control, were found to provide close approximations of the RMS power, the dynamic instruments are assumed to be more accurate in determining the true power.

Figure 4-6 illustrates typical current and voltage waveforms in a battery powered motor circuit system when controlled by a chopper operating at a nominal frequency of 400 Hertz. These oscilloscope photographs, as well as others illustrated later in this report, each result from three partial exposures of a Polaroid film (using an oscilloscope camera). The first exposure simply identifies the date and general

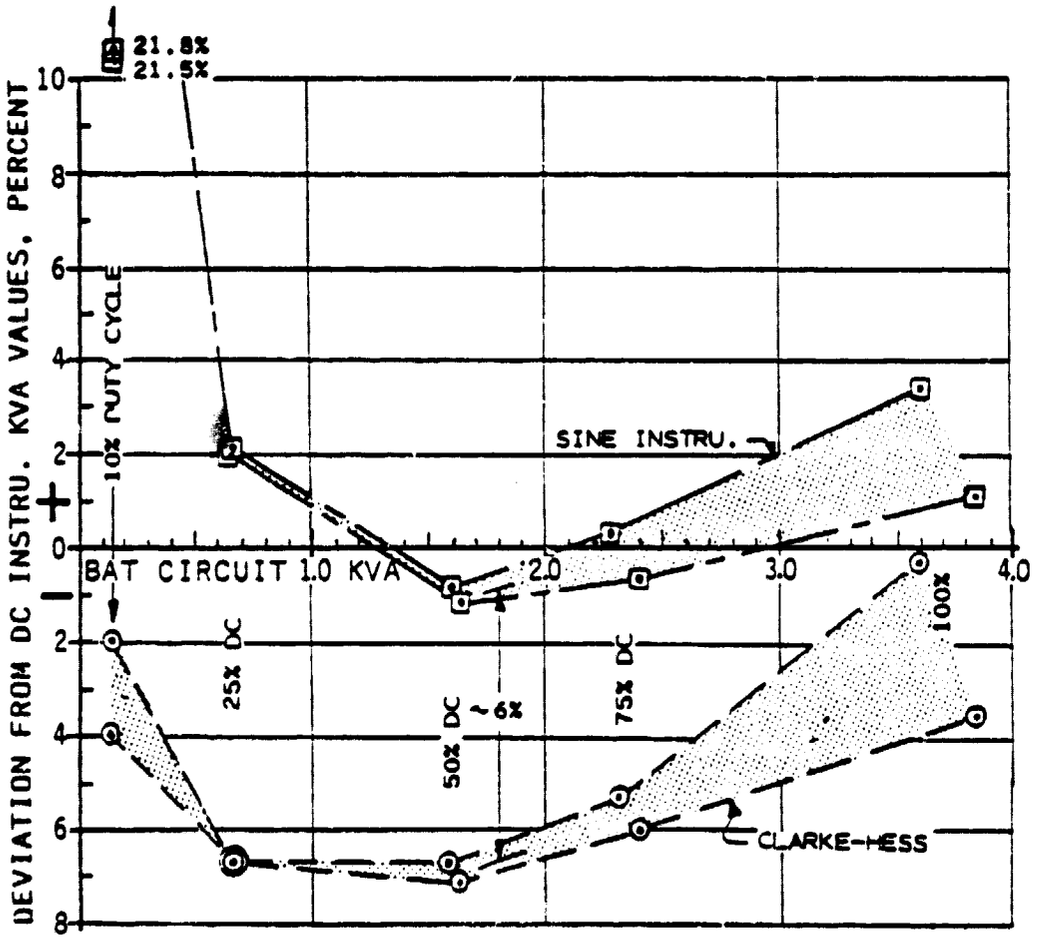

Figure 4-5 Typical Comparison of Dynamic Instruments in Measuring Chopper Controlled Power

subject and occurs near the top of the print. The other two exposures each record two traces on the oscilloscope grid and were typically separated in time by only a few seconds. In Figure 4-6 the bottom scope plot shows the voltage and current waveforms occurring in the battery circuit (i.e., the voltage and current flowing in the power circuit on the battery side of the chopper controller). The top plot of the left photograph shows the voltage and current waveforms on the motor side of the power circuit. In the right photograph the top plot shows the chopper current (as measured by coaxial resistor #2 when connected in the phantom-line "chopper alternate" set-up of schematic Figure 4-3) and chopper voltage (which for these tests was measured as was motor voltage, between the positive common ground and the "M" terminal of the controller). The RMS current, voltage and power values inserted along the right side of the photographs are those logged from the dynamic instrumentation during the test for which the photorecord was made. For the left hand photograph of the figure (which is typical of those later in this report) it should be noted that the current display is reversed in sign between the motor and battery circuit presentations. This sign reversal is due simply to the instrumentation common ground (as shown in the schematic Figure 4-3), plus the desire to switch the circuit selector and rapidly record data

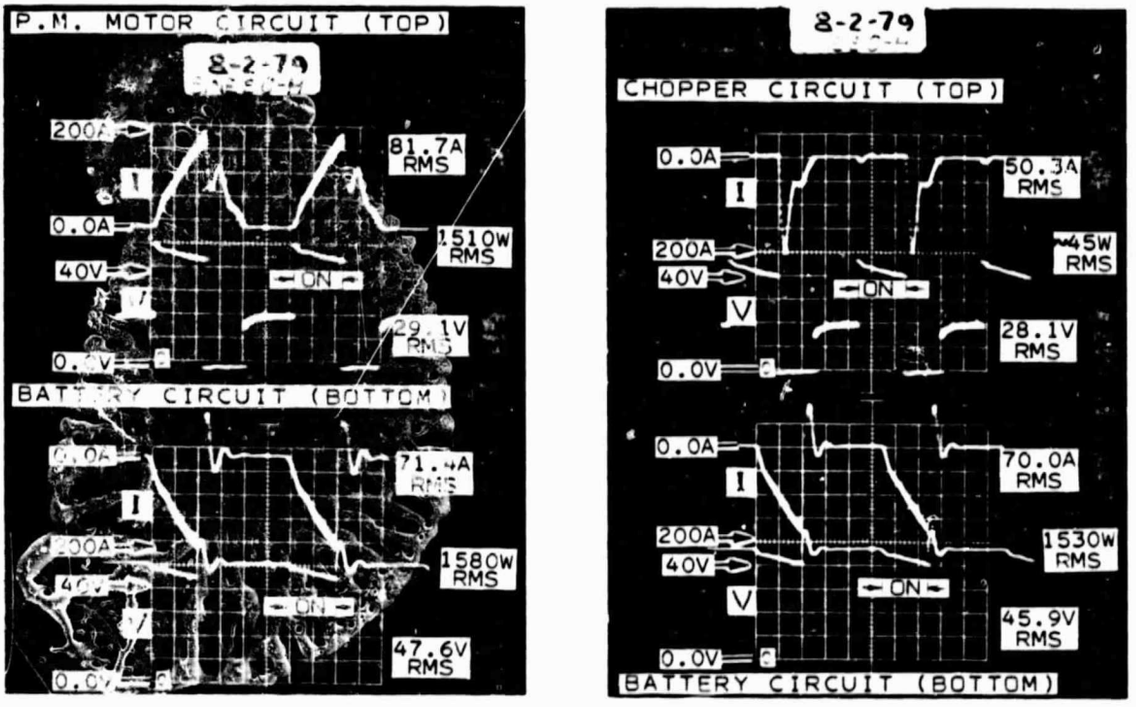

Figure 4-6 Chopper Caused Current and Voltage Waveforms in the Battery, Motor and Chopper Circuits (PM Motor with no added "choke" inductance, 38% Duty Cycle, 3.2 lb-ft torque)

from both circuits, to avoid appreciable changes due to battery voltage drop. The rapid switching from motor to battery circuit and the reversal of sign necessitated adjustment of the current trace vertical position for each exposure. Consequently, different zero current locations occur and some of the oscilloscope current traces do not have an identifiable zero current location. In some cases an obvious zero flat spot occurs on the trace as shown in Figure 4-6.

The oscilloscope records of this figure reflect an approximate 38% duty cycle (i.e., the chopper "switch" is closed 38% of the time) and a relatively low "cruising speed" torque of 3.2 lb-ft. Under these conditions the current continues to rise rapidly in both the battery and motor circuits with a noticeable drop in voltage, during the complete "on" period. As the chopper switches "off," battery circuit current is seen to drop sharply, reverse and rebound with but a slight time lag compared to similar but much milder oscillations in battery circuit voltage. Accordingly, the battery circuit current and voltage switch nearly simultaneously — which helps explain why the product of average voltage and average current (measured by typical DC instruments) was, in the battery circuit, consistently within 2 or 3 percent of RMS power as measured by the dynamic instrumentation.

In the motor circuit voltage and current clearly do not switch simultaneously. Current continues to flow long after the voltage abruptly returns to zero or becomes slightly negative. Integrating the product of instantaneous voltage and current is relatively more complex, and requires dynamic instrumentation to obtain sensible values for power. In these chopper controlled tests the motor voltage drops from 50 to about 43 volts during the on time of the controller. When the controller switches "off" the motor voltage falls to a slightly negative value as current continues to flow through the controller's free wheeling diode. With this PM motor and no added "choke" inductance, this "free wheeling" motor current reaches zero well before the next "on" period. When the motor current is zero the motor circuit voltage becomes an intermediate value indicating the motor's counter EMF (in this case approximately 20 volts, representing the motor speed of 2200 rpm during this test).

The right hand photograph of Figure 4-6 was taken about one-half hour after the left hand photograph. The chopper duty cycle setting, however, was precisely duplicated and to the extent practical the torque output was reestablished to the same conditions. This time delay and the resulting modest change in battery state-of-charge was necessary to allow altering the power circuit so that the second coaxial resistor sensed chopper current rather than motor current (i.e., in Figure 4-3 "coax #2" measures what is defined as chopper current when its center terminal connects, via the "chopper alternate" conductor, to the controller's plus terminal; it measures motor circuit current when its center terminal connects to the motor terminal). In the upper plot of the right hand photo, as the chopper "switch" turns off, current in the chopper circuit jumps to approximately the value previously reached in the motor circuit, and then decays rapidly as the motor circuit current decays. During this spurt of chopper current, however, very little voltage was present and

the power consumed by the chopper was low. A power value of 45 watts was the average of the two dynamic instruments' reading (too low for accuracy as this value is 0.5 and 0.1 percent of the instruments' measurement capability).

Measuring the small amounts of power consumed by the chopper was part of the "power balance" experiments which were the final and most demanding of the dynamic instrument precision and accuracy investigations. As discussed earlier, these experiments investigated the instrumentation precision by separately measuring the power in the motor and chopper subcircuits and comparing the sum of these to the power coming from the battery circuit. Several power balance attempts were made as the dynamic instrumentation, its switching circuitry and use procedures were investigated. The final and most successful of these power balance experiments is recorded in Table 4-2. To record chopper circuit power under the same conditions used for motor circuit power required a change in motor and chopper power circuitry, as discussed above in connection with the oscilloscope records. To accomplish the "power balance" experiment, then, two sets of "data point pairs" were recorded under essentially the same conditions. Data points 1 and 2, for example, recorded the voltage, current and power in the battery circuit and in the motor circuit; while data points 1A and 2A, somewhat later, re-recorded battery circuit data but now with chopper circuit data. In the left half of the table chopper power is assumed as the difference between the battery circuit and motor circuit powers. The percentage difference is shown as well as the numerical difference in watts. The table also shows, to the right, the chopper circuit power in watts and in percent of battery circuit power as measured by the "A" data point pairs. While these data are clearly inconclusive insofar as chopper power consumption is concerned (indeed the chopper may experience a mix of voltages and not simply motor circuit voltage as assumed for these tests), the trends of the two measuring methods seem consistent.

Table 4-2 Final "Power Balance Experiment*" to Investigate Dynamic Instrument Precision

INSTRU.	DATA PT. PAIR (BATTERY & MOTOR)	CHOPPER DUTY CYCLE	POWER MEASUREMENTS IN WATTS: BAT. CIRC. − MOTOR CIRC. =	(% OF BAT.)	CHOP. CIRC.	(% OF BAT.)	BAT. CIRC.	DATA PT. PAIR (CHOPPER & BATTERY)
SINE	1 & 2	10%	182 − 149 = 33	(18%)	26	(14%)	181	1A & 2A
	3 & 4	25%	674 − 596 = 78	(12%)	44	(6.6%)	659	3A & 4A
	5 & 6	50%	1615 − 1512 = 103	(6.4%)	55	(3.5%)	1572	5A & 6A
	7 & 8	75%	2376 − 2263 = 113	(4.7%)	55	(2.4%)	2279	7A & 8A
	9 & 10	100%	3917 − 3826 = 91	(2.3%)	29	(0.8%)	3798	9A & 10A
CLARKE-IESS	AS ABOVE	10%	147 − 139 = 8	(5.4%)	4	(2.8%)	143	AS ABOVE
		25%	616 − 591 = 25	(4.1%)	8	(1.3%)	612	
		50%	1519 − 1487 = 32	(2.1%)	16	(1.1%)	1479	
		75%	2250 − 2256 = -6	(-0.3%)	13	(0.6%)	215	
		100%	3734 − 3766 = -32	(-0.8%)	4	(0.1%)	3586	

*ASSUMES (AS MEASURED) BATTERY POWER = SUM OF MOTOR + CHOPPER CIRCUIT POWERS

Given the dual problems of measuring "small differences between large numbers" and measuring power values that are a minute fraction of either instrument's capability, these data were considered to illustrate a respectable degree of measurement precision by both of the dynamic instruments.

An unexpected conclusion, but one considered significant in the measuring of EV power consumption, resulted from the numerous experiments made with the two RMS-measuring dynamic instruments. The conclusion was later substantiated by the entire set of chopper controlled tests, using both the series and PM motors, and including the two chopper-controlled road tests. This conclusion is that conventional DC shunts and voltmeters, when installed in the power circuit on the battery side of the chopper controller such as tested, provide power and energy consumption accuracies commensurate with typical "good" vehicle instrumentation (i.e., within a few percent error). The error magnitudes typically indicated by comparative measurements (in the battery circuit) would be of concern in careful laboratory testing but not in road testing nor in normal vehicle use. (Power circuit measurements on the motor side of the chopper, by contrast, show large discrepancies when measured with DC shunts and voltmeters.)

5/ SYSTEM PERFORMANCE WITH VOLTAGE SWITCHING SPEED CONTROL

The motor/controller/battery system performance presented in this section used the 4-step voltage control circuitry previously shown in Figure 4-2. With this system a nominal cruising speed is selected by the choice of voltage switch positions — since DC motor speeds under given road conditions (i.e., a given torque) are essentially proportional to the applied voltage. When operating in traffic conditions requiring an intermediate speed, such intermediate speeds are accomplished by means of an on-off operation of the power contactor "throttle"; this results in intermittent periods of moderate acceleration mingled with periods of coast — in practice not unlike most conventional automobile driving in traffic. The 2-step series resistance positions on the contactor "throttle" are intended for motor start-up or "inching accelerations" only.

It will be noted that the voltage switching system for these dynamometer tests, as well as for the road vehicle from which this power circuit was duplicated, provide 48 volts nominal as the upper speed selection although both motors tested are rated at 36 volts. Use of moderately higher-than-rated voltage is considered both acceptable and appropriate for battery powered DC motors, particularly if they were rated for constant voltage operation. As long as the overvoltage and resulting motor speed are not excessive, the system will profit from higher efficiencies, particularly at the lower nominal voltage settings.

The permanent magnet motor whose performance data will be described, as previously indicated, was not designed as a traction vehicle motor and does not have the commutation capability or heavy wiring required to permit the brief-period high currents required of traction motors. Its performance characteristics, however, are typical of permanent magnet motors in general, which are quite different from series motors, and are presumed not appreciably different from a PM motor designed for the higher current capability of traction motors.

5.1 Power System With Series Motor

The basic performance characteristics of DC motors are usually presented in terms of speed-versus-torque and current-versus-torque curves. Horsepower curves may also be calculated from these speed and torque data. In this report horsepower is deliberately avoided since torque is the more important parameter for EV considerations. Figure 5-1 illustrates the characteristic curves for the series motor obtained from the dynamometer test data of this program. Unlike the motor manufacturer's curves as most often provided, these speed versus torque curves incorporate the "drooping" voltage characteristics of the battery pack. The voltage drop curves, corresponding to each of the nominal voltage selections, are shown in the upper plot as output volts per cell. (The nominal voltage of

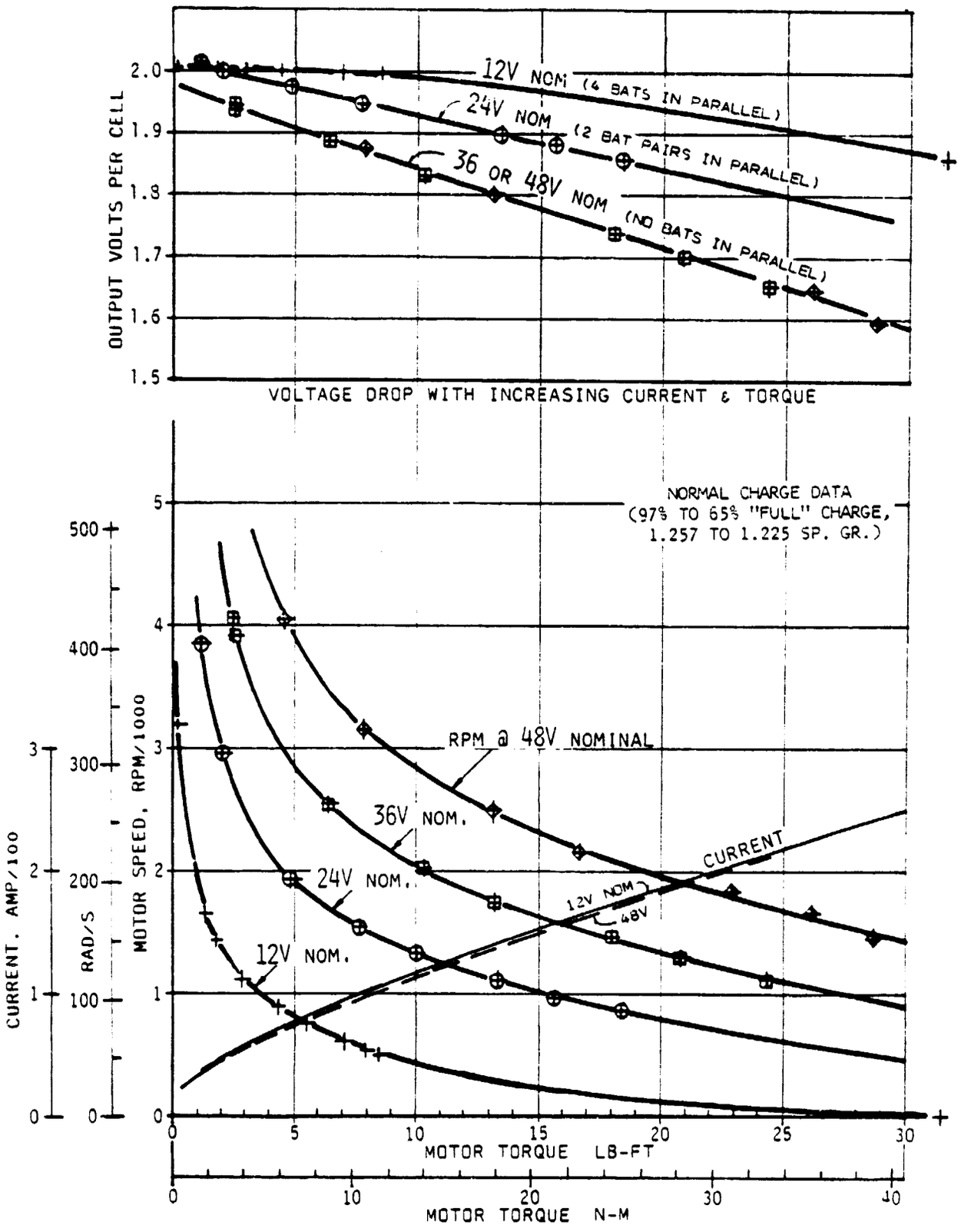

Figure 5-1 Series Motor Characteristics on Battery Power with Voltage-Switch Control

a lead acid cell being 2 volts, the number of cells in series for each of the nominal voltages is, accordingly, one half the stated nominal voltage.)

The torque of either series or PM motors is essentially directly proportional to current flow and is usually considered as independent of the applied voltage. In these tests, however, a slight variation due to voltage was evident and is so indicated in the curves of current versus torque. The current differences with voltage, however, are seen to be quite small and for vehicle design purposes, etc., the differences can be ignored.

Figure 5-2 shows the important efficiency characteristic of the motor and its motor circuit. The motor by itself is slightly more efficient than indicated here because these data include the voltage drop effects of the conductors between the voltage switch on the negative side and the current shunt on the positive side, as well as the voltage drop in the "throttle" contactor and the reverse switching contactor. The magnitude of these losses is treated in Section 5.4 along with all other circuitry losses in this voltage switching circuit. It will be noted, as discussed above, that the efficiency in the nominal 48 voltage selection is appreciably higher than when operating at a nominal 36 volts.

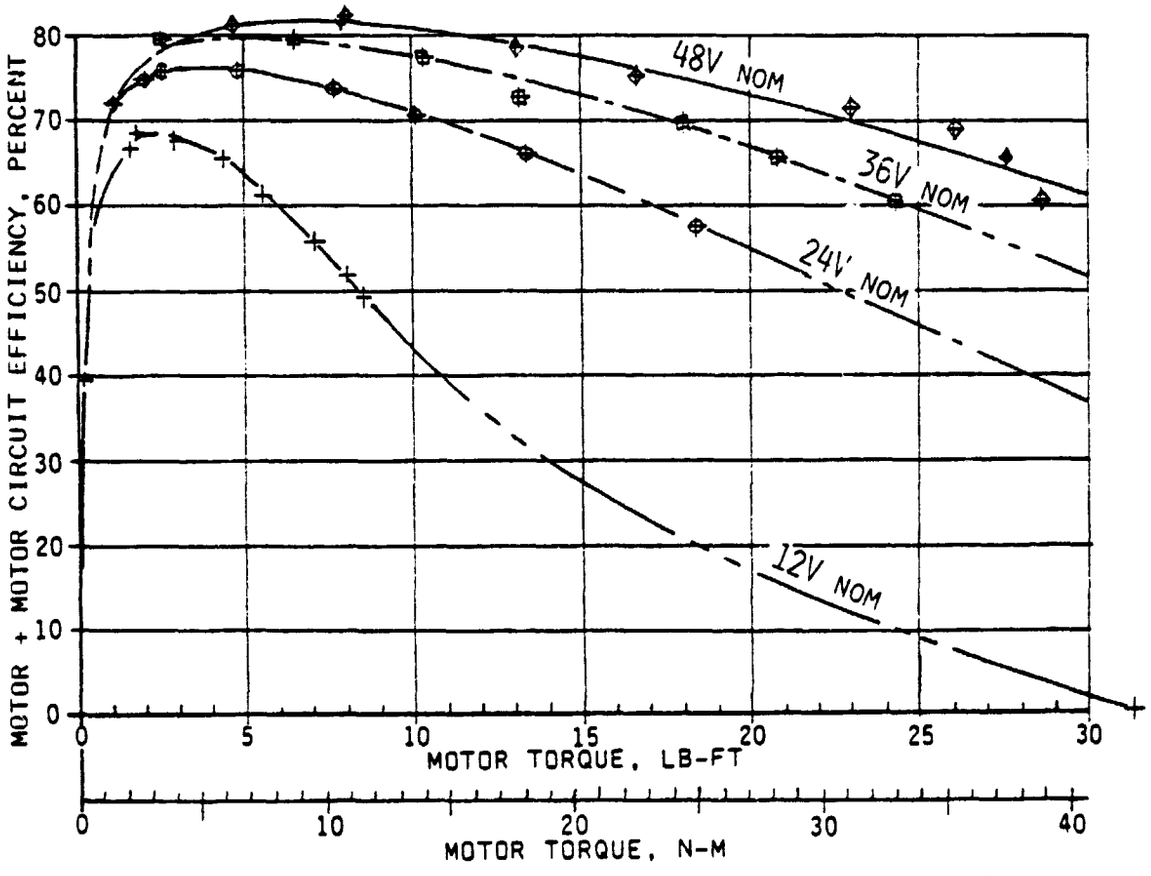

Figure 5-2 Motor Plus Motor Circuit Efficiency – Voltage Switched Series Motor

Tests to determine data point repeatability and the effects of hysteresis were also performed. The repeatability tests explored the testing system and instrumentation's ability to provide consistent and repeatable data by approaching the data points in different directions. Hysteresis experiments investigated actual hysteresis effects in the battery/motor system (such as might be caused by residual magnetic field effects when increasing versus decreasing current) as well as hysteresis effects in the instrumentation system.

Figure 5-3 summarises both the repeatability and hysteresis results of tests with the voltage switched series motor. Most of the numerous test data points generated for this program resulted from data point progressions along dynamometer "load lines" as indicated by the data points identified as 10 through 17 on the figure. Data points 10 through 13 were recorded by reaching a steady state operation at a given dynamometer load and a nominal 12 volt speed setting; followed by an open circuit ("throttle" off) and shift to 24 volts nominal and reacceleration to a new steady state condition for data point 11, etc. After data point 13 the dynamometer load was increased and data points 14 through 17 were obtained by backing down in voltage settings. The "flagged" data points and the curves shown more boldly on the plot (from a later test to determine repeatability) progressed along a given nominal voltage setting,

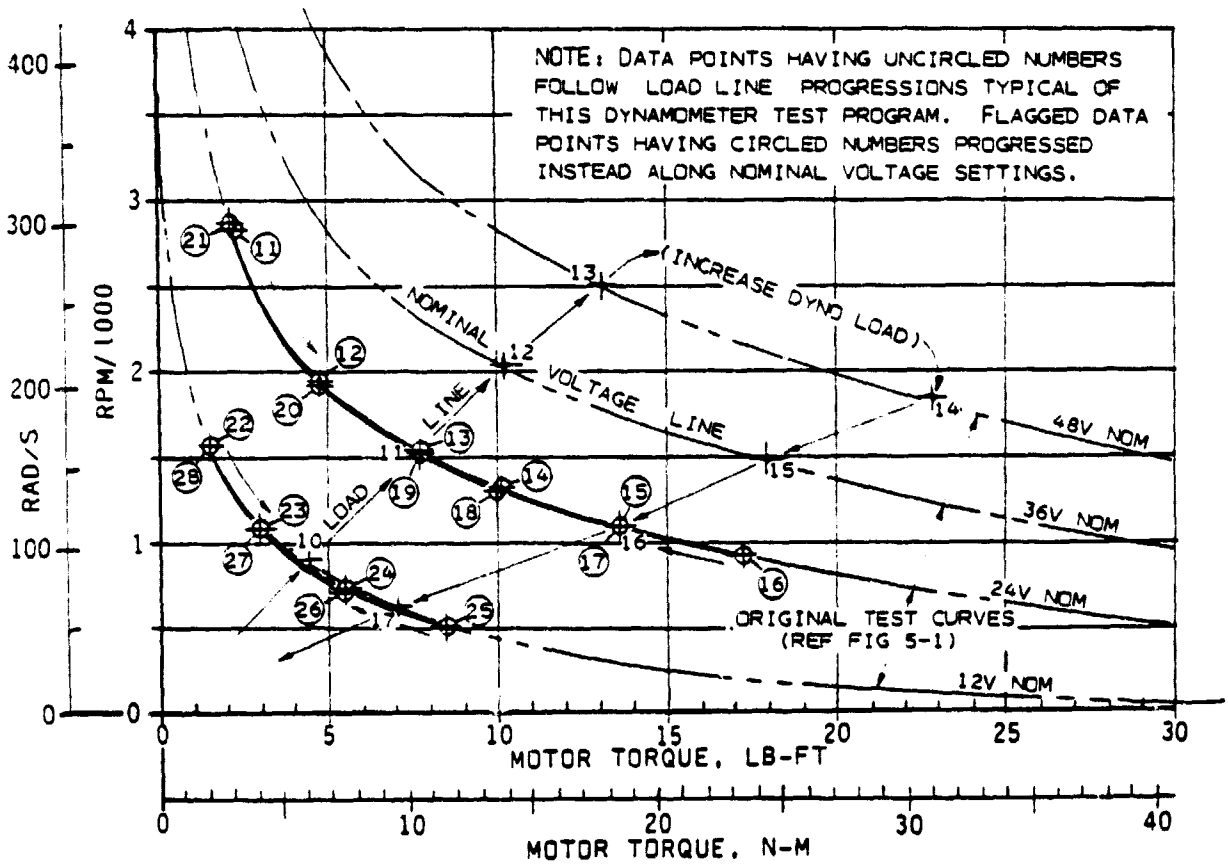

Figure 5-3 Repeatability/Hysteresis Data — Voltage Switched Series Motor

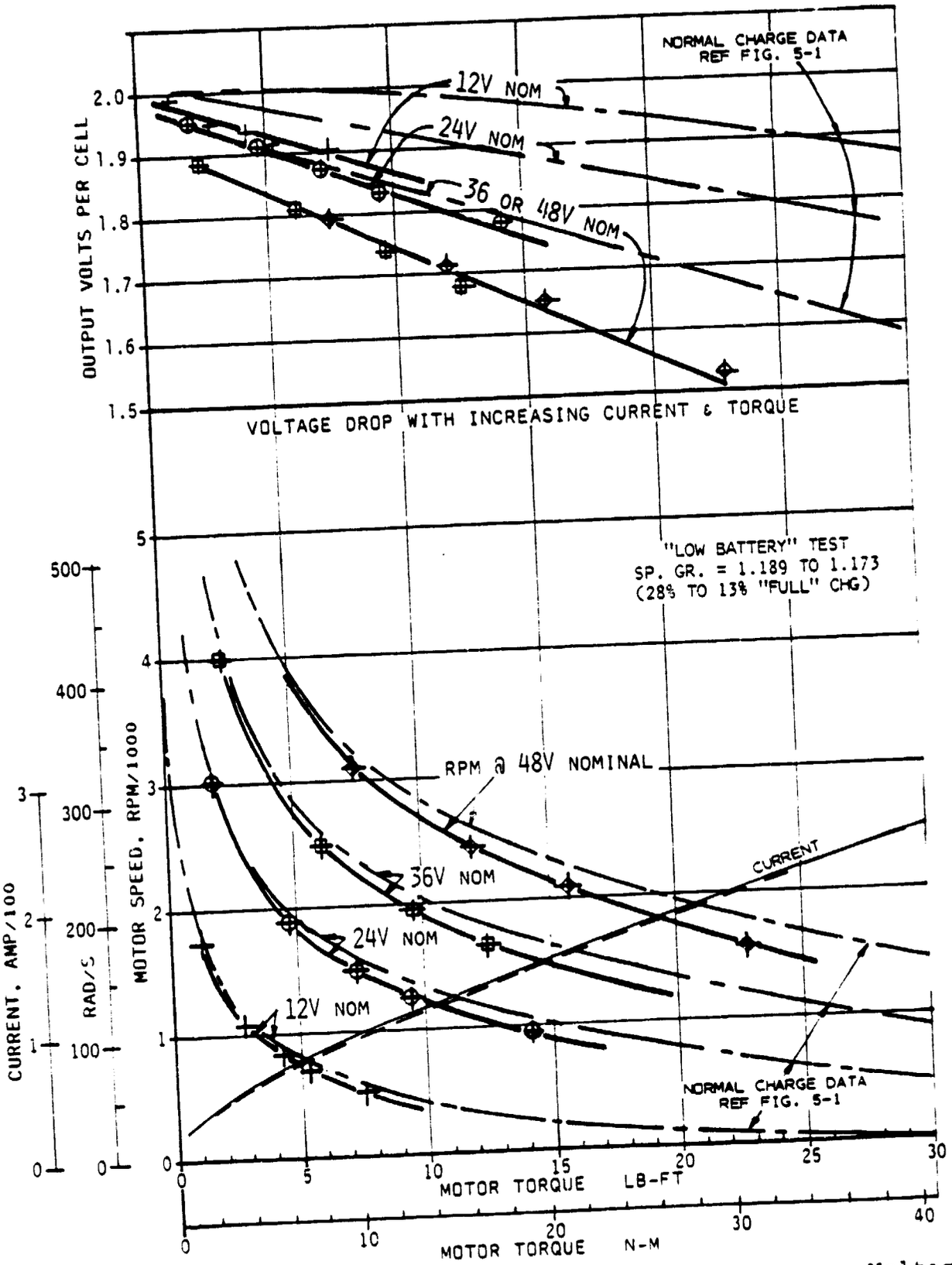

Figure 5-4 "Low Battery" Series Motor Performance – Voltage Switch Control

first incrementally increasing the dynamometer load (circled number data points 11 through 16 and 22 through 25) and later decreasing the load through nominally the same torque points (circled number data points 16 through 21 and 25 through 28). As clearly indicated, a high degree of repeatability and perhaps some slightly noticeable hysteresis is shown. Such repeatability, in general, is also indicated by the consistency of the data points falling on or quite near smooth curves (i.e., relatively little scatter of the test data is indicated).

Additional tests were performed to determine the performance effects of a nearly discharged or "low" battery. The results of these tests are shown in Figure 5-4. Here the primary effect is clearly the added amount of voltage drop from the battery, which reflects the normal discharge characteristics of batteries. This is shown in the upper plot where the bold curves indicate the low battery voltages per cell, while the lighter reference curves repeat the more fully charged drop data from Figure 5-1. The motor speed versus torque curves show a reduction in speed at a given torque and nominal voltage which reflects the added amount of voltage drop shown above.

Figure 5-5 shows the low battery effect on motor efficiency. Relatively little change in efficiency is indicated and most of the

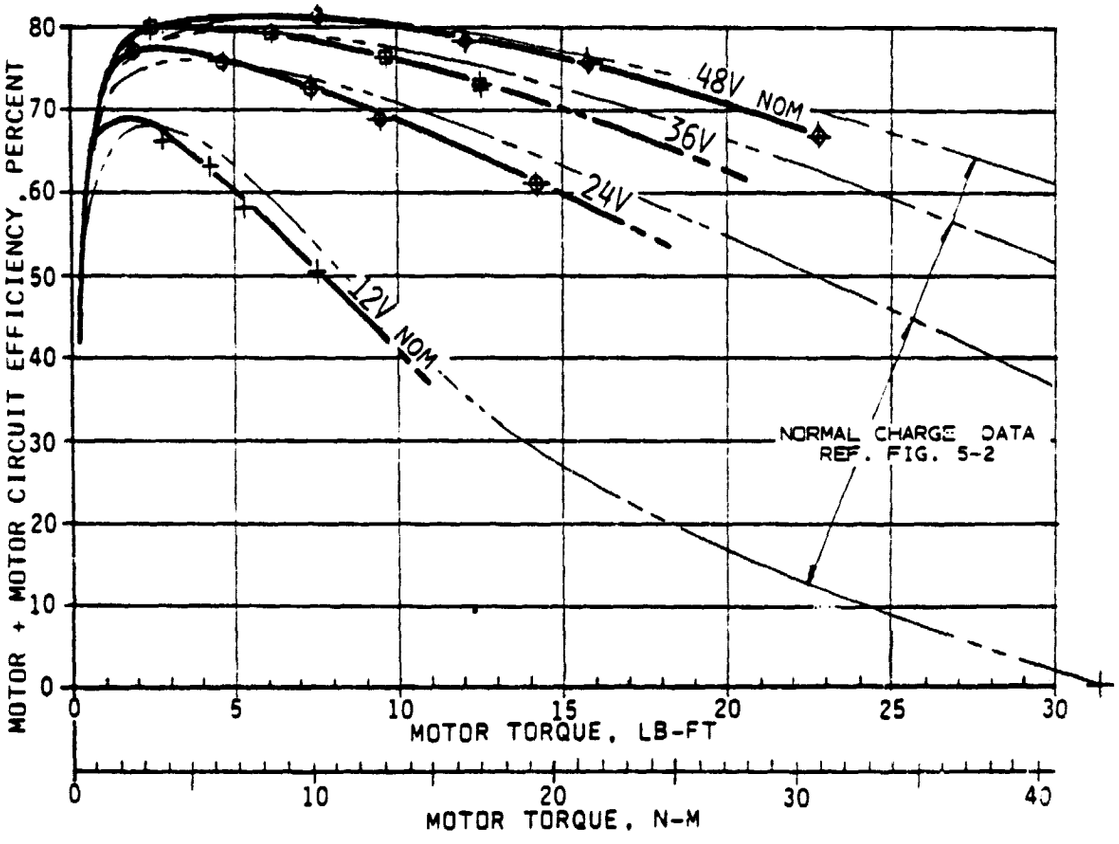

Figure 5-5 "Low Battery" Moderate Effect on Motor Efficiency

change shown is a modest reduction which again is attributable to the reduced voltage coming from the "low" battery. The curves, as they are plotted, also appear to show the "low" battery having a slight improvement in efficiency at very low torques. It is not clear whether this reflects an actual change in efficiency (possibly due to the motor and batteries being somewhat "warmed up" compared to the previous tests at a higher state of charge) or simply a different interpretation of the curve peak characteristic when based on relatively few low torque data points.

5.2 Power System With PM Motor

The basic tests with the permanent magnet motor were performed in essentially the same manner as tests of the series motor. The permanent magnet motor characteristically has a speed versus torque curve decidedly different from that of a series motor, as is shown in Figure 5-6. Due to its fixed magnetic field strength, the PM motor has a finite no-load speed and essentially a straight line speed versus torque curve, which sharply contrasts with the series motor curves being essentially asymptotic to the zero torque axis (meaning, among other things, that the series motor can "run away" and self-destruct if voltage is applied while it is unloaded). For EV applications, an interesting characteristic of the PM motor is the relative ease with which it can be used for regenerative braking (i.e., when the motor speed at a given nominal voltage setting appreciably exceeds its no-load speed, the motor becomes a generator and, if the circuit remains closed, returns current and energy to the battery). As shown in the upper plot of Figure 5-6, the voltage drop versus torque or current trend is much like that shown for the series motor. This, of course, is because the voltage drop versus current is a function of the battery's characteristics and not that of the motor.

The efficiency data for the permanent magnet motor, including the motor circuit losses previously mentioned, is shown in Figure 5-7. The PM motor tested is a higher speed motor than the series motor so its torque (for equivalent power output) is less. Even considering this difference, the PM motor's efficiency appears to drop off more rapidly at its high torque end. When operated at the lower voltages, however, the PM motor reaches higher efficiencies than the series motor. These efficiency differences, as well as other operating differences in the two motors, will be further illustrated in Section 5.3 and Section 7.

Tests were also conducted to obtain "low battery" performance data for the PM motor. Preparations for this low battery test required a period of steady state "cruise" operation of the motor to reduce the battery state of charge. Inadvertently too much discharging was accomplished which required a brief (approximately 90 minute) modest-rate recharge to bring the battery's specific gravity to the desired "low battery" state of charge (approximately 20% full charge or an sp. gr. of 1.185). The ensuing test of the recharged low battery system had surprising results, as indicated in Figure 5-8. As indicated in the upper plot, the voltage drop during these tests was less than that which occurred

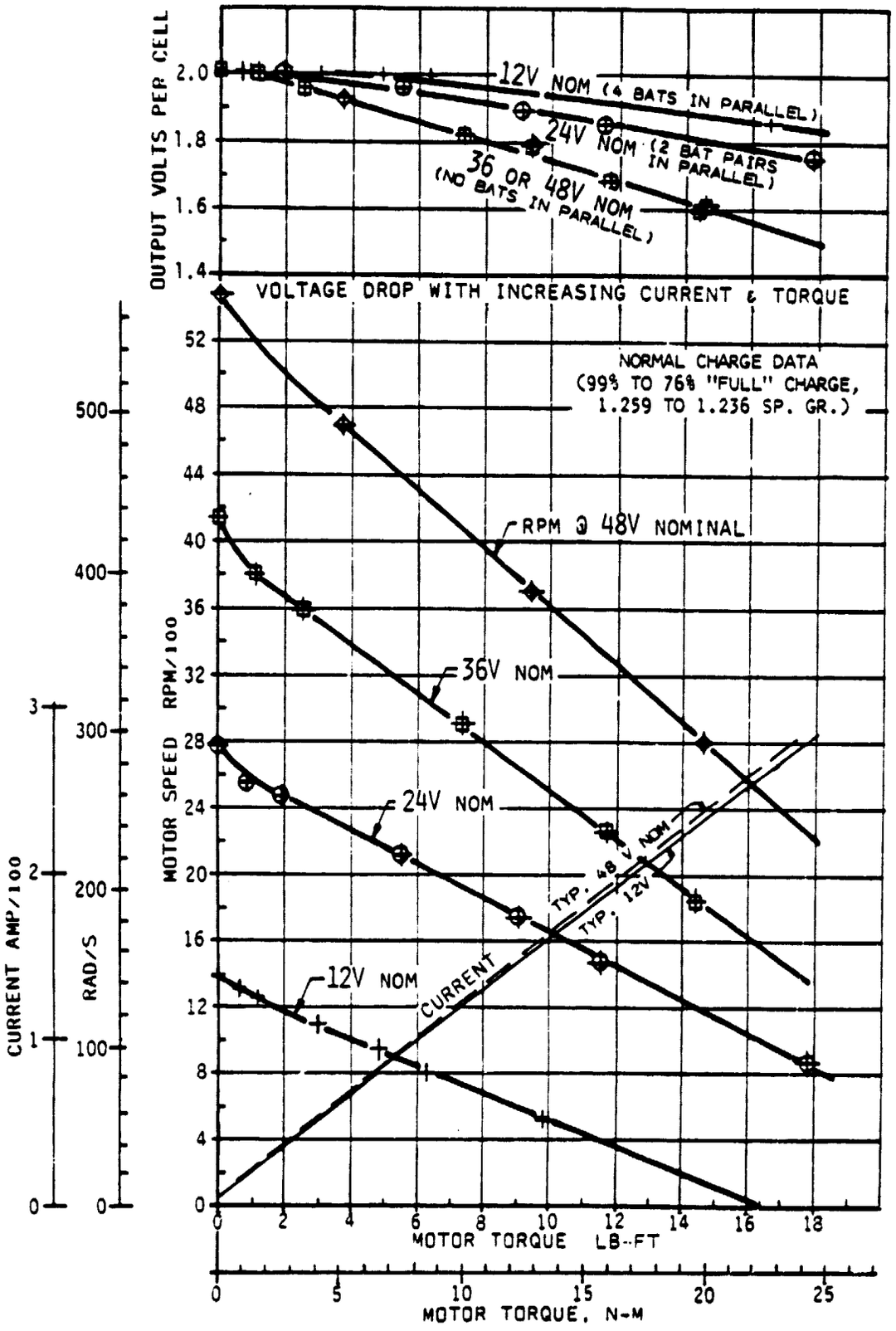

Figure 5-6 Permanent Magnet Motor Characteristics on Battery Power with Voltage-Switch Control

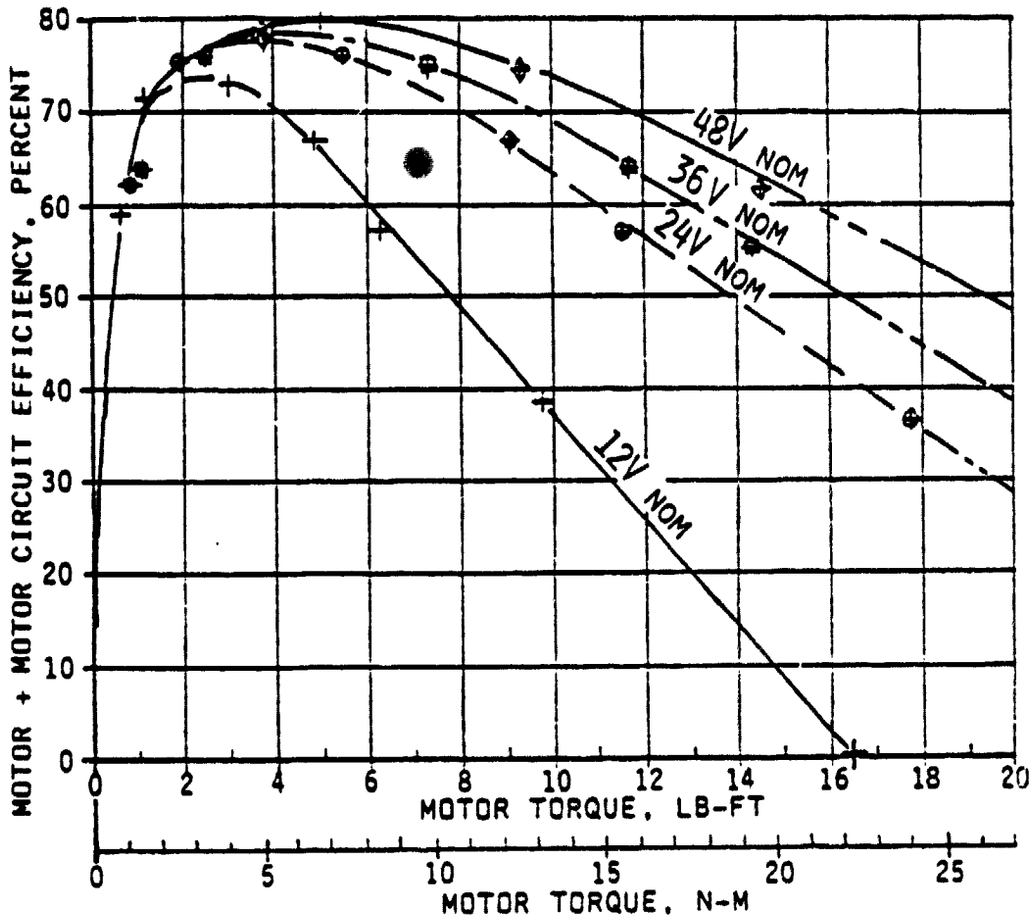

Figure 5-7 Motor Plus Motor Circuit Efficiency – Voltage-Switched Permanent Magnet Motor

during the tests of the system having a higher state of battery charge. The resulting speed versus torque curves also indicate a higher speed reflecting the comparatively higher voltages. These results indicate that the "surface charge" effects of a brief but incomplete recharge can be relatively lasting in their effect. A partial recharge, in other words, can, for a modest period at least, appreciably improve the performance of a battery powered system without having greatly changed the state of battery charge.

5.3 Comparison of Series and PM Motor for Traction Use

The previous motor efficiency versus torque curves did not provide a direct comparison of the two motors since they were designed for different speeds. By plotting efficiencies versus output power, in Figure 5-9, direct efficiency comparisons are shown. These curves show the PM motor to have higher efficiencies and wider useful power ranges at both of the lower voltage settings, but that the series motor excels at the higher and more important voltage settings. The limited useful power range at low voltage settings is emphasized by the closed-loop, return-to-zero trends of each curve.

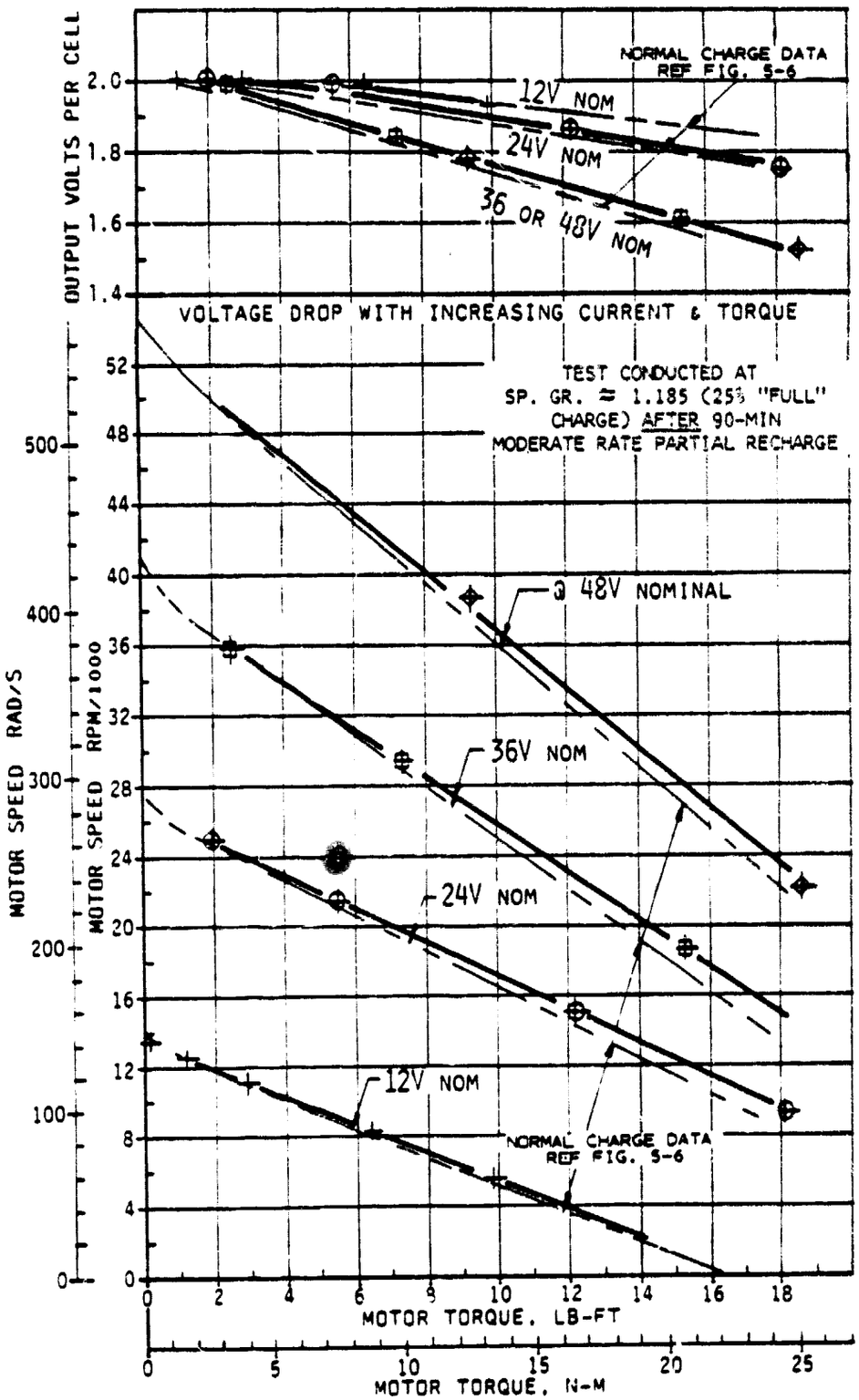

Figure 5-8 Partially Recharged Low Battery Performance — Permanent Magnet Motor with Voltage-Switch Control

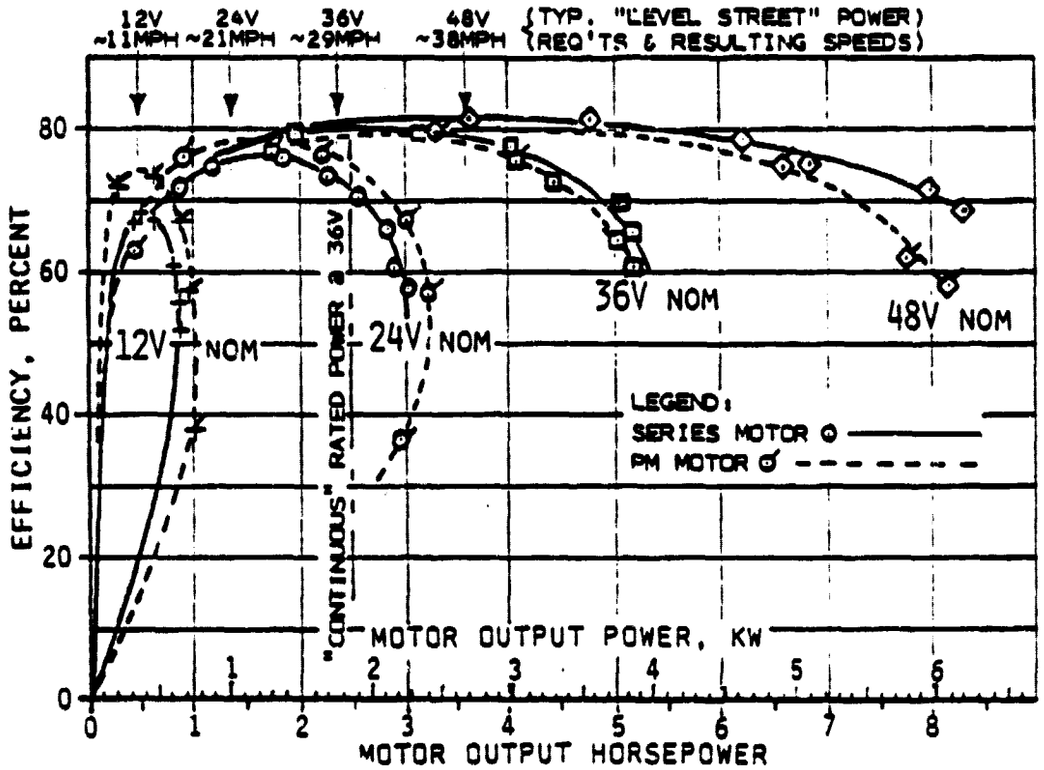

Figure 5-9 Comparative Efficiency of Series and PM Motors on Battery Power with Voltage-Switch Control

Figure 5-9 also illustrates the significant advantage of the 48 volt nominal setting, compared to a maximum of 36 volt nominal, in handling the temporary high torque, high power needs for acceleration and brief steep grades. The typical steady-state "level street" power requirements of the program's road test vehicle, at the optional speed or voltage settings, is shown at the top of the figure. Near maximum efficiencies, at steady state and somewhat beyond, are indicated for each setting.

For many vehicle traction applications the PM motor has a disadvantage due to its "constant slope" or "straight line" speed versus torque curves (ref. Figures 5-6 and 5-8) compared to the varying slope curves of the series motor (ref. Figures 5-1 and 5-4). This disadvantage is especially noticeable in EVs using a simple, single-speed-ratio drive train, as does the road test vehicle of this program. With a series motor in an EV, level road cruising occurs at the lower torque values where the speed versus torque curve is comparatively steep. When additional torque is required, as on upgrades, the speed slows appreciably so that power requirements and energy drain increase at a moderate rate only. As the EV's torque requirements continue to increase the series motor torque curves flatten to typically slow the rate of increasing power. In simpler terms, the characteristic speed versus torque output of a series motor is similar to the speed versus torque requirement of a road vehicle. The characteristic speed versus torque output of the PM motor does not match an EV's needs as conveniently.

Figure 5-10 illustrates, for this program's road test vehicle installations of the two motors, how differently the series and PM motor respond to increases in required torque. For the comparative road tests of this program (ref. Section 7), the motor-to-wheel speed reduction ratios were chosen primarily to provide comparable cruise speeds (and therefore comparable cruise power needs) when the controls are set for maximum speed, meaning ripple-free DC at 48 volts nominal. Performance was additionally confirmed as acceptable and comparable near the maximum design requirement of a 20% up-grade.

With the PM motor, the steady-state power required increased rapidly with small increases in grade slope but peaked at 15% grade. Such a response (good for maintaining nearer constant speed during moderate climbs) is more appropriate for EVs having a drive train with two or more speed reductions; permitting down-shifts for the steeper grades. The series motor, by contrast, required a more desirable (at least for single-speed-reduction drives) moderate increase in power with increasing grades over the full design range.

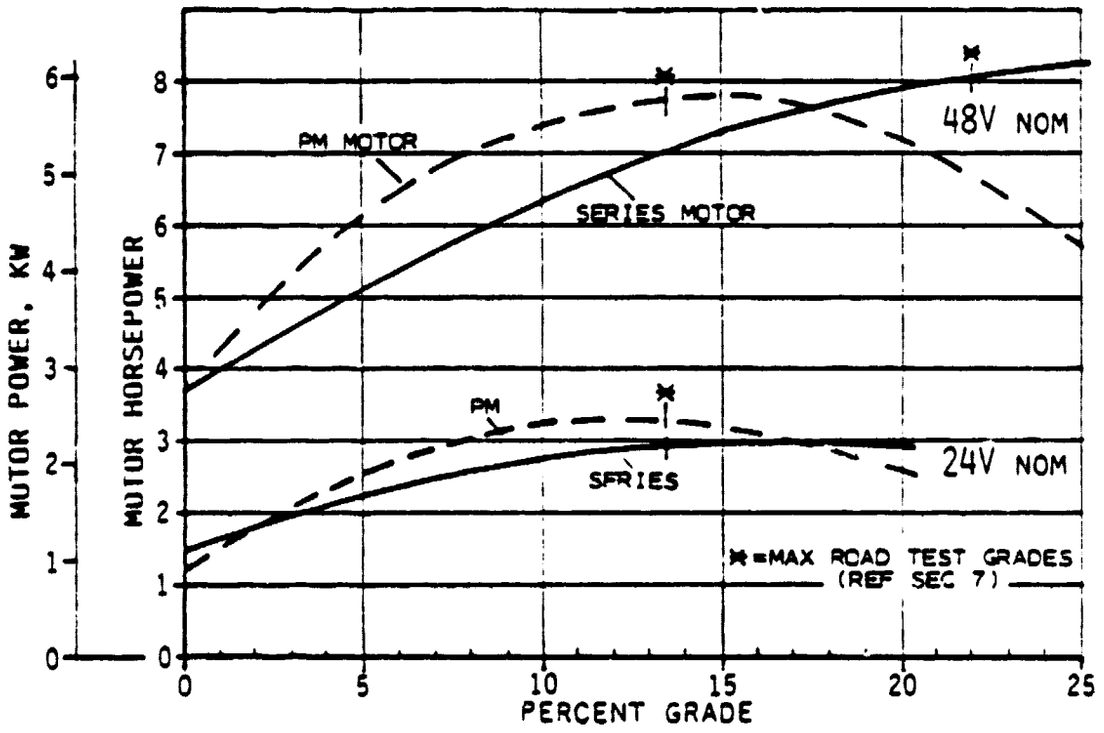

Figure 5-10 Power Requirements of EP-10 Road Test Vehicle For Steady-State Climbs of Varying Grade

5.4 Power Circuit Losses

The motor/controller/battery system performance data shown and discussed in this section has included the voltage drop effects on speed and motor performance but not the battery voltage drop effects on overall system efficiency. The voltage drop due to internal resistance of the batteries, as well as the voltage drop in the battery inter-connections and between the batteries and voltage switch, represent additional energy losses that need to be considered. The motor efficiency data just presented, however, did include voltage drop losses in the reverse and "throttle" contactors, as well as the conductors between the motor and the shunt or voltage switch. The sum of all of these voltage drops accounts for an appreciable energy loss and needs to be considered in this or any other EV power circuit. For this reason, these numerous specific voltage drops were carefully measured and recorded as presented here.

Figure 5-11 is a repeat of the motor circuit portion of the power circuitry. Shown at designated terminal points are labels A through R to identify particular segments of the power circuit. The circuit labeled C - D, for example, represents a master switch and the voltage drop between the attaching bolts at C and D was measured to determine the resistance of that (closed) switch. In a similar manner all circuit elements between G (at the shunt) and B (at the minus lead terminal of the voltage switch) represent those elements whose combined voltage drop is included in the motor circuit efficiency data previously shown.

Table 5-1 tabulates the resistance of the various circuit segments indicated in Figure 5-11. The table also separates and subtotals the resistances in the contactors involved. the numerous conductors (including their swaged or soldered-on terminals) and other components such as the master switch and shunt. Rather surprisingly, more than one half of the total resistance is in the three contactors in the circuit, with a large fraction of this due solely to the reverse contactor. This reverse contactor, as indicated in the note portion of the table, experienced a (presumably contact-point) resistance increase by a factor of approximately 7 during a 9-month period of intermittent EV operations. Presumably this contactor (which, along with the motor, represented essentially "unsprung" weight in the vehicle suspension) was adversely affected by the high accelerations it experienced perpendicular to its solenoid axis.

Power circuit components not covered in Table 5-1 include the voltage switch itself as well as the 8 conductors between the voltage switch and the 4 individual batteries. The measured resistance data for these components is shown in Table 5-2. Due to the voltage-switch series/parallel function, the 8 battery-to-switch conductors operate partly in parallel when the nominal setting is 24 or 12 volts, so halved or quartered accordingly. This effect is indicated in the table. The battery to switch conductors were of No. 2 copper cable (which has a nominal handbook resistance of .000159 ohm per foot) and had an average length of

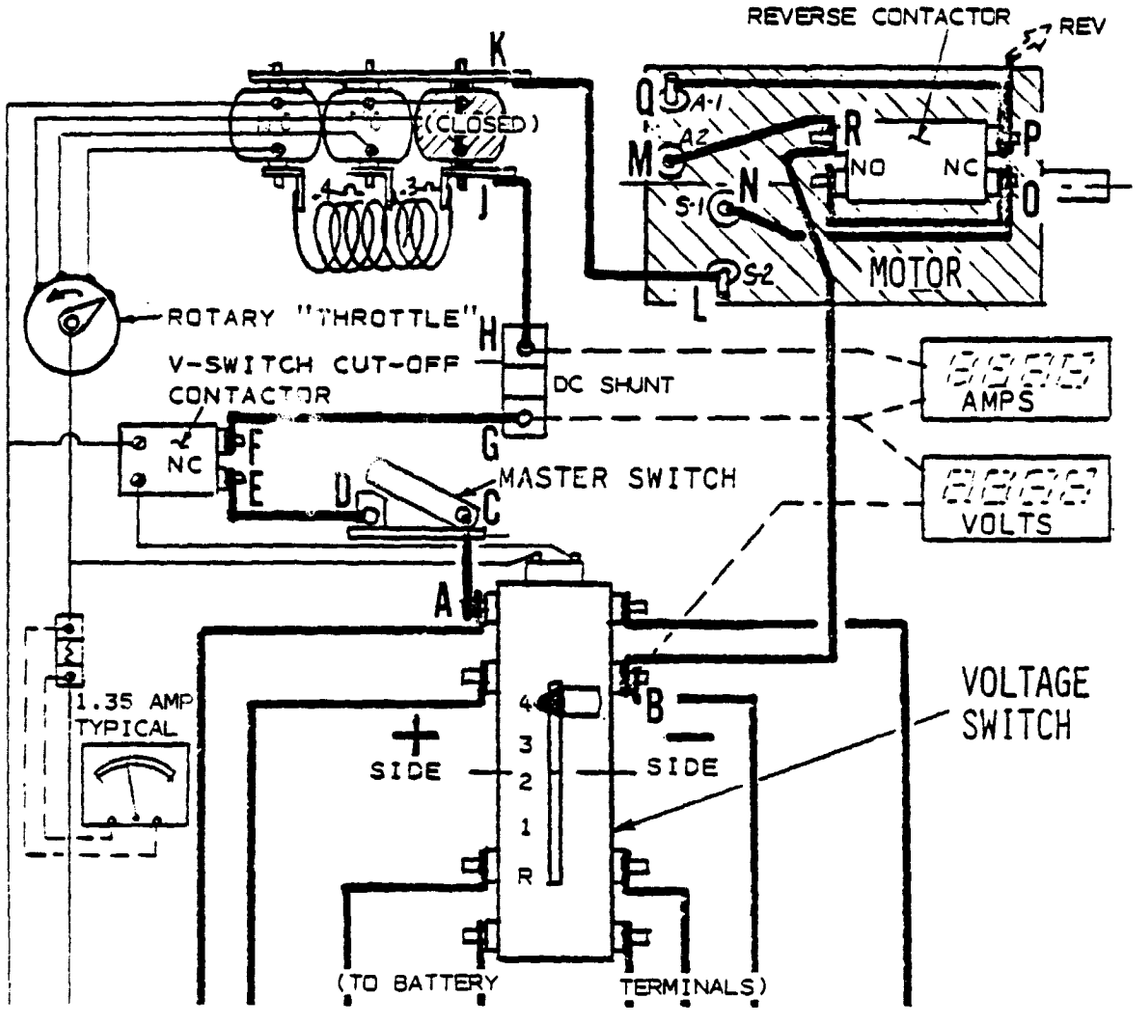

Figure 5-11 Motor Circuit Segment Schematic with V-Switch Control

Table 5-1 Sources of Motor Circuit Resistance

CIRCUIT SEGMENT (REF FIG. 5-9)	SEGMENT RESISTANCE (OHM)	RESISTANCE BREAKDOWN BY COMPONENT					
		CONTACTOR		COND'R & TERMINALS		OTHER	
		SUB-SEGMENT	RESIST. (OHM)	SUB-SEGMENTS	RESIST. (OHM)	SUB-SEG. & NAME	RESIST. (OHM)
A - G	.00177	E - F	.00114(1)	A-C, D-E & F-G	.00060	C-D M. SWITCH	.00003
G - L	.00220	J - K	.00026(2)	H-J & K-L	.00161	G-H SHUNT	.000332
N - Q	.00346	O - P	.00327(1)	N-O & P-Q	.00019	-	-
M - B	.00095	-	-	M-R & R-B	.00095	-	-
TOTALS	.00838 (100%)		.00467 (56%)		.00335 (40%)		.00036 (4%)

NOTES: (1) THESE COMPARATIVELY HIGH-CYCLE-LIFE, EXPENSIVE, NORMALLY CLOSED (NC) CONTACTORS AVERAGED R ≃ .00048 OHM WHEN NEW; SEE RELATIVE SELDOM USE (ESP. O-P UNIT). (2) THESE LOWER-RATED, CHEAPER CONTACTORS AVERAGED .00030 OHM WHEN NEW, WITH READINGS AS LOW AS .00015 OHM AFTER A BRIEF PERIOD OF CYCLING.

Table 5-2 Battery Conductor and Voltage-Switch Resistances

VOLTAGE SETTING	BATTERY-TO-SWITCH CONDUCTORS					VOLTAGE-SWITCH		
	NO. USED	AVERAGE R (Ω)	PARALLEL PATHS	FACTOR	EQUIVALENT R_{TOT} (Ω)	SERIES PATHS	AVERAGE R (Ω)	EQUIVALENT R_{TOT} (Ω)
48V	8	.00053	0	8	.00424	3	.00032	.00096
36V	6	.00054	0	6	.00324	2	.00032	.00064
24V	8	.00053	2	8/2	.00212	4	.00016	.00064
12V	8	.00053	4	8/4	.00106	6	.00016	.00096

approximately 37 inches. The measured resistance shown in the table can be closely approximated by using the handbook resistance value and adding .00003 ohm for each well-crimped or soldered terminal and its tight-nut connection.

The internal voltage switch resistances are seen to be relatively low. This is because this switch was designed with relatively large bus bar stock and flexible strap conductors and utilized silver plated contact surfaces.

The total resistances within the voltage switch power circuit, which combines the resistance of all of the above tabulated circuit elements and segments, is shown in Table 5-3. As indicated by the loss column at the right, significant percentages of the battery energy can be dissipated in the circuit components even when they are carefully designed and selected to minimize such losses.

Table 5-3 Total Power Circuit Losses with V-Switch Control

NOMINAL VOLTAGE SETTING	RESISTANCE OF CIRCUIT COMPONENTS (OHMS)						PERCENT LOSS AT 100 AMP
	CONDUCTORS BAT→V-SW.	CONDUCTORS V-SW→MOT.	VOLTAGE SWITCH	SHUNT & M. SW.	CONTAC-TORS	TOTAL	
48V	.00424	.00335	.00096	.00036	.00467	.01358	2.83%
36V	.00324	"	.00064	"	"	.01226	3.41%
24V	.00212	"	.00064	"	"	.01114	4.64%
12V	.00106	"	.00096	"	"	.01040	8.67%

NOTE: ADDITIONAL 12V CONTACTOR HOLDING COIL & SWITCH CURRENT AVERAGES 1.35 AMP (16 WATTS)

5.5 Circuit and Battery Loss Effects on Motor Performance

DC motor performance data provided by many manufacturers is based upon the motor terminals being supplied a constant voltage, usually of one value only. Some manufacturers, if the motor is intended primarily for operating with batteries, provide performance data based upon the "drooping" voltage-vs-current characteristic of a particular battery set. In either case the provided data, by itself, is inadequate for EV performance engineering, since the manufacturer's data has not incorporated the effect of the EV's power circuit resistance nor that of its particular battery pack. Either above type of data, however, will serve as a starting point to calculate the vehicle-installed performance of the motor.

For performance prediction purposes the most important changes due to system resistances occur in the motor speed-vs-torque data. Once this new data is attained, it is a simple further step to determine new efficiency curve data and, if desired, data for a new power curve.

Figure 5-12, which was provided for series motors of the model tested, is an example of motor performance data as typically provided by the manufacturer. Figure 5-13 is an expanded set of performance data, as predicted for the motor/controller/battery system used for this test program. The 36 volt nominal RPM curve, which incorporates the effect of both the power circuit and battery resistance, is seen to depart significantly from the constant 36 volt curve. In addition, for this control system, performance data for the other nominal voltages was required. By comparison with Figure 5-1 and others, these predicted curves are seen to closely match those of the actual dynamometer tests.

Having a speed versus torque curve and a current versus torque curve for a given DC motor design, as in Figure 5-12, most of the additionally desired speed, power, and efficiency data can be determined — assuming that one has additionally been told (or can measure) the resistance of a motor's armature circuit (and field circuit, if it is in series with the armature). For a given motor design, the current at a particular torque remains constant and independent of voltage; accordingly, when torque of the motor is known, the motor current is also known or can be determined by reading the value from a curve. The motor speed, N, under a new set of voltage and system resistance conditions can be determined by using the following equation:

$$N_2 = N_1 \frac{E_{OC(2)} - I(R_{B(2)} + R_{C(2)} + R_A + R_F)}{E_{T(1)} - I(R_A + R_F)} \qquad \text{(EQ 5.1)}$$

where N_2 is the new speed to be determined; N_1 is the known motor speed at current I when operating under conditions (1) for the performance data provided; $E_{OC(2)}$ is the open circuit voltage under the new (2) conditions; $E_{T(1)}$ is the motor terminal voltage under the initial (1) conditions; R_A is the resistance of the motor's armature and brushes, R_F is the resistance of the motor field; $R_{B(2)}$ is the effective internal resistance of the battery under the new (2) conditions; and $R_{C(2)}$ is the total resistance of all power circuit components between the battery and motor for the new (2) conditions.

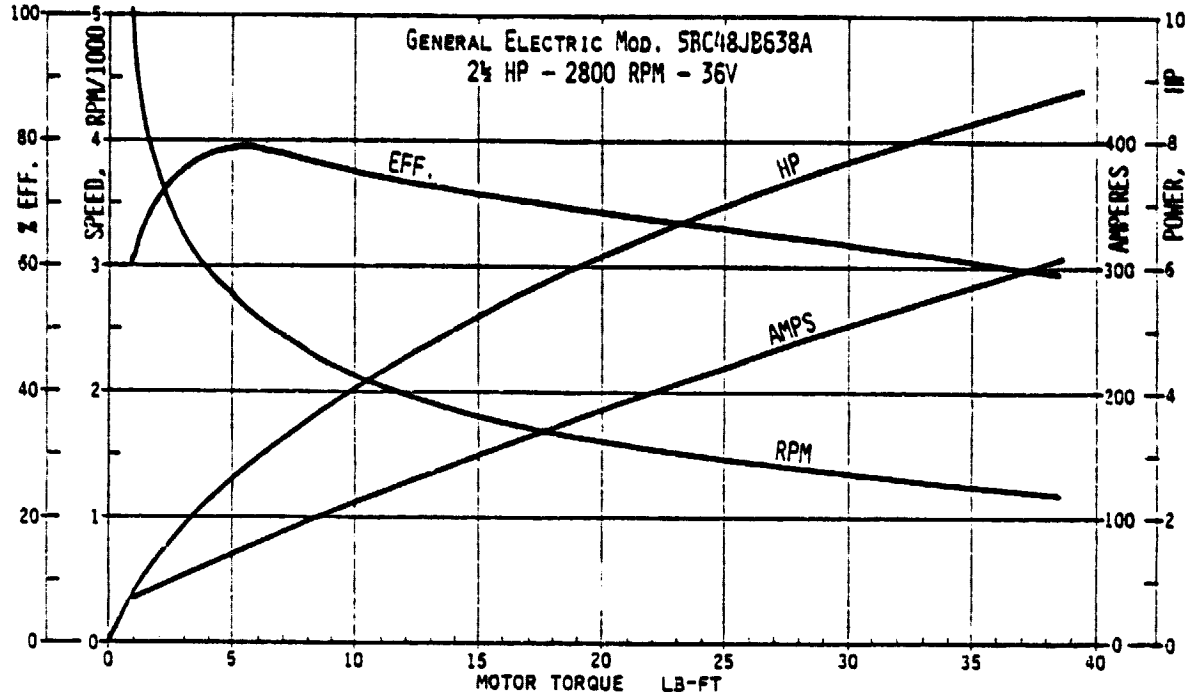

Figure 5-12 DC Motor Performance Data Typically Provided by Manufacturers

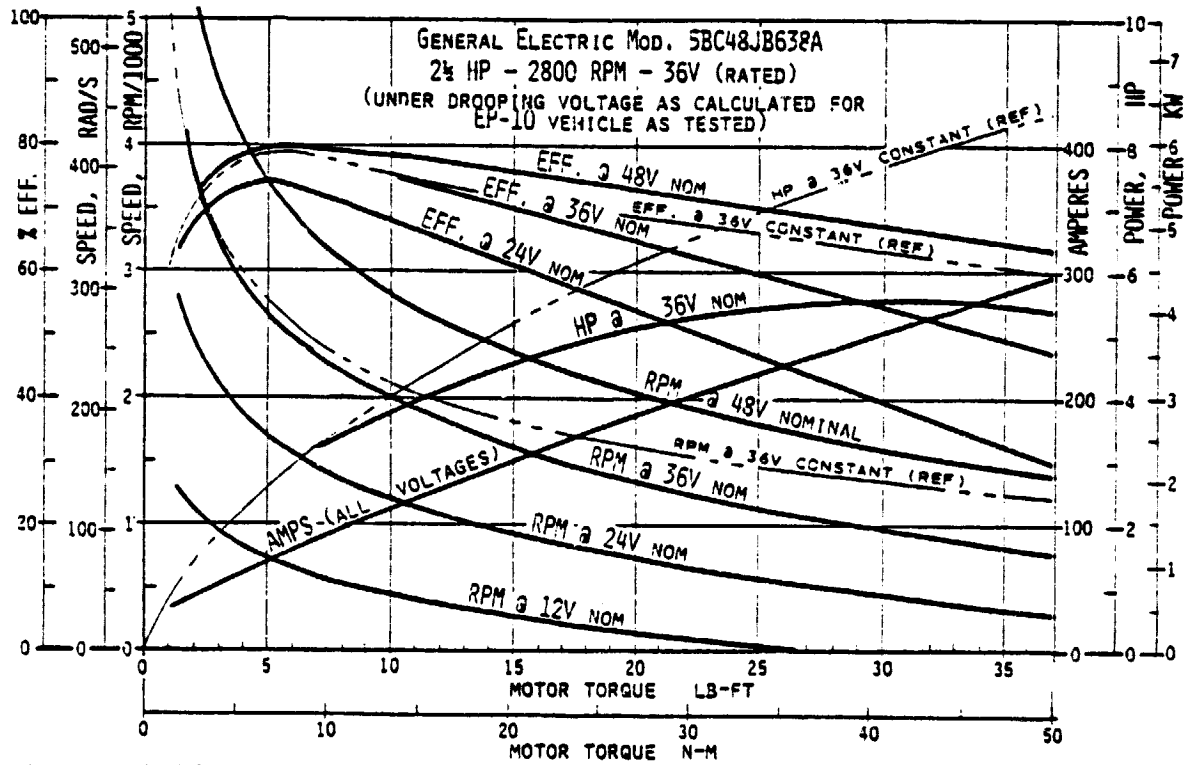

Figure 5-13 DC Motor Performance Data Modified and Expanded to Show Installed Performance for a Particular EV

If the field coils of the motor are not in series with the armature (for example, if a shunt motor or a PM motor is used) the resistance R_F drops out by equaling zero.

When the motor performance data provided are based upon testing or operating at a constant voltage, the $E_{T(1)}$ in equation 5.1 is simply that voltage value (e.g., for Figure 5-12 calculations $E_{T(1)}$ became 36 volts). When the performance data provided already reflect the drooping voltage of a battery energy source, the new speed equation becomes:

$$N_2 = N_1 \frac{E_{OC(2)} - I(R_{B(2)} + R_{C(2)} + R_A + R_F)}{E_{OC(1)} - I(R_{B(1)} + R_{C(1)} + R_A + R_F)} \qquad \text{(EQ 5.2)}$$

where $E_{OC(1)}$ is the open circuit voltage value used to prepare the provided (1) performance data; and $R_{B(1)} + R_{C(1)}$ make up the actual or assumed total resistance of the battery and conductor circuit for the provided (1) data. (If not stated with the performance data provided, the manufacturer can provide the battery resistance used or assumed. Similarly, a telephone call will usually produce resistance values for a given motor's armature and field circuits.)

Open circuit voltage values for lead-acid batteries, when charged, are very near 2.08 volts per cell. Therefore, a nominally 6V battery will have an open circuit value very near 6.25 volts; a nominal 12 volt battery near 12.5 volts, etc. Four 12 volt batteries in series, as in much of this test program, when labeled 48 volt nominal provide an open circuit value of 50 volts.

Lead acid battery resistance can vary considerably, depending on the battery configuration, size and intended use. Fortunately the typically used EV battery, of the golf-car or GC-2 group, is said to have an effective resistance essentially the same for all manufacturers and near .003 ohm per 6 volt battery (".0028 to .0030 ohm at full charge and .0030 to .0033 ohm at discharge"). Twelve of these batteries in series, for example, will have a combined effective battery resistance of about 12 x .003 or .036 ohm, not including resistance of the inter-battery connectors. If series-parallel voltage switching is used, it is important to realize that two factors reduce the effective battery resistance when switched to a lower battery output voltage. For example, if the 12 battery set mentioned above is switched to 6 parallel connected pairs in series, this connection provides 2 current paths through the batteries and 1/2 as many batteries in series. The effective resistance is then 1/4 the all-series connection or about .036/4 = .009 ohm.

The effective resistance of the 12 volt, group 27 deep discharge batteries used on this test program was less well known. Based upon some earlier tests on one make of battery, an effective resistance of about .036 ohm was calculated for 4 batteries in series or the nominal 48 volt setting, meaning .009 ohm per battery. For a 36 volt setting the battery resistance value used was then .027. For the 24 volt series-parallel setting, as discussed above, the resistance value became .036/4 or .009 ohm

effective. For the 12 volt setting, with another doubling of current paths and half as many batteries in series, the effective resistance became .009/4 or just over .002 ohm.

The additional important circuit resistance was the total of the numerous circuit component resistances in series for each nominal voltage. These numerous circuit components were discussed in Section 5.4 and their measured resistance totals tabulated in Table 5-3 (the resistances estimated for the calculations were similar).

The motor armature and field resistances were measured on the actual motor used in the test program. The armature, plus its commutator brush resistance measured approximately .029 ohm. The field resistance measured .0117 ohm.

To calculate data points for the installed motor's performance at 48 volts nominal, for example, as discussed above, the effective battery resistance was .036 ohm, armature resistance .029 ohm, field resistance .0117 ohm and .0136 ohm was used for the remaining circuitry. Equation 5.1 then became:

$$N_2 = N_1 \frac{50 - I(.036 + .0136 + .029 + .0117)}{36 - I(.029 + .0117)} = N_1 \frac{50 - I(.0903)}{36 - I(.0407)} \quad \text{(EQ 5.3)}$$

By selecting a number of convenient current values and reading the original (N_1) speed values for each, a set of new speed values (N_2) was determined for plotting the 48 volt nominal curve.

To calculate motor efficiencies in the usual way it is necessary to know the voltage applied at the motor terminals. For this, the open circuit voltage is reduced by the IR voltage drop in the battery and circuit only, or:

$$E_T = E_{OC(1)} - I(R_{B(2)} + R_{C(2)}), \text{ OR}$$
$$E_T = 50 - I(.036 + .0136). \text{ FOR 48V NOM} \quad \text{(EQ 5.4)}$$

Having the terminal voltage values, efficiencies are calculated by the more readily available equation:

$$EFF. = \frac{T_{LB-FT} \times RPM}{7.043 \times E_T \times I} \quad \text{(EQ 5.5)}$$

Horsepower values are also calculated by a readily available equation:

$$HP = \frac{T_{LB-FT} \times RPM}{5252} \quad \text{(EQ 5.6)}$$

6/ SYSTEM PERFORMANCE WITH CHOPPER CONTROL

Performance tests using the electronic chopper controller were performed after tests with the voltage switch were completed. Ripple-free DC operation of both types of motors, accordingly, had already been dynamometer tested and their performance details illustrated. The early dynamometer tests using the chopper controller — including numerous partial tests during the dynamic instrumentation development and checkout — were performed with the permanent magnet (PM) motor.

6.1 The Effect of Added "Choke" Inductance

Before obtaining the detailed performance data for the PM motor using the chopper, the test program called for investigating the effect of adding series inductance in the motor armature circuit by means of a choke. Advice from engineers involved in the manufacture or use of chopper controllers varied. In general, it was implied that series motors typically have sufficient inherent inductance for suitable performance with a chopper but that PM motors, which have no field windings, should show significant improvements with the addition of choke inductance. The manufacturer of the chopper being tested, EVC, Inc., state in their literature, "The motor circuit inductance should be at least 0.5 millihenries." "With a PM motor," one engineer stated, "250 microhenries is a minimum and any addition up to 3 millihenries should help."

Four locally available chokes were selected to obtain a range of inductances approximating that mentioned above, while having relatively high current capacities and relatively low resistances. All of the chokes chosen were of laminated iron core construction. Table 6-1 describes the four initially selected and tested chokes as well as a fifth (numbered C-6) which was specially wound and introduced later in the program.

Table 6-1 Description of Test Program Chokes

ASSIGN. NO.	INDUCTANCE (MHY)	RESIST. (OHM)	WEIGHT (LB)	APPROX. SIZE W X D X H (INCHES)	CONDUCTOR GAGE & COILS
C-1	0.20[2]	.0027	5.0	3.8 X 3.0 X 3.0	#6, ~7-TURN
C-2	1.49[1] 1.32[2]	.0060	37	5.8 X 7.5 X 6.1	UNKNOWN
C-3	0.41[1]	.0040	34	9.0 X 4.5 X 9.0	"
C-4	3.00[1]	.0163	81	6.2 X 8.5 X 10.2	"
C-6	0.34[2]	.0025	5.9	4.4 X 3.0 X 3.2	#4, 12-TURN

REF. INDUCTANCE DATA ON TESTED MOTORS (NON-ROTATING DATA)
OHIO P.M. MOTOR : ARMATURE (& COMMUTATOR) 0.024 MHY.
G.E. SERIES MOTOR: ARMATURE 0.018 MHY; FIELD 0.005 MHY;
ARM. & FIELD IN SERIES: 0.037 MHY (FWD.), 0.024 MHY (REVERSE)

NOTES: [1] NAMEPLATE RATING. [2] MEASURED BY GEN. RADIO LCR BRIDGE.

Screening tests were performed to compare the performance, efficiency, and current and voltage waveforms of the permanent magnet motor/chopper/battery system — when using no choke and with each of the four chokes having widely varying characteristics. These tests were performed at two power settings; one representing low speed cruise of the road test vehicle (approximately 36% chopper duty cycle and 3.2 lb-ft motor torque) and one intermediate speed on a moderate grade condition (approximately 52% duty cycle and 7.4 lb-ft torque). The resulting changes in efficiency are shown in Figure 6-1. As indicated, even the small, 5 lb choke (C-1) showed an improvement in efficiency of 4 to 5 percentage points while the larger C-3 and C-2 chokes added a few additional percentage points of efficiency. The largest and highest inductance choke (C-4)

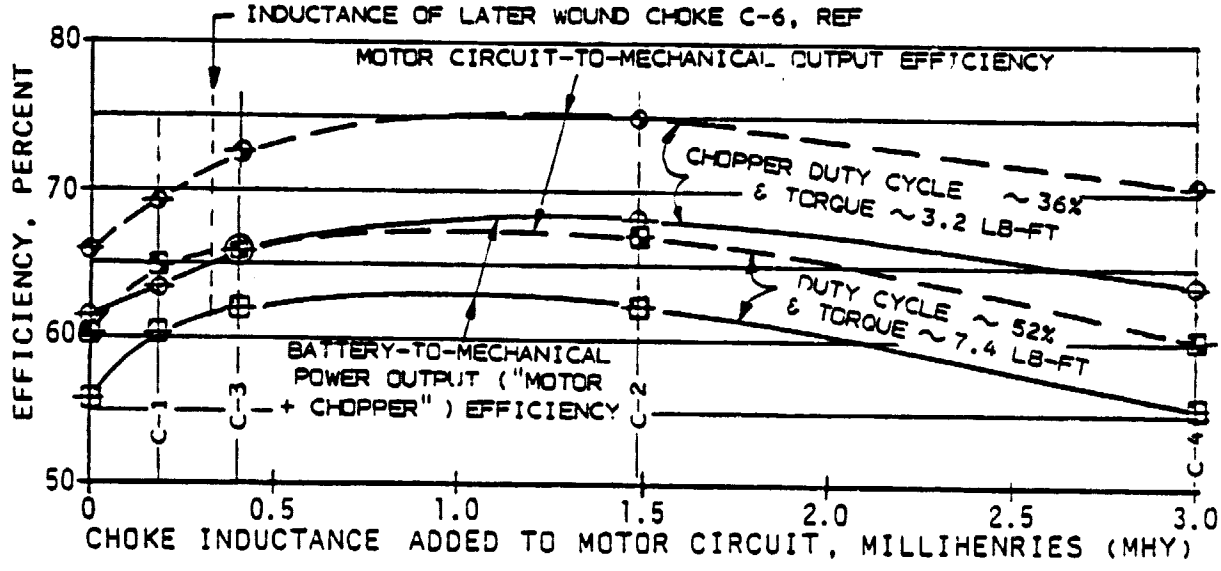

Figure 6-1 Efficiency Data Resulting from Choke Screening Tests

caused an efficiency drop to approximately that of the motor alone; doubtless due in large part to the considerably higher resistance in its winding. As a result of this screening test, the small choke C-1 was chosen to use with the PM motor during its chopper-controlled testing. Chokes C-3 and C-2, although they provided the highest system efficiency, were rejected because of their high weight (34 and 37 lb or 15.4 and 16.8 kg respectively).

It should be recalled that the chokes initially tested and discussed above were chosen from ready-built, available units primarily for their combined range of inductance. After a study of the comparative efficiency data and the explanatory oscilloscope traces, as well as preliminary tests of choke effects with the series motor, an improved choke (C-6) was wound on the same type and size of laminated core used for choke C-1. Nevertheless, none of the chokes tested were specifically designed nor were their core configurations chosen to best meet the inductance needs of the tested motor/circuit/battery/controller system.

It is understood that engineers competent in the analysis of power circuit impedance needs can, after some study, specify inductance characteristics – or perhaps added capacitance elsewhere in the circuit – to more readily define or converge on an optimum system.

The oscilloscope records of current and voltage waveforms made during the choke screening tests do much to explain the differences in efficiency. Figure 6-2 shows the oscilloscope records for the moderate speed, higher torque tests made as the inductance was increased from the no-choke test to that with the largest choke that still increased system efficiency. The change in the fluctuations of motor circuit current with each on-off cycle of the chopper, as shown in the sawtooth curves at the top of the motor circuit plots, illustrates a major cause of the lower efficiency when the circuit inductance is low. The motor circuit current excursion with no choke, for example, is seen to be some 280 amperes (since the current scale is 50 amp per graduation) while this excursion reduces to some 30 or 40 amperes with the large choke C-2. A marked reduction in acoustic noise was also evident as the circuit inductance was increased.

This reduction in current excursions is seen to also reduce the variations in motor circuit voltage; the motor circuit voltage plots becoming increasingly closer to "square waves" as the inductance increases. The added inductance also "flattens out" and simplifies the current and voltage waveforms in the battery circuit (note that the sign of the current in the battery circuit is reversed from that of the motor circuit, i.e., in the battery circuit an increase of current is downward). The battery circuit current, as well as voltage, approaches a square wave shape as the motor circuit inductance increases. It may also again be noted that in the battery circuit the voltage and current waveforms switch at essentially the same time, whereas in the motor circuit, current flows continuously while voltage switches "off" and "on". Accordingly, the determination of power (voltage times current) is appreciably simpler in the battery circuit than in the motor circuit, as previously concluded and discussed near the end of Section 4.

The detailed current, voltage and power values listed to the right of each of the oscilloscope plots are data recorded by the Sine dynamic instrument (with the power values approximately confirmed by the Clarke-Hess instrument). The efficiency data shown at the bottom of each photograph (and as used in the preceding Figure 6-1) was obtained by dividing the motor's dynamometer output power in watts by the battery circuit power indicated; accordingly, the efficiencies shown represent that of the motor and chopper combined.

Subsequent to the choke selection screening tests discussed above and early tests using the C-1 choke, additional tests were performed with no choke to determine the choke effect on performance through a more complete range of motor torques.

These specific no-choke tests were performed at 75% and 25% duty cycles only (at 100% duty cycle chopper action ceases and the over-

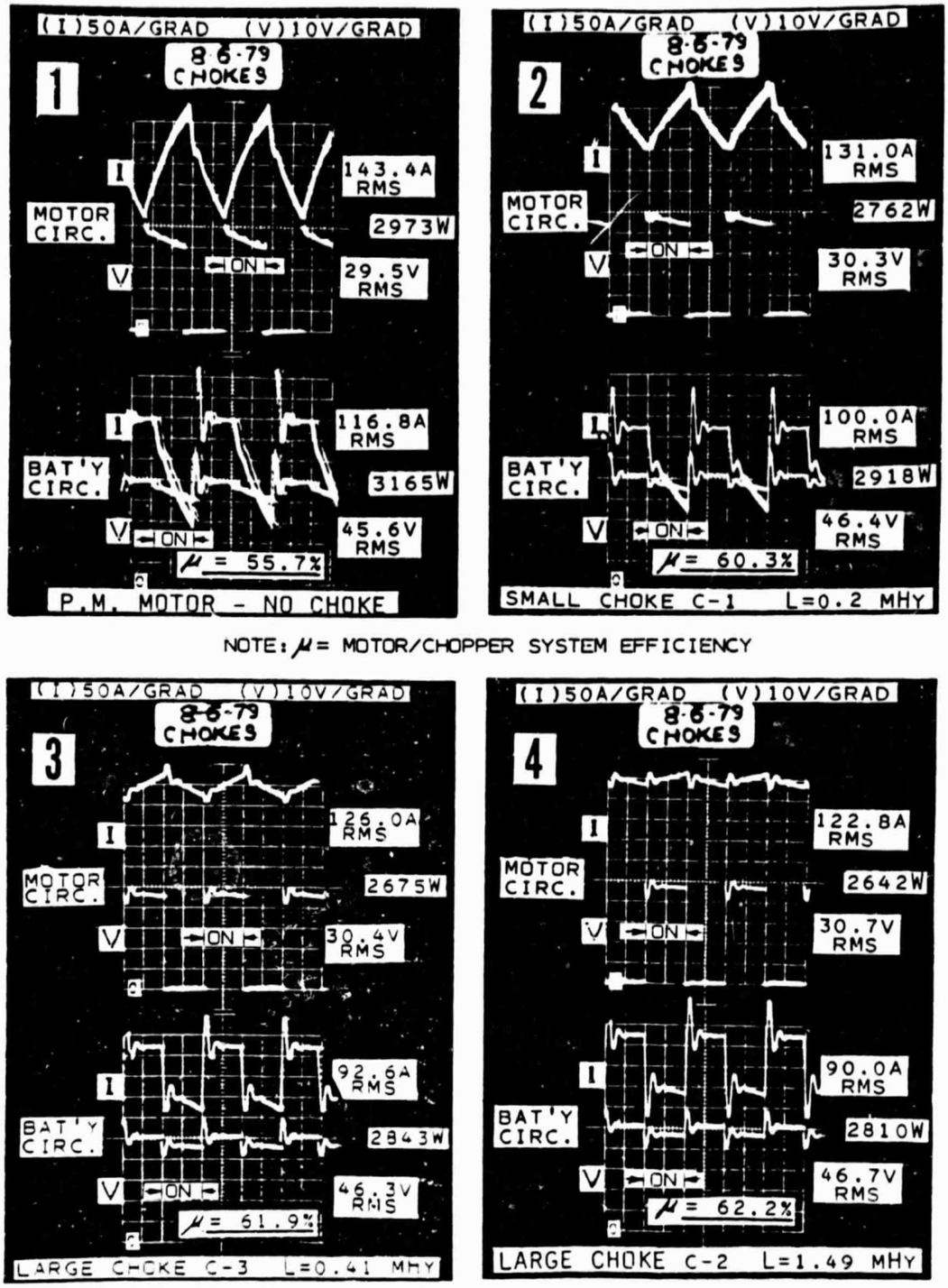

NOTE: μ = MOTOR/CHOPPER SYSTEM EFFICIENCY

Figure 6-2 Current and Voltage Waveforms, Power Values, and Motor/Chopper System Efficiencies as Varied by Added Motor Circuit Inductance (at 52% chopper duty cycle and motor torque 7.4 lb-ft)

all effect of added choke inductance is a loss of efficiency due to the added resistance of the choke windings). The result of this test is shown in Figure 6-3. As indicated here, the efficiency improvements caused by the added choke inductance decreased with increasing motor torque. At the higher torque and lower efficiency regions of the curves, the efficiencies without the choke were somewhat higher than with the choke.

After evaluating some of the unexpected results from added choke inductance in the PM motor circuit, it was decided to investigate the effect of added choke inductance with the series motor. Unexpectedly, considerable improvement in efficiency was indicated in the "low speed cruising" torque regime of the series motor. This led to some additional series motor tests with a small but improved choke (C-6) and to the use of this improved choke later during road tests with both types of motors. These added choke tests are discussed below.

6.2 Chopper Controlled System With Series Motor

The series motor performance when using a chopper controller (with no added choke inductance) is shown in Figure 6-4. For comparative

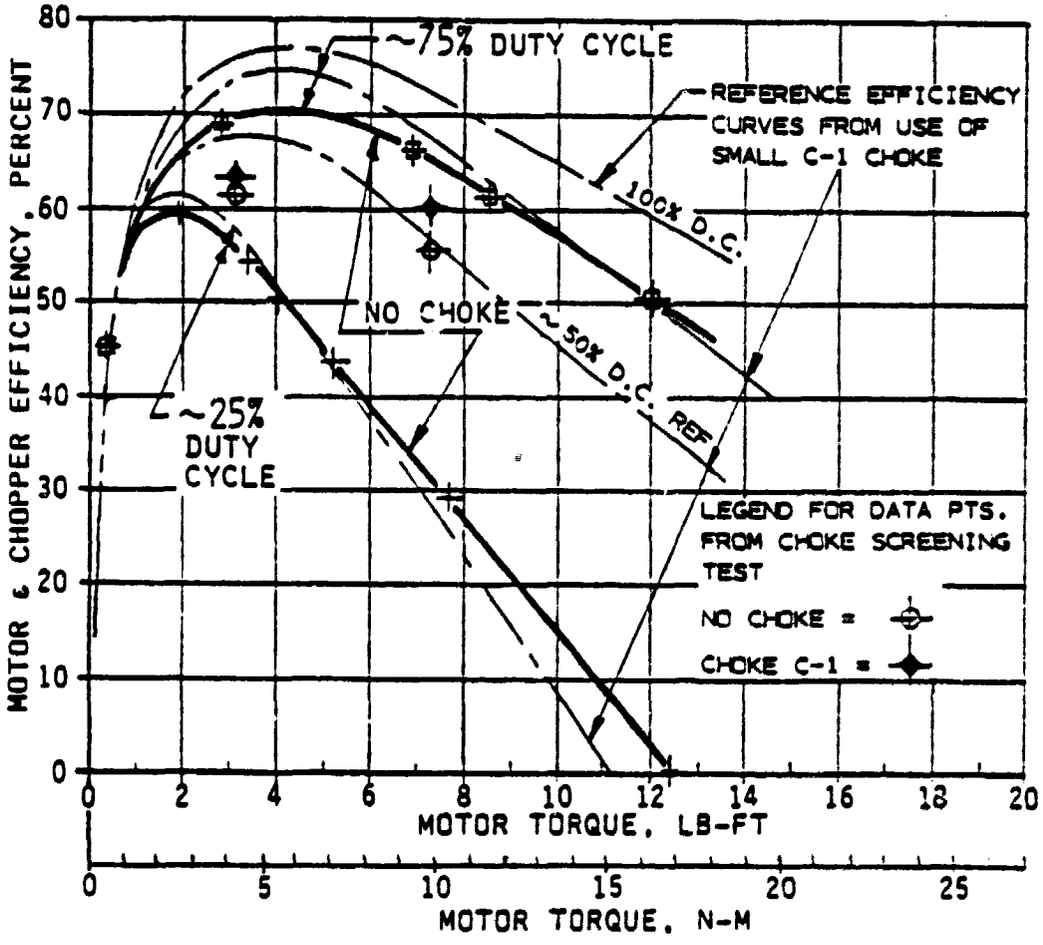

Figure 6-3 Effect of Small Choke C-1 on PM Motor Efficiency

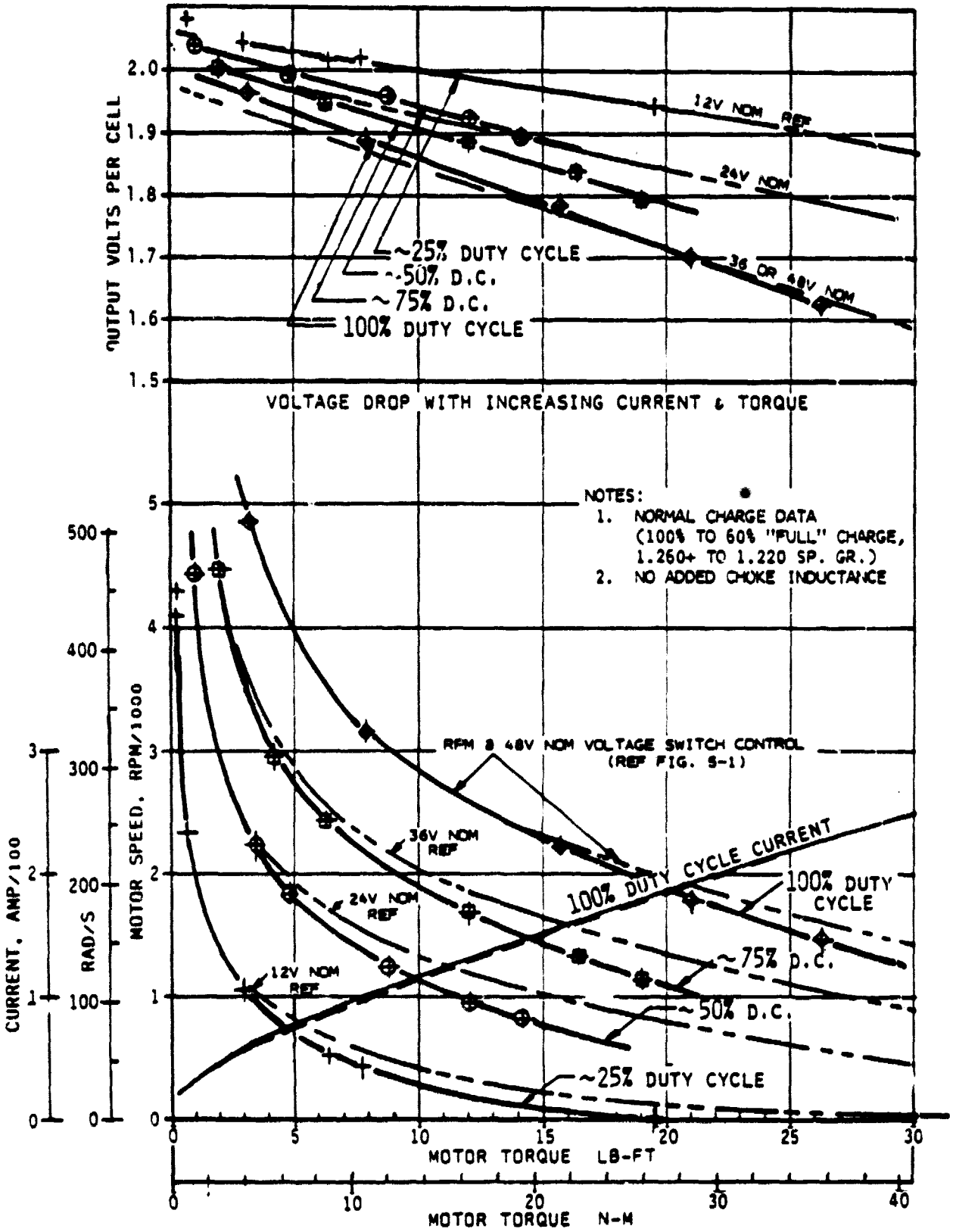

Figure 6-4 Comparison of Chopper Controlled and Voltage Controlled Series Motor

purposes the performance under the voltage switching control mode is shown as phantom line curves. The characteristic speed versus torque curves are seen to have a similar shape to those at roughly corresponding voltage settings, except that the speed at a given torque is noticeably lower. The upper plot, showing voltage drop versus increasing current or torque, is seen to show that the battery voltage drop is quite comparable for the two types of operation.

The efficiency of the motor and chopper system is shown in Figure 6-5. Again, the efficiency in operating with voltage switching control system is shown as phantom or reference lines. While the efficiencies determined at the several duty cycle settings are decidedly lower than those under the voltage switching mode at roughly comparable fractions of maximum voltage, it should be understood that these curves do not reflect comparable vehicle operating conditions. For example, with a voltage switching speed control system the driver might well elect to operate at a 24 volt nominal speed setting and operate through a relatively broad range of torques at that nominal voltage. With a chopper controller, on the contrary, if the chopper duty cycle is low, the torque will almost assuredly be low, since the driver will respond to a higher torque need with more throttle which means a higher duty cycle. If one

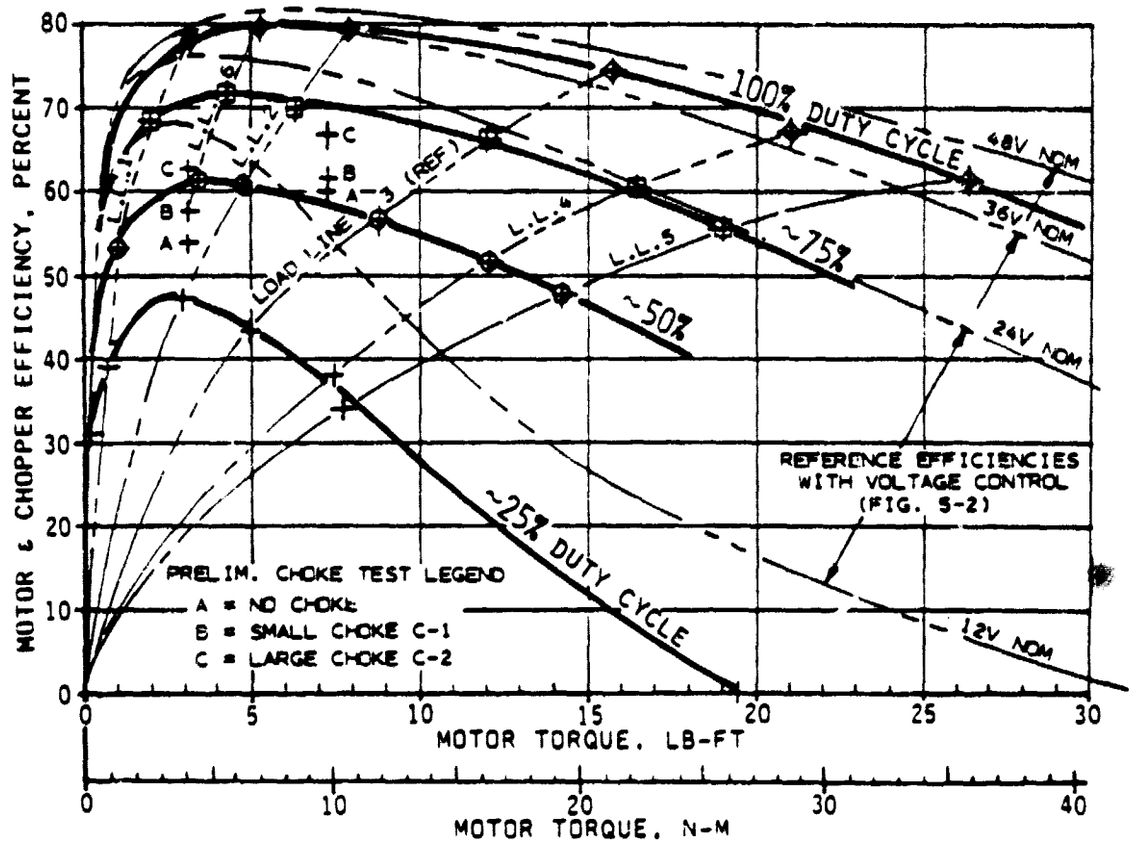

Figure 6-5 Chopper Controlled Series Motor Efficiency (without choke) and Preliminary Choke Test Results

assumes that the chopper controlled motor is geared to the vehicle drive train with an appropriately selected gear ratio, the vehicle would be expected to operate along one of the load lines indicated in the figure, or something similar, and not along a constant duty cycle line. During periods of acceleration and climb the throttle would often be fully "down" and the system would then operate along the 100% duty cycle line.

The preliminary choke tests using the series motor with chokes C-1 and C-2 resulted in the data points marked A, B and C on Figure 6-5. The several percentage point improvements noted in the preliminary tests indicated that additional choke tests with the series motor were desirable. This finding, combined with the previous PM motor choke test data, led to the preparation of a new, specially wound choke for additional tests. Choke C-1, which had been wound rather loosely and not stabilized by sealing the windings with electrical varnish, had developed an intermittent short presumably due to vibration. The new choke, numbered C-6, was wound on the same type of iron core used for C-1, but used a higher gage conductor and as many turns as the core could contain. Its measured inductance was 0.34 millihenry compared to approximately 0.20 for choke C-1, due to having 12 turns compared to 7. The resistance of choke C-6, however, was nearly identical to that of C-1 (ref. Table 6-1) due to its higher gage winding.

New series motor tests were performed using the new choke, C-6, added in series with the armature and field windings. The resulting increase in efficiencies over the lower torque range is shown in Figure 6-6.

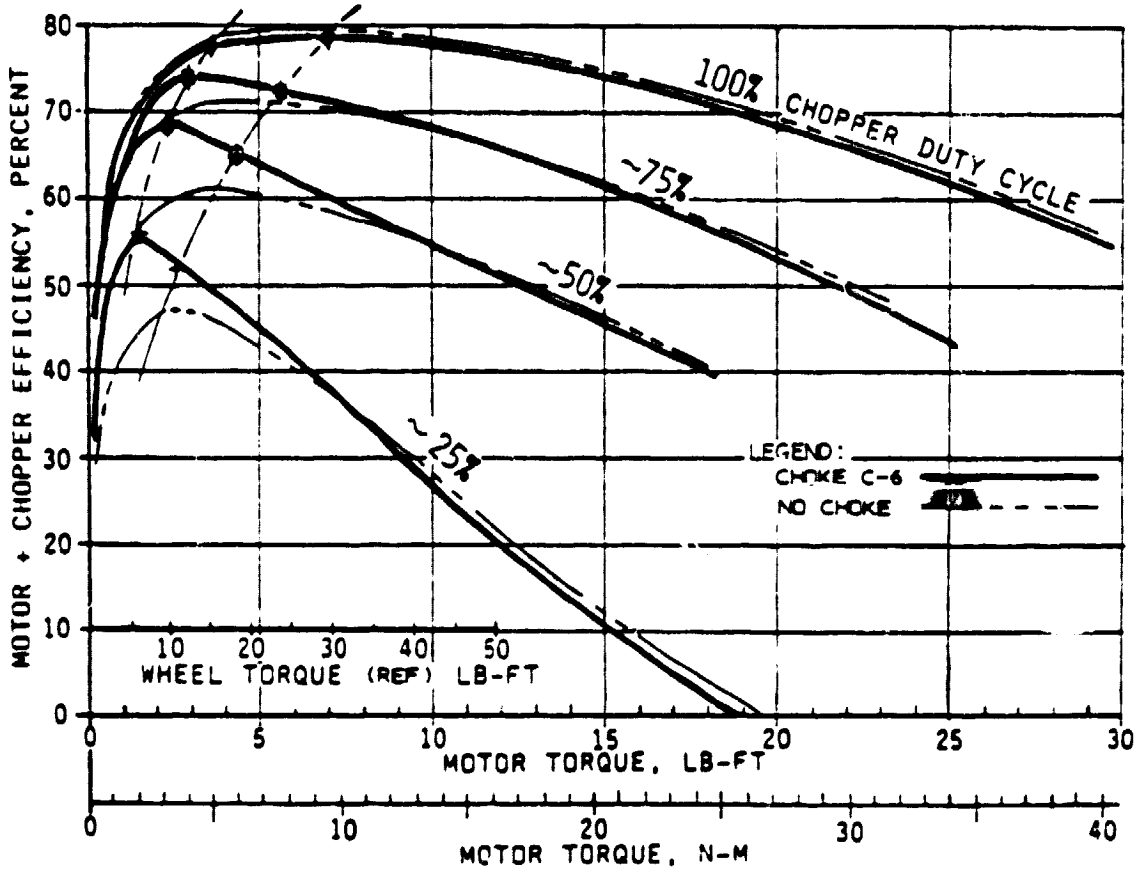

Figure 6-6 Chopper Controlled Series Motor Efficiency with Choke C-6

These tests were not expanded to the high torque regions so the curve differences at the higher torques are estimates based upon test data with the PM motor. The efficiency differences shown in the lower torque ranges, where efficiency is important for level-road, lower speed cruising, are rather significant. This choke, C-6, therefore, was used in all chopper-controlled road tests that followed.

Again, as in testing with voltage-switch control, tests were performed with a "low battery" to determine the reduced voltage effect on the motor speed torque curves and upon efficiency. The results are shown in Figure 6-7. The reduction of motor speed when using a nearly discharged battery is relatively comparable to that seen when under voltage switching control. Again, as shown in the upper plot, there is relatively little difference in the motor system efficiency between operating with a nearly charged or nearly discharged battery (the battery's discharge efficiency is, however, decidedly less due to its increased voltage drop as discharge is approached).

6.3 Chopper Controlled System With PM Motor

Rather surprisingly, the characteristic speed versus torque curves for the PM motor were found to change quite markedly when operating under chopped DC power. These differences are shown in Figure 6-8. It is noted that at 100% duty cycle (i.e., no chopping) the PM motor's typically straight line characteristic still exists with the speed being somewhat lower at a given torque, presumably due to additional voltage drops within the system. Under chopped power, however, as the percent duty cycle or "on time" decreases, a decided curve exists which approaches that of a series motor.

The upper plot of Figure 6-8, as with the series motor, shows that the battery voltage drop with chopper control is quite similar to that for voltage reductions of similar magnitude.

The basic efficiency data for the chopper controlled PM motor, using the earlier small choke C-1, is shown in Figure 6-9. As with the series motor, the efficiencies at the several percentage duty cycle operations are appreciably lower than those at comparable percentage voltage values. However, as previously discussed in connection with Figure 6-5, these efficiency curves for the two types of controls are not directly comparable.

As discussed in Section 6-2, a new and more effective choke, C-6, was prepared for use with the series motor and to use during the road tests. This new choke had almost exactly the same resistance as the previous choke C-1 but a measured inductance of .34 millihenry compared to .20 for the widely tested choke C-1. Using the data on efficiency versus choke inductance from Figure 6-1, the efficiency curves for the PM motor with choke C-6 were modified to show modest low torque improvements as indicated in Figure 6-10. No change was made to the 100% duty cycle curve since there was no circuit resistance change and there is no chopping

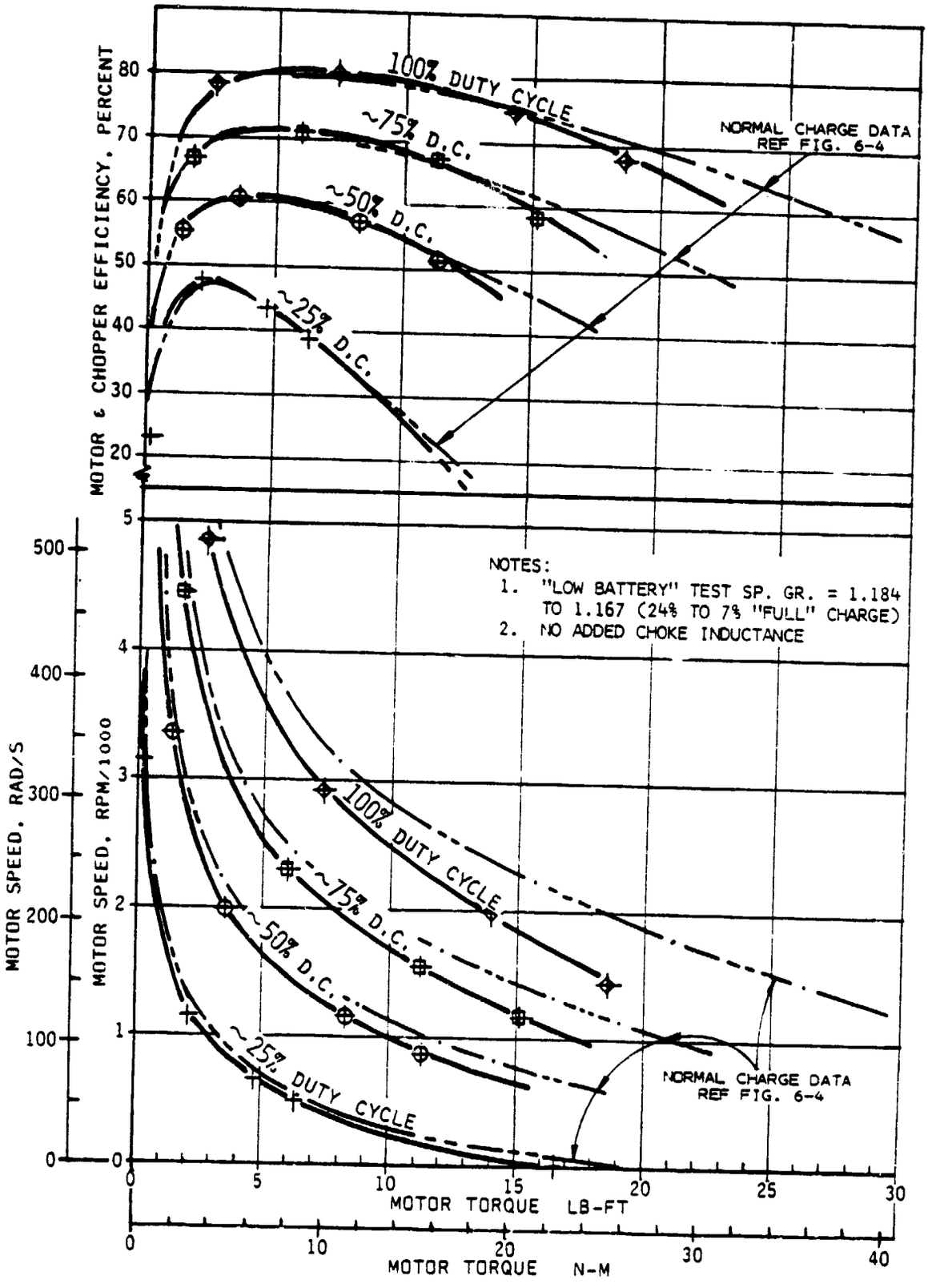

Figure 6-7 "Low Battery" Effect on Speed and Efficiency of Chopper Controlled Series Motor

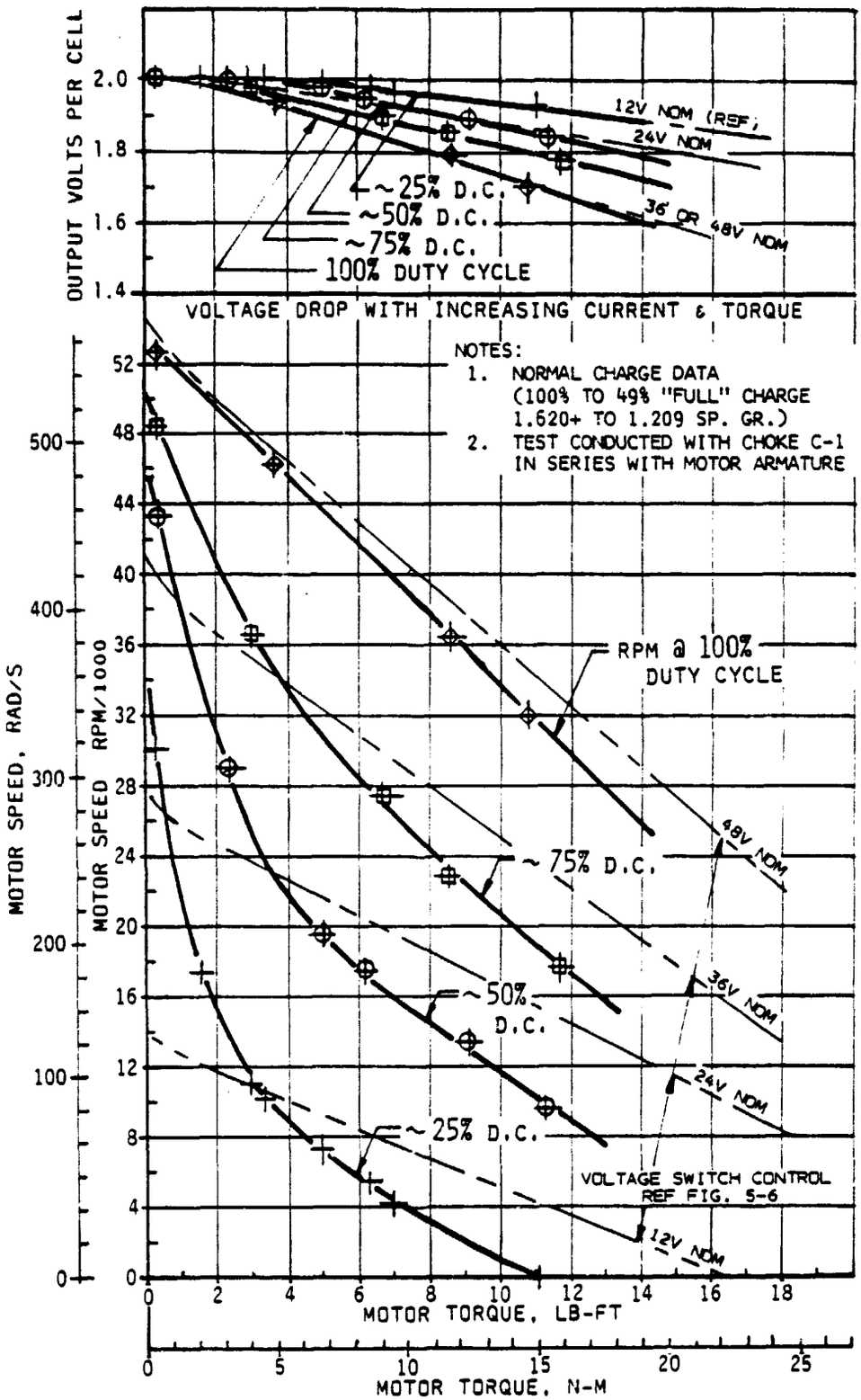

Figure 6-8 Comparison of Chopper Controlled and Voltage Controlled Permanent Magnet Motor

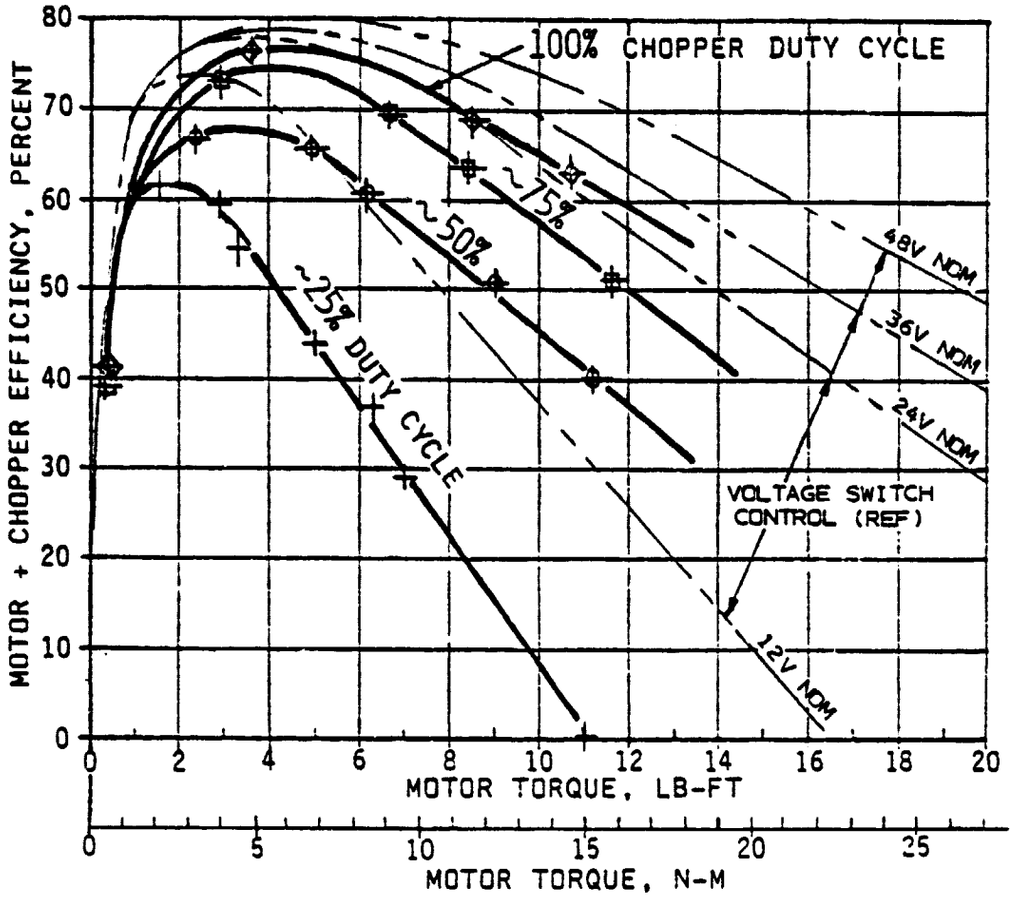

Figure 6-9 Efficiency of Chopper Controlled Permanent Magnet Motor with Choke C-1

at that duty cycle. The primary purpose of Figure 6-10 was its use in estimating the efficiency of the road test vehicle discussed later in Section 7.

6.4 Chopper Power Consumption

In discussing the dynamic instrumentation comparisons and precision investigations in report Section 4, some data were presented on power consumption of the chopper itself. Much of these data were determined by seeking "small differences in large numbers" and all of it involved considerable uncertainty. The magnitude of the chopper power measuring task was also indicated in the chopper voltage and current waveforms shown in Figure 4-6. Here the oscilloscope traces show 200 amp pulses of current immediately following a potential of over 40 volts in the chopper circuit, but the current pulse continues to be appreciable only while the voltage is very low.

In a final effort to better approximate the chopper power consumption by using the existing instrumentation (whose power range for precise measuring was many times the power used by the chopper) a test was performed using three types of instruments: the Sine instrument, the

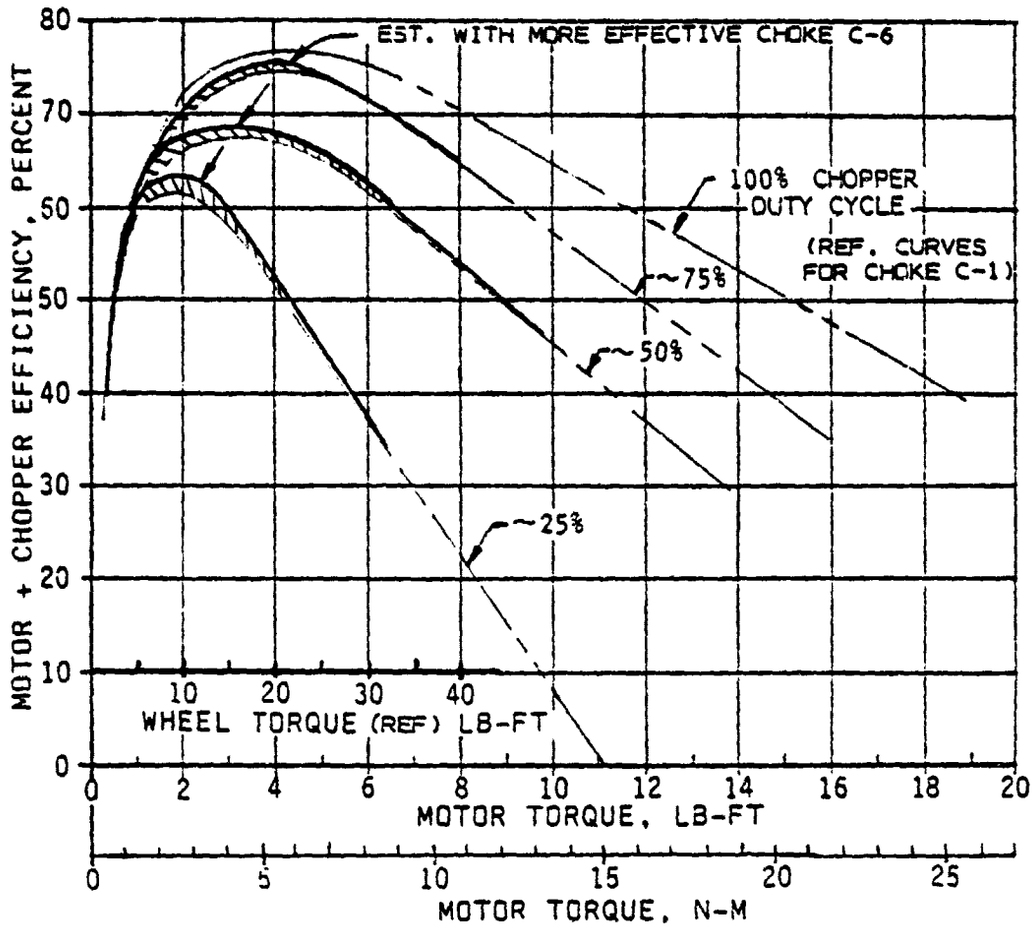

Figure 6-10 Improved Efficiency of Chopper Controlled PM Motor with Improved Choke C-6

Clarke-Hess instrument and DC instrumentation which is generally presumed to be quite inadequate for such current and voltage waveforms. The resulting data are shown in tabular form in Table 6-2 and in curve form in Figure 6-11.

Figure 6-11 also shows a present "best estimate" of the chopper power consumption as approximately the average of the data provided by the two dynamic instruments. In this case the "best estimate" is closely approximated by the DC instruments.

Table 6-2 Chopper Controller Power Consumption Data When Discharging Into Resistance Load

DATA PT. PAIR (CHOPPER & BATTERY)	CHOPPER DUTY CYCLE	SINE INSTRUMENT			CLARKE-HESS			DC INSTRUMENTS		
		CHOP. WATTS	(% OF)	BAT'Y WATTS	CHOP. WATTS	(% OF)	BAT'Y WATTS	CHOP. V-A	(% OF)	BAT'Y V-A
1 & 2	25%	26	(3.9%)	561	12	(2.0%)	600	17.3	(2.6%)	670
3 & 4	50%	40	(2.1%)	1918	16	(0.9%)	1809	39.4	(2.0%)	1959
5 & 6	75%	41	(1.6%)	2630	12	(0.5%)	2386	29.3	(1.1%)	2571
7 & 8	100%	18	(0.5%)	3864	16	(0.4%)	3678	2.2	(0.1%)	3800

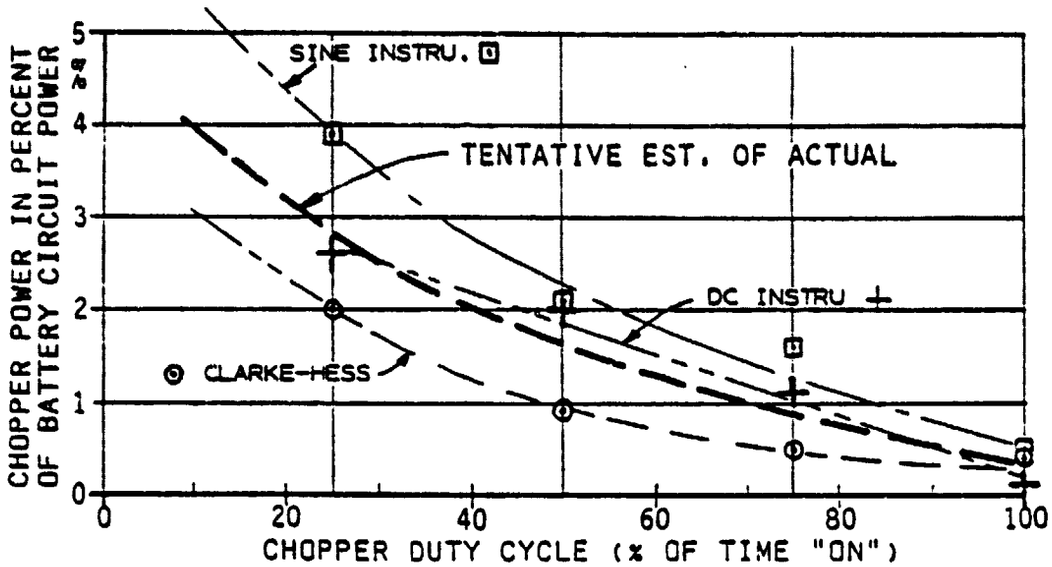

Figure 6-11 Best Test-Based Estimate of Chopper Power Consumption

The chopper's electronic circuit also required a source of 12 volt DC power. This control circuit power was separately measured by a simple DC instrument and was found to vary with duty cycle as shown in Figure 6-12.

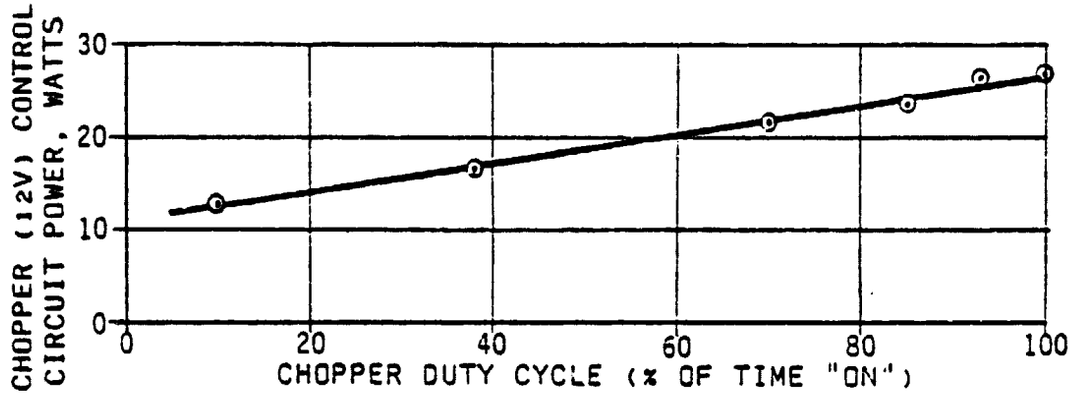

Figure 6-12 Electronic Circuit Power Needs of Chopper Are Small

As indicated by Figures 6-11 and 6-12, the chopper's own power requirements are not very great. The efficiency costs of chopper use — as indicated by the general test data of this section — are instead due to losses induced in the combined motor/controller system circuitry by (a) added I^2R losses due to fluctuating currents and (b) added voltage drops through the chopper, including across the transistor switches themselves.

This test program did not attempt to evaluate any gains or losses in battery performance, battery life expectancy, etc., that possibly may result from chopper-caused current or voltage fluctuations as compared to ripple-free battery discharging. The battery voltage drop as a function of current, which was measured and its effects illustrated, appeared similar whether the battery current was ripple-free or chopper-modulated.

7/ ROAD VEHICLE TEST CONFIRMATION

The four motor/controller/battery systems tested during this program, as illustrated and discussed in previous sections, were duplicates of systems to be later road tested in a small electric vehicle (EV). The road test vehicle used was 3E Vehicle's EP-10 "Sport Roadster," a small, light, 3-wheel EV designed to carry two persons plus a few bags of groceries or other parcels. While this test vehicle is considerably lighter than most EVs now being developed, its general performance will be indicative of larger EVs having a similar battery weight to gross vehicle weight (BW/GVW) ratio.

This BW/GVW ratio is by far the most important parameter in maximizing EV performance and range, assuming the same type of batteries (such as deep discharge lead-acid) is used. Probably next in importance are the losses in the mechanical drive train and rolling resistance of tires. In this respect the EP-10 is equal to or better than most EVs. In aerodynamic drag, however, the EP-10 carries a decided penalty, so at the higher speeds its torque and energy increase proportionally faster than conventional vehicles. This is because (a) open or semi-open roadsters are notorious for high drag coefficients and (b) aerodynamic drag provides an increasing fraction of total resistance as vehicle weight reduces.

7.1 The EP-10 Test Vehicle

The basic configuration of the EP-10 test vehicle is shown in Figure 7-1. This 2-person vehicle was designed as a simple and austere but structurally efficient, relatively safe, vehicle for neighborhood and urban use only. Two performance versions were built and tested, as listed in Table 7-1. Both versions used the same integrated body/structure, which is a bonded composite of various materials. The different performance versions use different wheels and brakes, different lights, different numbers of batteries and slightly different motors and motor-to-wheel speed reduction ratios. Both have front wheel drive with an efficient single speed reduction roller-chain drive.

The integrated body structure of the vehicle is a labor intensive design developed specifically to be marketed as a kit for fabrication by the owner-builder. This design was not marketed, however, due to insufficient interest in a construction kit of this complexity. The EP-10 prototype versions, accordingly, have instead been repeatedly used as an instrumented test vehicle for investigating variations in drive trains, suspension systems, maneuverability, as well as testing of alternative motors and power controls.

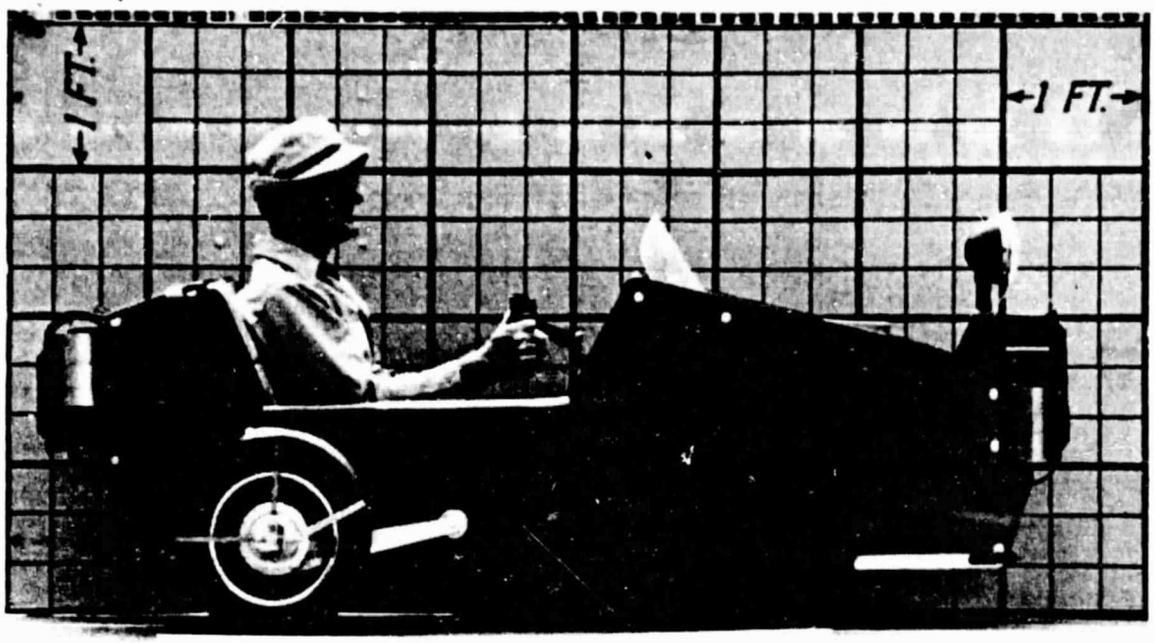

Figure 7-1 The EP-10A "Sport Roadster" Neighborhood EV

Table 7-1 Two Performance Versions of the EP-10 Electric Mini-Car

	MODEL EP-10A "MOTORIZED BICYCLE"		MODEL EP-10B MAX. PERFORMANCE	
PERFORMANCE				
MAXIMUM SPEED (LEVEL ROAD)	30 MPH (48 KM/H)		45 MPH (72 KM/H)	
MAXIMUM (IMPRACTICAL) RANGE	(100 MI) (161 KM)		(85 MI) (137 KM)	
PRACTICAL URBAN DRIVING RANGE	25-35 MI (40-56 KM)		20-25 MI (32-40 KM)	
TYPICAL ENERGY MILEAGE (ON BOARD)	13 MI/KWH		9 MI/KWH	
" " " (110V METER)	7.8 MI/KWH		5.4 MI/KWH	
WEIGHT STATEMENT	LB	(KG)	LB	(KG)
BATTERIES (57 LB EA)	228	(103)	285	(129)
MOTOR, CONTROLS, CONDUCTORS	62	(28)	65	(29)
CHASSIS & BODY	195	(88)	210	(95)
CURB WEIGHT	485	(220)	560	(254)
DRIVER & PACKAGES	200	(91)	200	(91)
NORMAL GROSS WEIGHT	685	(311)	760	(345)
DESIGN MAX. GROSS WT (2-PERSONS)	825	(374)	900	(408)

For the test program of this report, the EP-10 was an intermediate configuration of those listed in Table 7-1. It had the higher capacity rear tires and brakes of the EP-10B but for test data consistency, used only 4 traction batteries as did the EP-10A. With both types of motors tested the vehicle was geared for a level road maximum speed of approximately 38 mph (61 Km/h). This required a higher speed reduction ratio for the PM motor, of course, due to its higher operating speeds (5.167:1 vs 4.40:1 for the series motor).

The gross vehicle weight (GVW) for the subject test program was maintained at 725 lb. (329 kg) (with the exception of one test to investigate steep climb capability with a high GVW and low state of battery charge). Table 7-2 lists the breakdown of the test program GVW. To allow for variations in the amount of instrumentation, driver weight, etc., a variable amount of lead shot ballast was carried.

Table 7-2 The EP-10 Test Vehicle Operating Weight & Balance

I T E M	WEIGHT (LB)	CG ARM (IN):::	REACTION F.AXLE	REACTION R.AXLE	MASS (KG)
CURB WEIGHT, EP-10 (REWEIGH 10-6-79)	492	23.28	249	243	223
TEST DATA INSTRUMENTATION NORMAL(MIN): 3-CHA.RECORDER(5.0),TEMP. RECORDER(3.0),SHUNT(0.5),TEMP.PANEL METER & MOUNT(1.0). WIRING (0.5)::	10	~10	2.2	7.8	4.5
DYNAMIC(CHOPPER TESTS): SINE INSTRU. PLUS TACH.SYSTEM(15.0),12VDC/110VAC INVERTER (7.0),CAMERA & INSTL (~3)	25	~10	5.4	19.6	11
SAFETY GEAR & TOOL KIT FIRE EXT.(4.0); CABLE CUTTER(4.0); WRENCHES, FUSES, ETC (2.0)	10	-8	-1.7	11.7	4.5
DRIVER & PERSONAL GEAR (MIN ALLOW.)::	188	10	40.9	147.1	85
GVW FOR LRC ROAD TESTS::	725	(18.77)	295	429	329

NOTES: (1) ::SHOT-BAG BALLAST ADJUSTMENT FOR LIGHT INSTRUMENTS OR DRIVER.
(2) :::CG LOCATION IN INCHES FORWARD OF REAR AXLE.
(3) BATTERY WT/GVW RATIO = 228/725 = 31.4%.

7.2 Test Vehicle Performance Analysis

The estimated performance of the EP-10, at its test GVW, was recalculated specifically for this program. This new calculation was made in part because of the altered GVW from the earlier design analysis. Another reason was to incorporate an improved basis for estimating the drag effects of typical winds and the rolling resistance effect of typical urban streets.

Torque requirements, rather than horsepower, are the more important criteria for matching an electric motor's capability to a road vehicle's requirements. The torque needs of a vehicle stem primarily from (a) wheel and tire rolling resistance, (b) aerodynamic drag due to the vehicle's shape and size, and (c) additional temporary torque needs as required for vehicle acceleration or the climbing of grades.

Figure 7-2 shows tire rolling resistance (RR) coefficients as a function of vehicle speed. The EP-10 uses bias ply tires (the only type produced in these small sizes) and the subject analysis used coefficient data from the figure's bias ply curve. The suitability of this curve (even for the small EP-10 tires) had been generally confirmed by rolling resistance tests conducted by 3E Vehicles during development of this vehicle. Tests of the 4.80-8 tires used on the rear wheels, conducted at low speed and with no prior warm-up, indicated an RR coefficient of .012 (at the wheel load of the present test vehicle GVW). The 5.30-6 front tire, in a

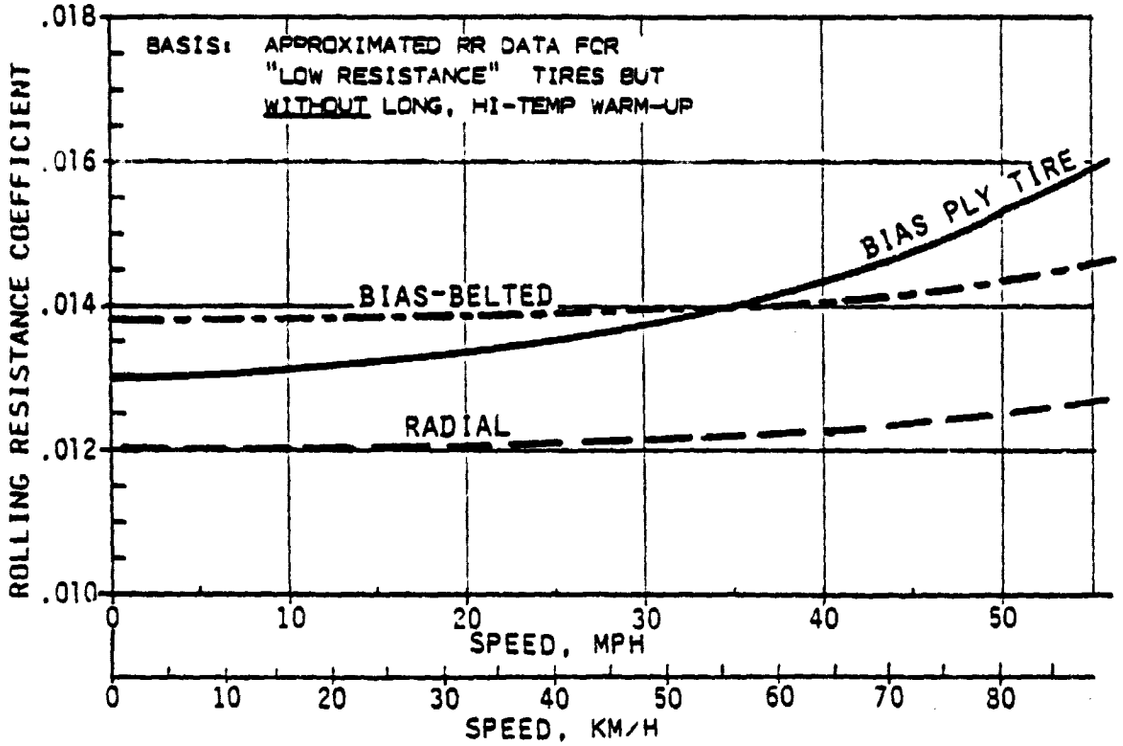

Figure 7-2 Representative Tire Rolling Resistance Data for EVs

similar test, demonstrated an RR coefficient of .015 at its test GVW load. The average of these three matches the .013 shown for the generalized bias ply curve.

Many persons involved in EV design or performance will consider the rolling resistances of Figure 7-2 too high. The figures are "high" primarily because they provide but a small allowance for tire warm-up. Since RR testing is performed to compare one tire with another, for consistently comparable data it is necessary that test tires be "warmed-up" to reach an equilibrium operating condition. Two test and analysis programs (references 3 and 4) were recently performed to find a less time consuming method for RR tests. Data extracted from the two studies is consistent in the amount of RR increase to contend with if tires do not experience an extended, loaded, moderately high speed warm-up. This warm-up effect data is shown in Figure 7-3. An RR increase factor of 1.25 is suggested for EV use of typical tire RR data.

To the basic tire rolling resistance data from the above curve was added a +.002 coefficient increment to allow for some slight added resistance due to brake shoe drag and/or wheel alignment (this is a small allowance since the vehicle uses drum brakes that are not self-adjusting and wheel alignment drag is minimized in a 3-wheeled configuration). Some appreciation for the likely equivalent RR effect of today's disc brakes can be gleaned from reference 5, a paper describing a development program to reduce disc brake drag for the new GM X-cars. Reported lab tests showed 2.0 lb-ft drag torque for a previous design reduced to 0.5 lb-ft for the new design. When road tested, however, the new X-car design brake

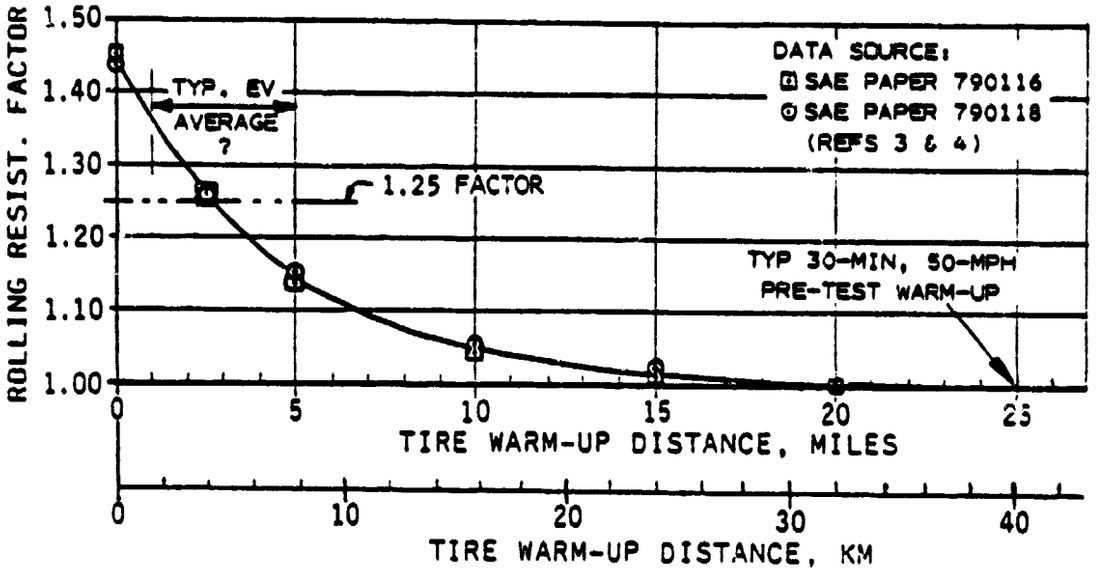

Figure 7-3 Typical Tire Test Warm-Up Effect on Rolling Resistance

averaged about 1.5 lb-ft drag torque. After factoring in the tire's rolling radius and load per tire, this means an equivalent RR coefficient exceeding .002 for brake drag alone. Many disc brakes, presumably, will not do as well.

Aerodynamic drag is computed as a function of the frontal area of the vehicle and its estimated or otherwise determined drag coefficient. The EP-10 vehicle has a frontal area of 9.1 sq ft (0.85 sq m) and, due to its boxy lines and open cockpit, a relatively high estimated drag coefficient of .70. For operations in still air the aerodynamic drag is calculated by multiplying together the frontal area, drag coefficient, and the dynamic pressure of air at the velocity of the vehicle. To allow for some added aerodynamic drag due to typical or "average" winds, the previous EP-10 analysis applied a "5 mph built-in head wind." A more recent analysis of this type of wind effect, conducted by Jet Propulsion Laboratory for the Electric and Hybrid Vehicle Program (reference 6) provided equations for calculating a more logical drag increment. For the EP-10 this typical drag increment as a function of vehicle speed is shown in Figure 7-4.

Two tabulations of total "drag" or resistance force are considered appropriate in view of the incremental values discussed above. One tabulation, which includes no incremental wind factor and no allowance for the texture and small-scale up-and-down grades (waves or bumps) experienced in typical street paving, is appropriate for highly controlled test runs for which the wind factor and road texture effects are either eliminated or separately accounted for. A second resistance tabulation, which includes wind factor and street texture increments suitable for the operating locale, is more appropriate in calculating typical vehicle performance. In either case, the vehicle resistance forces are readily converted to driving wheel torque requirements by multiplying the force values by the rolling radius of the wheel-tire combination. For the EP-10 this has been done as listed in Table 7-3.

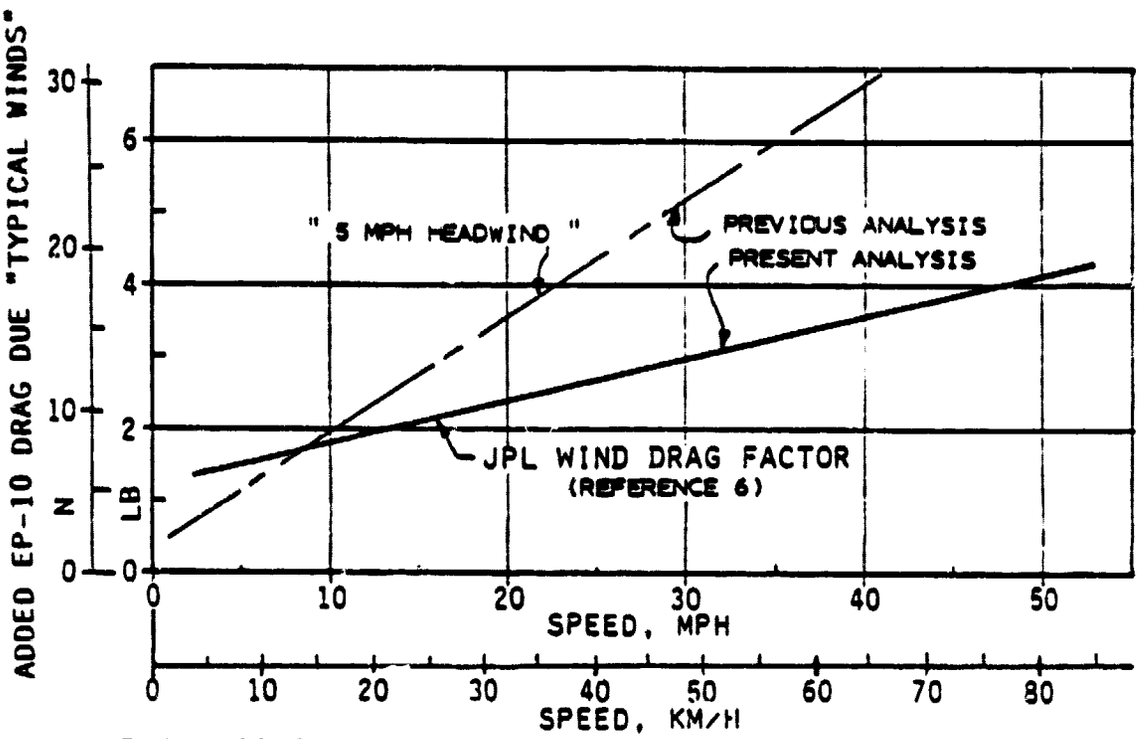

Figure 7-4 Added EP-10 Aerodynamic Drag Due to "Average" Winds

Line 1 of Table 7-3 simply repeats the bias ply rolling resistance data from Figure 7-2 after adding the .002 brake and alignment allowance. Line 2 converts this resistance coefficient to a resistance force by multiplying by the test vehicle GVW. Line 3 tabulates the aerodynamic drag force while line 4 totals these two basic resistance forces. Wheel torque requirements at the various speeds — for the no-wind, smooth level surface test conditions — then results as listed in line 5.

3E Vehicles' previous vehicle test experience has indicated an incremental rolling resistance coefficient of about .004 which permits typical "black top" neighborhood and urban street performance to correlate with smooth surface rolling resistance basic data. This incremental factor is applied in line 6 of the above table, while line 7 applies the incremental wind effect factor taken from Figure 7-4. The resulting "typical street" drag and wheel torque requirements for the EP-10 vehicle are listed in lines 8 and 9 of the figure.

The above .004 incremental RR coefficient is too high to use for nicely leveled interurban highways or high speed freeways, which can keep RR values comparable to those of the typical steel test wheel. Urban or neighborhood streets, however, which are more typical roadways for an EV, are usually rougher textured, contain small waves or bumps, and are much more frequently dug up and patched.

The wheel torque data of Table 7-3 is summarized in curve form by the two lowest curves shown in Figure 7-5. This figure also shows added increments of wheel torque as required for either various rates of acceleration or various steepnesses of grades to be climbed.

Table 7-3 Wheel Torque Requirements of the EP-10 Test Vehicle

LINE	DRAG ITEM (FOR GVW=725 LB)	SPEED IN MPH (KM/H)					
		5 (8.0)	10 (16.1)	20 (32.2)	30 (48.3)	40 (64.4)	50 (80.5)
1	ROLLING RESIST. COEF, C_{RR}	.0150	.0151	.0154	.0158	.0164	.0173
2	ROLLING RESIST."DRAG" (LB)	10.88	10.95	11.17	11.46	11.89	12.54
3	NO-WIND AERO. DRAG (LB)	0.41	1.63	6.52	14.66	26.07	40.73
4	"TEST RUN" TOTAL DRAG (LB)	11.29	12.58	17.69	26.12	37.96	53.27
5	" " TORQUE (LB-FT)	6.68	7.44	10.47	15.45	22.46	31.52
$5_{(SI)}$	" " " (N-M)	9.06	10.09	14.20	20.95	30.46	42.74
6	GRADE/TEXTURE EST (LB)	2.90	2.90	2.90	2.90	2.90	2.90
7	WIND FACTOR $\Delta DRAG_A$ (LB)	1.56	1.85	2.44	3.03	3.57	4.24
8	"TYP STREET" DRAG (LB)	15.75	17.33	23.03	32.05	44.43	60.41
9	" " TORQUE (LB-FT)	9.32	10.26	13.63	18.97	26.30	35.76
$9_{(SI)}$	" " " (N-M)	12.64	13.91	18.48	25.72	35.69	48.49

The increments of both acceleration torque or climbing torque are, of course, strictly functions of the GVW to be accelerated or lifted. For the EP-10 vehicle, at its test GVW and known drive wheel rolling radius, these equations simplify to the two shown below; the equation for acceleration includes a 1.1 factor to account for the rotational inertia of the vehicle's wheels and motor.

$$\text{Accel:}\quad T_{w(A)} = 1.1 \times GVW \times \frac{MPH/S}{21.94} \times \frac{7.1"}{12"} = 21.51\ (MPH/S)$$

$$\text{Climb:}\quad T_{w(c)} = GVW \sin(\arctan \frac{\%GR}{100}) \times \frac{7.1"}{12"} = 429 \sin(\arctan \frac{\%GR}{100})$$

$$\simeq GVW \frac{\%GR}{100} \times \frac{7.1"}{12"} \simeq 429 \frac{\%GR}{100};\ \text{(for typ. low \%GR)}$$

Figure 7-5 makes it quite obvious that operating torque requirements (and, therefore, the power and energy requirements) can greatly exceed that required in a steady state level road operation. For example, a low speed "test" cruise of 18-20 mph (29-32 km/h) requires some 10 lb-ft (13.6 N-m) of torque at the wheel. Yet at this speed, one might desire ten times that torque to temporarily accelerate at 4 mph/S (1.79 m/S^2) or climb a 20% grade.

7.3 Performance With V-Switch Control

The road test program planned and executed for each of the four motor/controller combinations is summarized in Table 7-4. Since level-road propulsion requirements are neither very demanding nor time-consuming to confirm by tests, the program emphasized a variety of grade climbs to explore both the magnitude and duration of the higher torque operations.

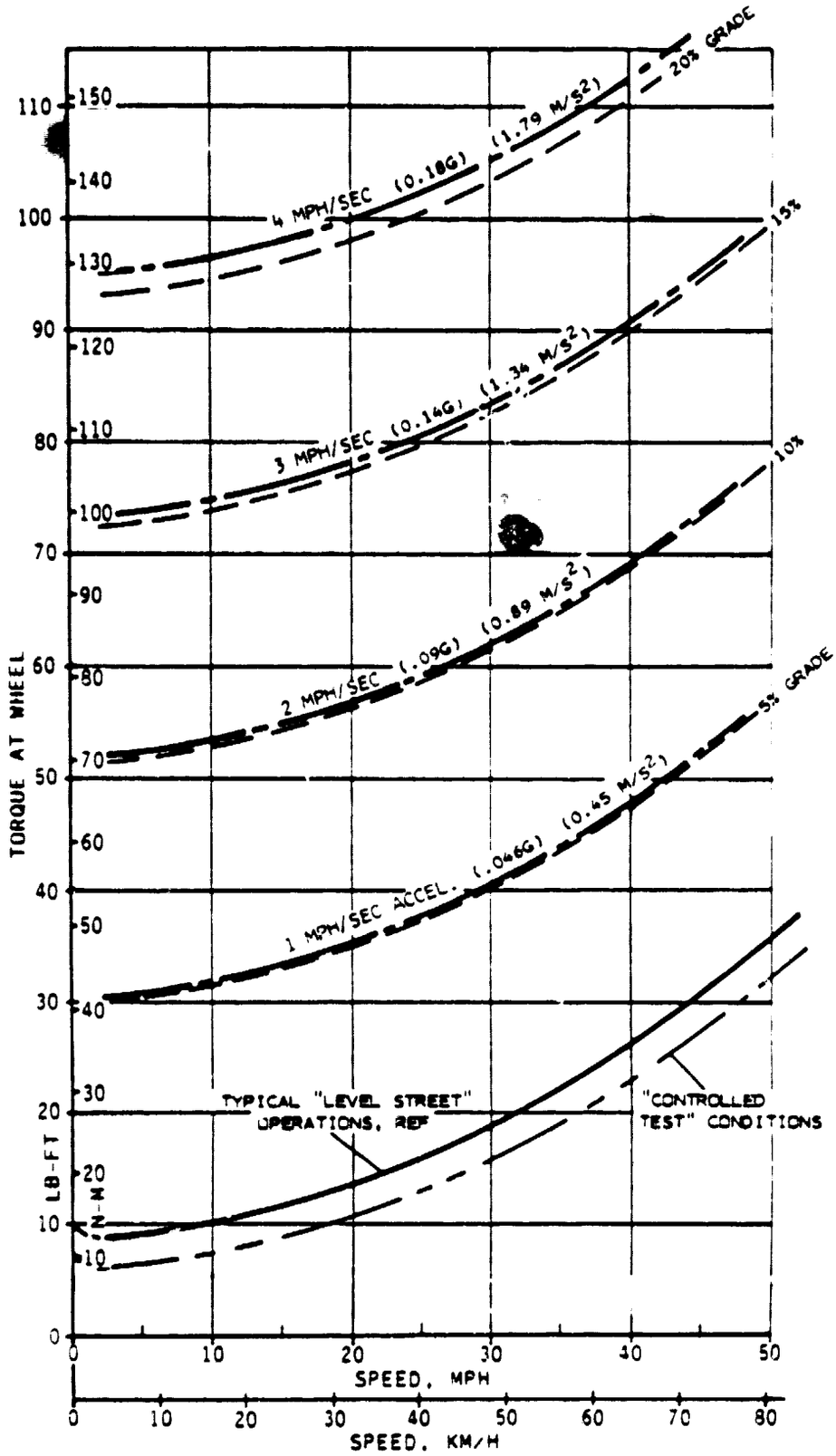

Figure 7-5 Torque Required by EP-10 Test Vehicle Including Acceleration or Climb

Table 7-4 Road Test Data-Run Program

SERIES	TEST RUN DESCRIPTION	NOM. VOLTS or DUTY CYCLE	GRADE	REMARKS
I	HILLY NEIGHBORHOOD CLIMBS			
I-1	LOW POWER, MODERATE SLOPE	12Vor25%DC	4.7%	STEADY STATE (S.S.) REACHED
I-11	MOD. POWER, MOD. SLOPE	24Vor50%DC	5.0%	" " "
I-111	BRIEF STEEP CLIMB (LG ≈ 200'W) *	24Vor50%DC	13.5%	TYP NOT S.S. (SOME ACCEL.)
I-1111	" " " (LG ≈ 300'E) *	36Vor75%DC	10.0%	" " " " "
I-11111	" " " (LG ≈ 200'W) *	48Vor100%DC	13.5%	" " " " "
II	LONG COAST THEN CLIMB			
II-0	DESCEND PARKWAY(1.0 OR 1.3 MI)	(BRAKING)	6.4%	REGEN.BRAKE WITH PM/V-SW
II-1	CLIMB PARKWAY (~1/3 UP)	48Vor100%DC	6.8%	S.S. PRIOR REDUCED GRADE
II-11	" " (~3/4 ")	48Vor100%DC	7.6%	" AFTER " "
III	REDUCED SPEED "LEVEL" CRUISE			
III-1	LOW POWER CRUISE	12Vor25%DC	~0%	
III-11	MODERATE POWER CRUISE	24Vor50%DC	~0%	
III-111	SAE "B" CYCLE RUNS	VARIED	~0%	
IV	STEEP EXTENDED CLIMB		MAX	
IV-1	UP PRIVATE DRIVE (600',260'OVER 20%)	48Vor100%DC	22.5%	SUBSTITUTE 10% GR,PM MOTOR
V	URBAN TRAFFIC TRIP			
V-1	ARTERIAL URBAN STREET (OUT-BOUND)	VARIED	±2%	2.5 MI,7 LIGHTS,14 STREETS
V-11	" " " (RETURN)	"	±2%	" " " "
VI	LEVEL ROAD SPEED RUNS			
VI-1	0.4 MI INCL. 0.100 MI MARKED (WEST)	48Vor100%DC	~0%	STOPWATCH TIMED 1/10 MI.
VI-11	" " " " (EAST)	48Vor100%DC	"	" " "
VI-111	" " " " (WEST)	36Vor75%DC	"	" " "
VI-1111	" " " " (EAST)	36Vor75%DC	"	" " "
VII	SAE SCHEDULE "C" RUNS			
VII-1	1 3/4 CYCLES,ABOVE 0.4 MI (WEST)	VARIED	~0	
VII-11	" " " " (EAST)	"	"	

NOTES: (1)*WITH PM MOTOR & V-SWITCH CONTROL REGENERATIVE BRAKING USED AND RECORDED WHILE DESCENDING OPPOSITE SLOPE.
(2) PROGRAM MILEAGE VARIED FROM 15.6 TO 18.4 (25.1 TO 29.6 KM) DEPENDING UPON NUMBER OF RUN REPEATS.

The 3E Vehicles' experimental shop is located in a hilly suburban area having a variety of both brief and extended street slopes. The streets selected for test program use were each "surveyed" for both slope and slope duration and their profiles plotted for correlation with strip-chart data. Figure 7-6 shows the simple but accurate "grade gage" being used to measure the maximum 22.5% grade for this program (a private access road, since this slope exceeds that permitted for streets by most municipalities). The climb test also included a 1.0 or 1.3 mile (1.6 or 2.1 km, choice depending on cross-street selected for turn-around) arterial boulevard with a grade mostly near 7%. This long climb was not performed with the PM motor and chopper combination due to time-at-current limitations (previously discussed) as well as test results from the shorter climbs. The maximum 22% grade climb was not planned for the PM motor with either control system, but an 8 to 10% medium duration (approx. 700 ft or 215 m) grade was substituted.

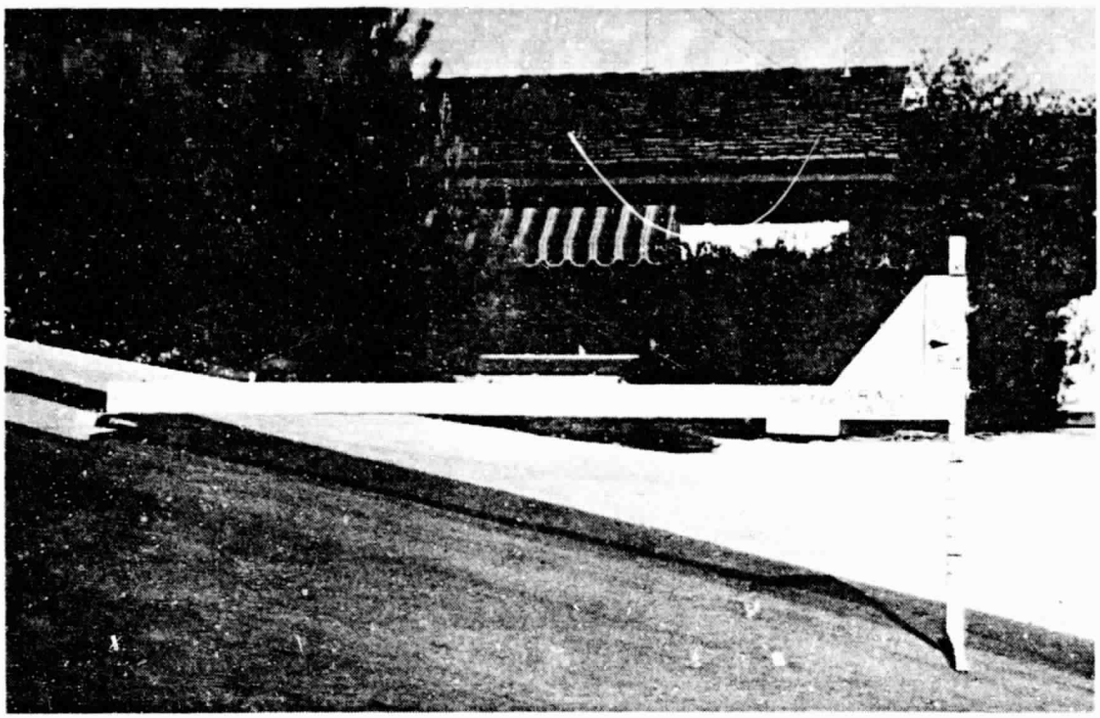

Figure 7-6 Convenient Grade-Gage Illustrating Maximum Test Grade

The vehicle torque requirements plot previously shown in Figure 7-5 can be considerably complicated (but made to present much useful information) by adding to it torque available from the vehicle's propulsion system as well as data on the efficiencies of operating that propulsion system. This was done for each of the four test vehicle motor and controller combinations prior to conducting the road tests. The resulting composite torque required/torque available plot for the test vehicle with the series motor and V-switch combination is shown in Figure 7-7. It is seen that this plot has an additional ordinate showing the motor current in amperes. This is convenient for road test purposes since current is readily measured; it is also technically sound since ripple-free DC current is a direct function of motor torque.

Obtaining motor current values to plot requires the conversion of wheel torque to motor torque. The conversion factor for this plot was the 4.40:1 speed reduction ratio times the estimated chain drive efficiency of 0.96 or an overall torque factor of 4.224:1. Having the wheel-to-motor torque ratio, the motor current data for a given nominal voltage setting and various wheel torques can be determined from the data of the previous Figure 5-1. In a similar manner the motor and motor circuit efficiency data points for each of the nominal voltage curves were taken from Figure 5-2.

Figure 7-7 is seen to also have a number of boldly indicated data points reflecting road test data collected during the various road test operations. The road test data points of this figure are seen to fall quite close to the torque available curves that were previously plotted from the dynamometer test data. The vertical location of these data points (which were determined from strip chart records of motor current, confirmed in many cases by point-data read from a more accurate digital multimeter) are also seen to reasonably correspond to the percent grades indicated.

Three test data points are shown for the steep, 22% grade; two labeled "low battery." Performance during the near-full-charge first test was so good (sprite, steady climb at 210 amperes with only a moderate brush temperature rise) that a repeat 22% climb, but with a "low battery," was planned as the day's final test run. Again, similar performance with differences reflecting only the somewhat lower voltage. The vehicle's lead-shot ballast was then replaced with a second (155 lb) man for a third climb at a GVW of 850 lb (386 kg). The current drain increased and voltage and speed reduced as expected, but still no hesitation or undue motor temperatures (brush temperature peaked at 295°F or 146°C). Clearly these "golf-car" motors had been developed with such short-period torque and current needs an understood reality.

The composite torque required/torque available plot for the vehicle powered by the permanent magnet motor with V-switch control is shown in Figure 7-8. With this motor the motor-to-speed reduction ratio was 5.167:1 (resulting, with the 96% drive efficiency, in a wheel-to-motor torque ratio of 4.96:1). As with the series motor, the road test point-data is seen to correlate well with both the nominal voltage curves and the percent grade torque and current requirements.

Figure 7-8 is seen also to have additional data in terms of estimated time limits for given values of motor current. These data were derived from an extra series of relatively prolonged time-at-current dynamometer tests for the PM motor — in which the cut-off time-at-current criteria was a motor brush temperature of 400°F (204°C). Motor brush temperatures were continuously recorded during the entire road test program (with all of the motor and controller combinations). The maximum brush temperature recorded during particular data runs is shown except when the temperature rise was relatively modest. Motor field temperatures were also monitored by means of an analog meter and logged when approaching a high value. In general, the motor field temperatures remained sufficiently below "safe limits" (212°F or 100°C) to be of little interest during the tests.

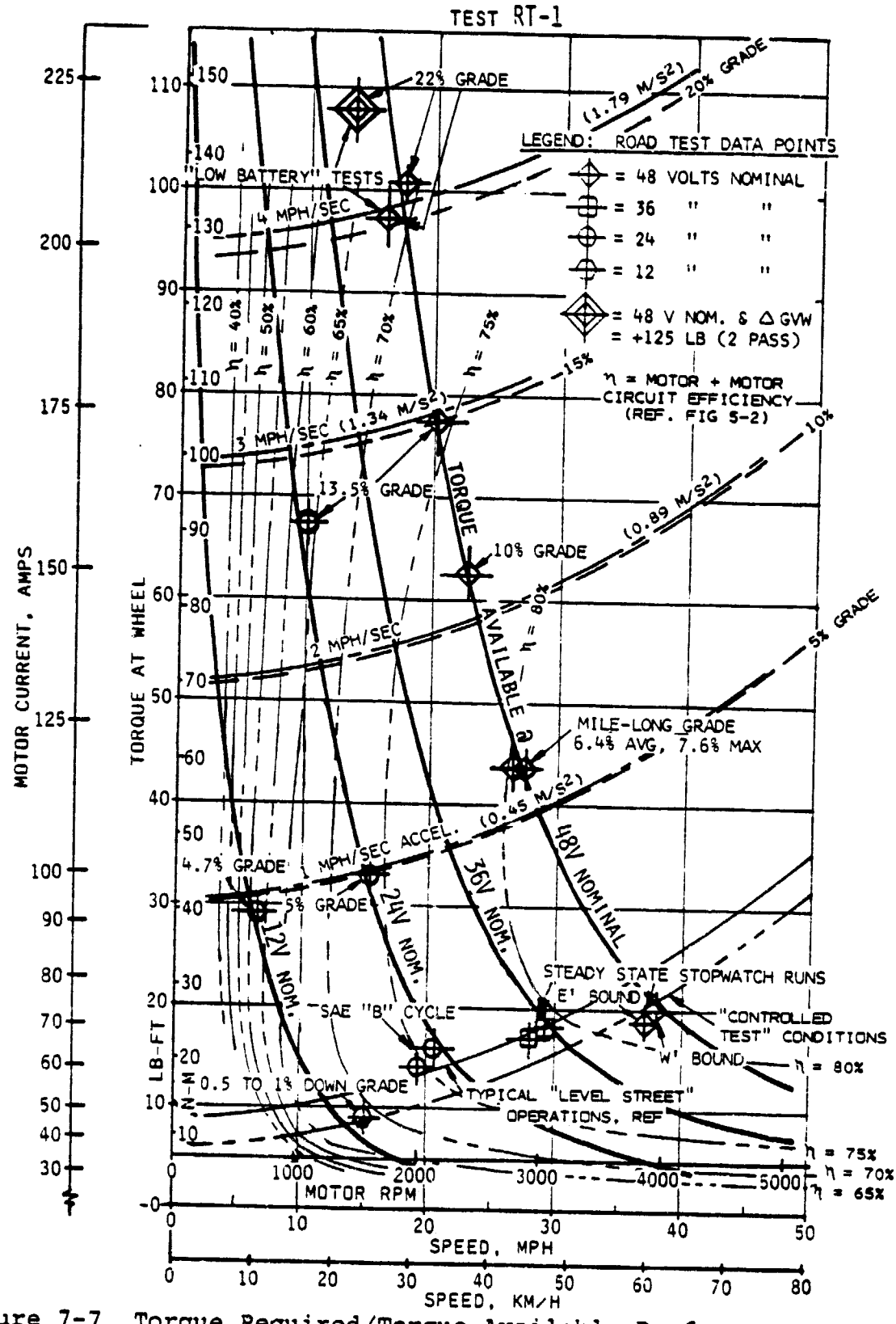

Figure 7-7 Torque Required/Torque Available Performance Envelope Including Road Test Data Correlation – For EP-10 Vehicle with Series Motor and V-Switch Control

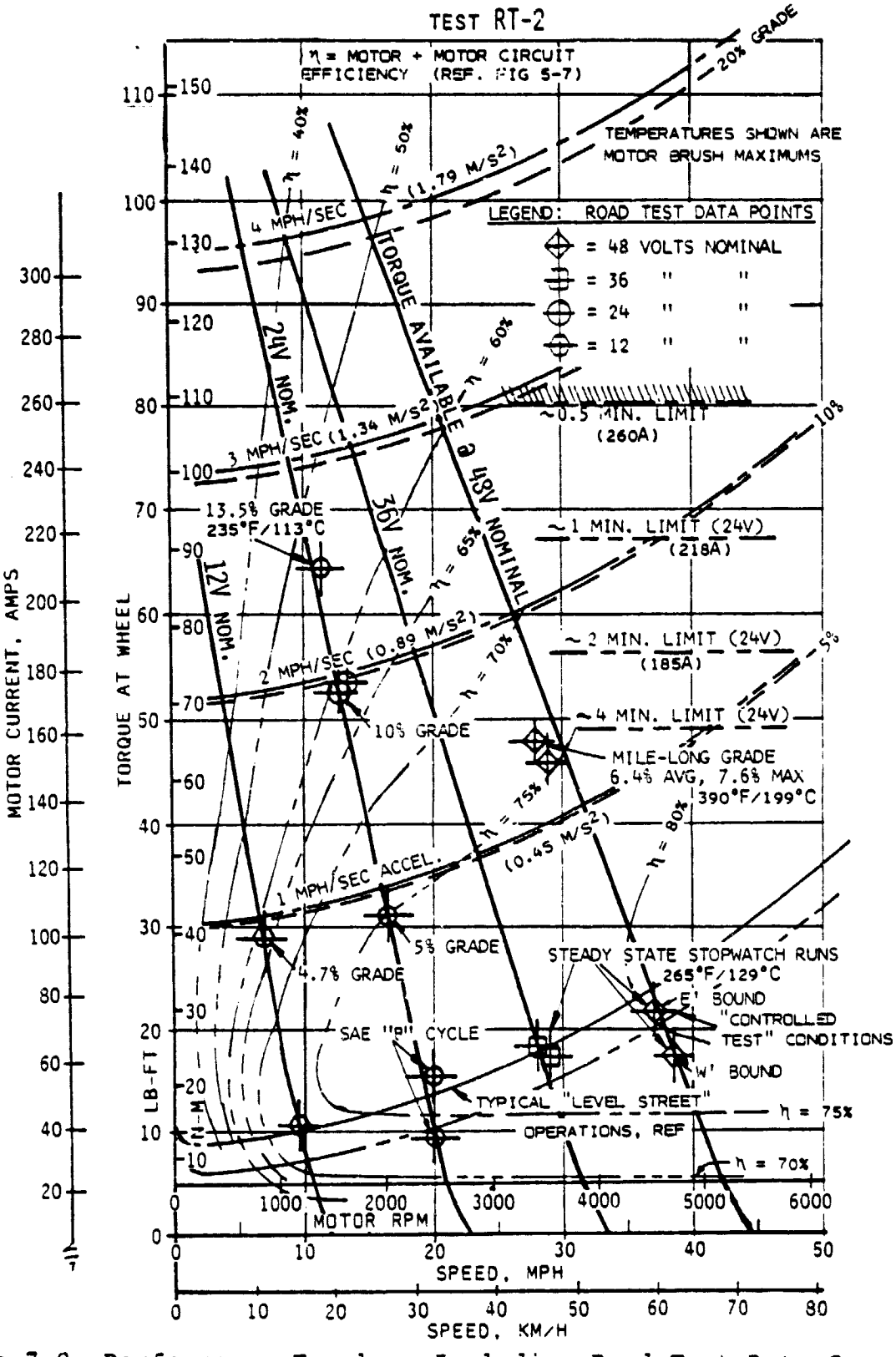

Figure 7-8 Performance Envelope Including Road Test Data Correlation – For EP-10 Vehicle with PM Motor and V-Switch Control

7.4 Regenerative Braking With PM Motor

Permanent magnet motors, due to their fixed magnetic field strength, have the potential for regenerative braking without the control circuit complexity necessary with wound-field-pole motors. As the PM motor speed exceeds its no-load value, at any given circuit voltage, current flow changes direction and the motor becomes a generator.

3E Vehicles' interest in regenerative braking for the simple EVs concerns primarily its use as a speed stabilizer on downgrades (not unlike down-shifting a conventional car or truck). EVs when not under power are, in internal combustion car terms, "free wheeling" machines. As such, they otherwise require larger and heavier brakes than normal to absorb downgrade braking energy. Interest in recapturing energy to extend EV range or performance is only secondary. It is believed that most paper studies of regenerative braking's energy-saving potential have (a) used unrealistic efficiencies for the system's components and (b) overestimated the amount of deceleration performed by braking.

The road test program using the PM motor with voltage-switch speed control, as briefly noted in the data run Table 7-4, explored regenerative braking during the series I "brief steep climbs" and series II "long coast then climb." In these experiments, a down-shift in nominal voltage at or right after the hill's crest resulted in braking to a moderate speed commensurate with the local downgrade (the data recorder's current shunt leads had been provided with a polarity switch, activated at voltage down-shift, to record the reversed current flow).

Figure 7-9 is the strip-chart record of current, voltage and speed during the series II long descent (using regenerative braking) and subsequent reclimb. The descent and climb were each just under one mile (1.6 km) in length with a nearly constant grade of 6.8%, except for a brief reduction to 5% some 3/10 below the crest (reflected by a current reduction and speed increase on the climb record).

As indicated by the brief comparative analysis data provided, about 19% of the circuit energy expended during climb was "returned" during descent. The battery's state-of-charge "return," however, is seen to be under 15% (the charge being a function only of the amount of current that passes through a cell, independent of the voltage that caused it). This fraction of charge returned seemed rather small (compared to some studies) especially since almost the entire descent was generating current and friction braking was used only during the last 8-10 seconds. Accordingly, an after-test analysis was made to determine the current flows one theoretically could expect.

Figure 7-10 is a plot of the test vehicle's required power versus speed — to either overcome road loads (i.e., rolling resistance plus aerodynamic drag) or to climb various grades (the same amounts of power must be somehow absorbed during descent). The percent grade data shown is rigorous, since it depends only on vehicle mass and the laws of physics; the

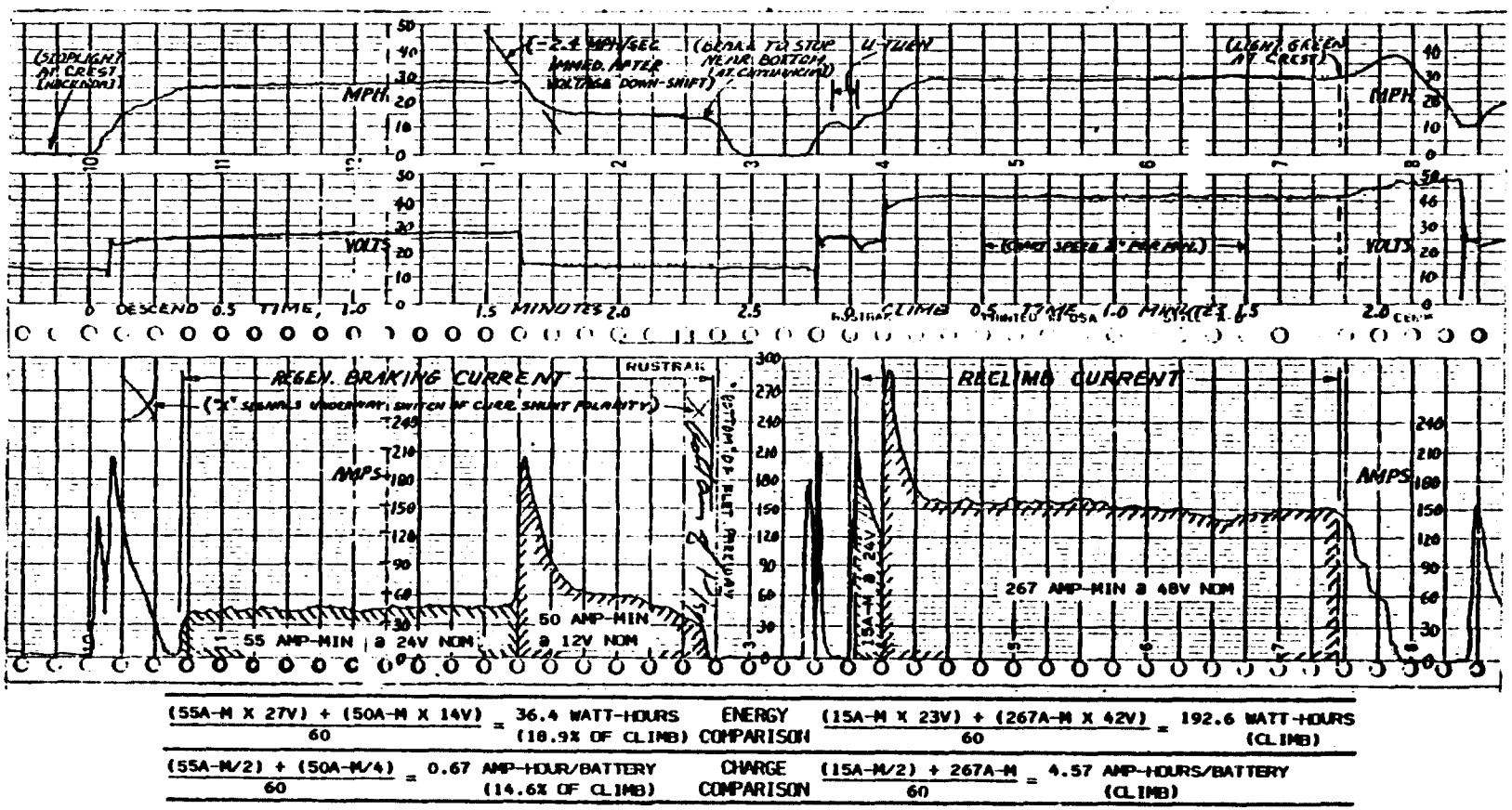

$\frac{(55A\text{-}M \times 27V) + (50A\text{-}M \times 14V)}{60}$	= 36.4 WATT-HOURS (18.9% OF CLIMB)	ENERGY COMPARISON	$\frac{(15A\text{-}M \times 23V) + (267A\text{-}M \times 42V)}{60}$	= 192.6 WATT-HOURS (CLIMB)
$\frac{(55A\text{-}M/2) + (50A\text{-}M/4)}{60}$	= 0.67 AMP-HOUR/BATTERY (14.6% OF CLIMB)	CHARGE COMPARISON	$\frac{(15A\text{-}M/2) + 267A\text{-}M}{60}$	= 4.57 AMP-HOURS/BATTERY (CLIMB)	

Figure 7-9 Strip-Chart Record of Regenerative Braking Descent and Reclimb, with Comparative Energy and Charge/Discharge Analyses

road load curve is approximate, since it depends on aerodynamic and rolling assumptions discussed earlier. The plot illustrates several points. For example, a 2% grade should sustain a coast of some 15 mph (24 km/h), and on the tested 6.8% grade, this relatively high drag vehicle would reach only about 48 mph (77 km/h) without braking. More importantly, the power available for current regeneration was about maximum at the speed attained during the 24V nominal descent (i.e., the road load curve there is approximately parallel to the 6.8% grade line, meaning near maximum separation).

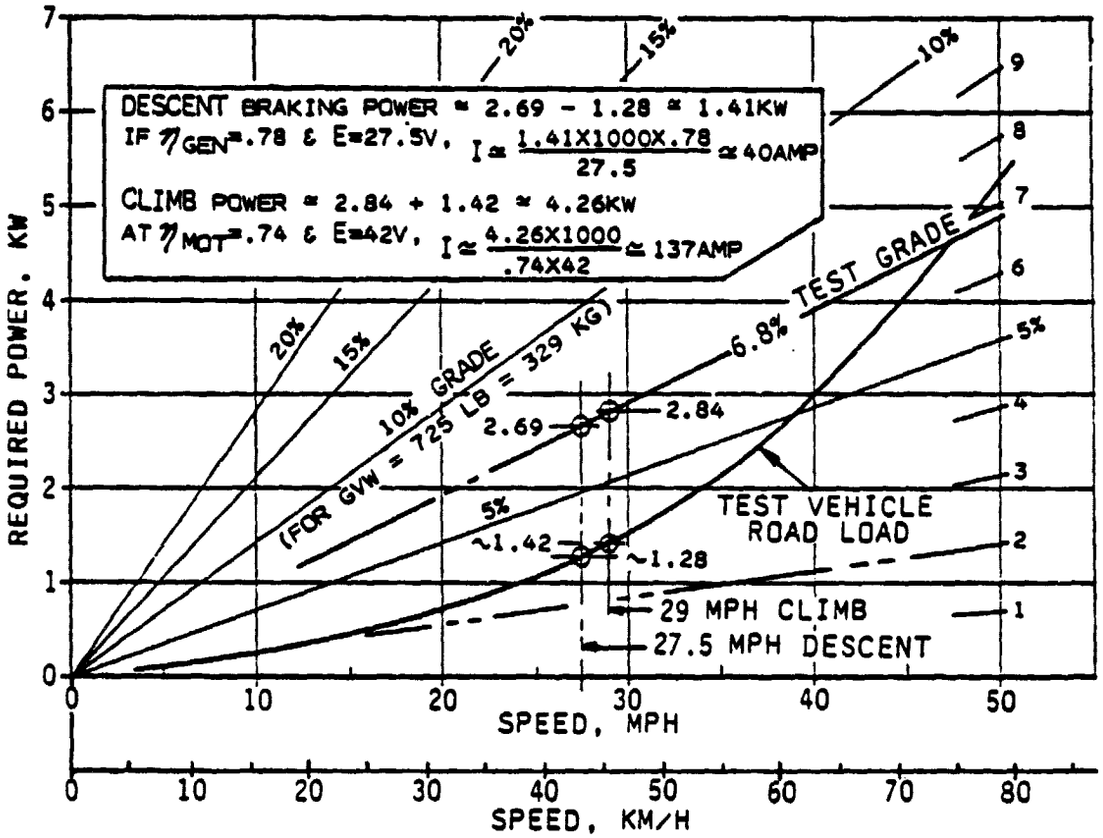

Figure 7-10 Test Vehicle Power Needs for Road Loads and Climbs — With Elementary Analysis of Climb and Braking Currents

The analysis data inserted in Figure 7-9 shows that one would calculate and expect a regenerative current of about 40 amp (where the recorder said 46 to 48) and a climb current of some 137 amp (where the recorder said 150 - 155). While discrepancies of this amount, between calculated versus real test data, are not bad, part of that shown can be presumed due to wind effects on aerodynamic drag. The data log for this test shows a measured wind velocity, at mid-slope, of "3 to 5 mph from 11 o'clock, climbing." While the data significance does not merit the effort of recalculating the aerodynamic drag, such a mild tailwind on descent and headwind on climb should increase both calculated currents by amounts on the order of the discrepancies above.

The regenerative braking test, in summary, did demonstrate a desirable potential to brake descents with at least some energy return and without the need of dissipating the energy in brake heating. This was relatively easy to accomplish with a PM motor, although the method requires a conscious action by an informed driver and is not automatic upon brake pedal use. Similar braking action, but not the energy return, could be accomplished with a series motor by dissipating the generated current into resistors (as, for example, do diesel-electric locomotives). For the simpler and more economic EVs, it is quite possible that total systems effectiveness would favor the least complex electrical control, accept "free wheeling" descents, and size friction brakes to accept the extra heat energy.

7.5 Performance With Chopper Control

For the road test program when using chopper control, two types of data recording instrumentation were used. These were (a) the multichannel strip chart recorder just discussed, which uses conventional galvanometers as used for recording ripple-free DC data, and (b) the Sine dynamic instrumentation system from which simultaneous but single point data was recorded by means of a remotely operated photopanel. For both types of instrumentation, voltage and current were sensed in the motor circuit where excursions of the chopped current are relatively mild. As discussed earlier in Sections 4 and 6, the battery circuit power values, as determined by the product of the measured average current and average voltage (although these average values differed somewhat from RMS values measured by the dynamic instruments), were within some 2% of those power values as measured by the dynamic instrumentation. In correlating the road test data with vehicle performance predictions as derived from the dynamometer tests, the strip chart recorder data was used primarily, with the photopanel point-data from the Sine instrument used primarily as a confirmation and accuracy check. Figure 7-11 shows copies of two of the SX-70 Polaroid color prints used to record the point-data. The figure also shows the use of a portable digital multimeter whose output accurately indicates vehicle speed, provided by the 5.00 mph/volt tach generator also used for the strip chart recorder speeds. (The digital tachometer of the dynamometer tests malfunctioned when powered by the inverter and/or with its magnetic pick-up near the chopper.)

Figure 7-12 again illustrates a torque requirement/torque available plot; this time for the series motor under chopper control. The current ordinate, for chopper control, is seen to be complicated by the need for a separate ordinate for each of the four duty cycles tested. Again, these current values at the various duty cycles were determined as functions of wheel torque by applying the previously discussed wheel-to-motor torque ratio and using dynamometer data from Figure 6-4. The motor-plus-chopper efficiency data for this plot was similarly derived from Figure 6-6.

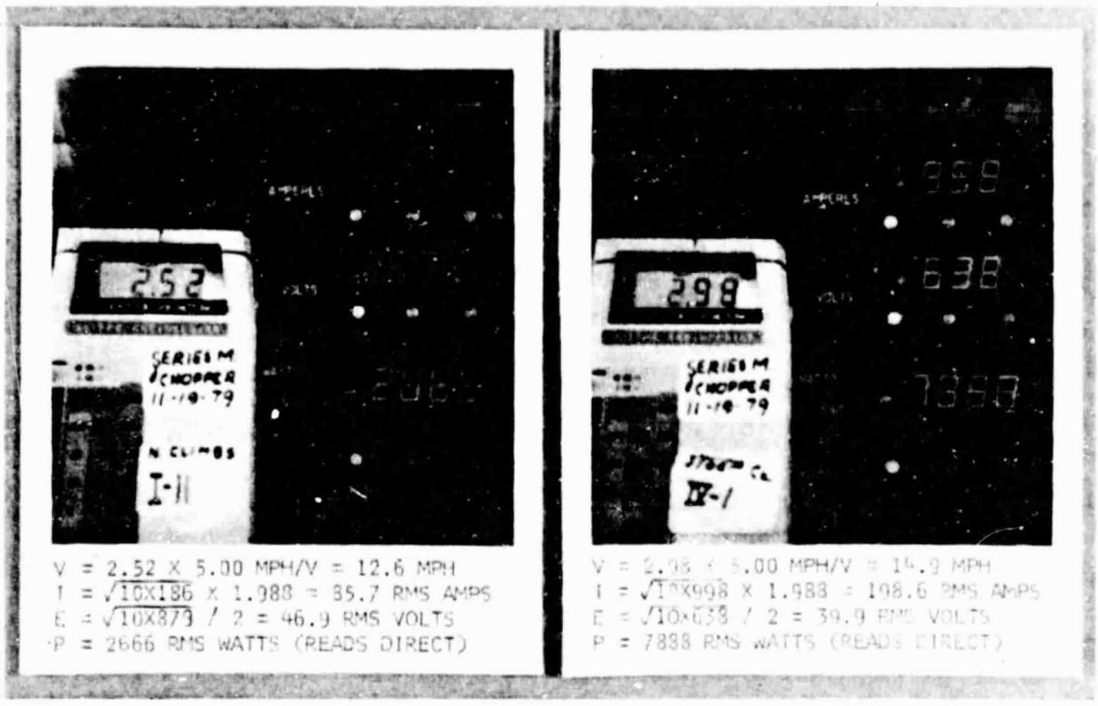

Figure 7-11 Typical Road Test Photo Data-Point Records from Sine Instrument and Improvised Speed Meter

The correlation of road test data points with performance predictions is seen to be not quite as good as that obtained with the V-switch control system. For the duty cycles other than 100%, this is believed mostly attributable to the reduced ability to set a precise duty cycle under the road test conditions. For vehicle control under road and traffic conditions, the 10-turn precision potentiometer used for the dynamometer tests was replaced by a nominal 300° potentiometer whose active range between 0 and 100% duty cycle was found to be some 120°. The resulting thumb-dial settings of the duty cycle, while suitably responsive and rapid for traffic operations, were less exact than those of the dynamometer test program. Again, however, the correlation of road test data with predictions appears to quite adequately confirm the process.

The final torque required/available plot, for the PM motor with chopper control, is shown in Figure 7-13. As in the preceding figure, a multiple scale current ordinate is shown to cover the four duty cycles being tested. For this plot, the current versus torque and the efficiency data were derived from Figures 6-8 and 6-10, respectively. Again, for the most part, reasonably good correlation between the road test data points and the predicted curves and current values is indicated. For this plot, however, the below-100% duty cycle road test points nearly all fall at a lower speed than predicted by the dynamometer data. In addition to the inability to precisely set the road test duty cycle, as discussed above, these road test data points also reflect some additional voltage drop within the battery pack. As will be shown in Table 7-5 that follows,

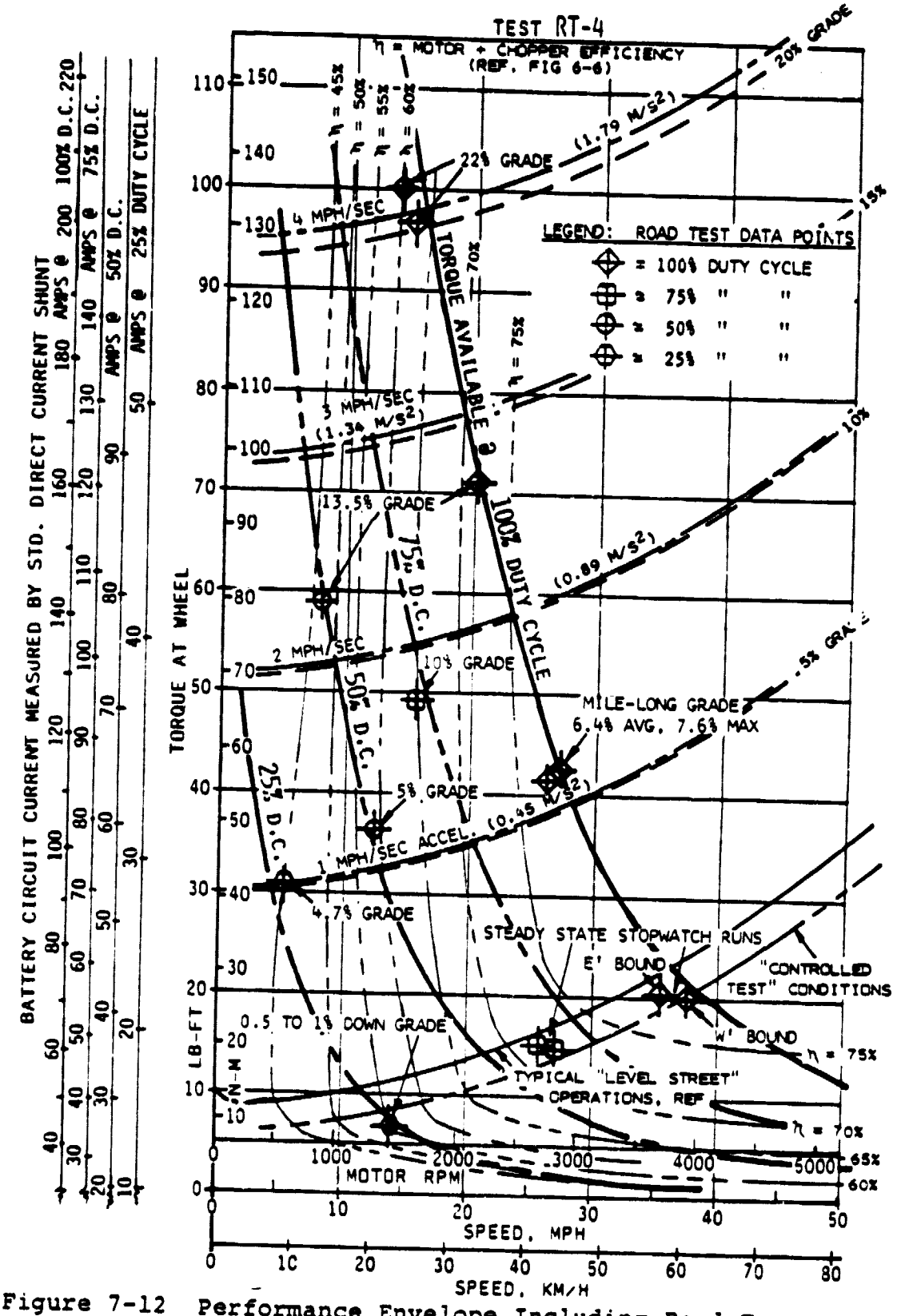

Figure 7-12 Performance Envelope Including Road Test Data Correlation – For EP-10 Vehicle with Series Motor and Chopper Control

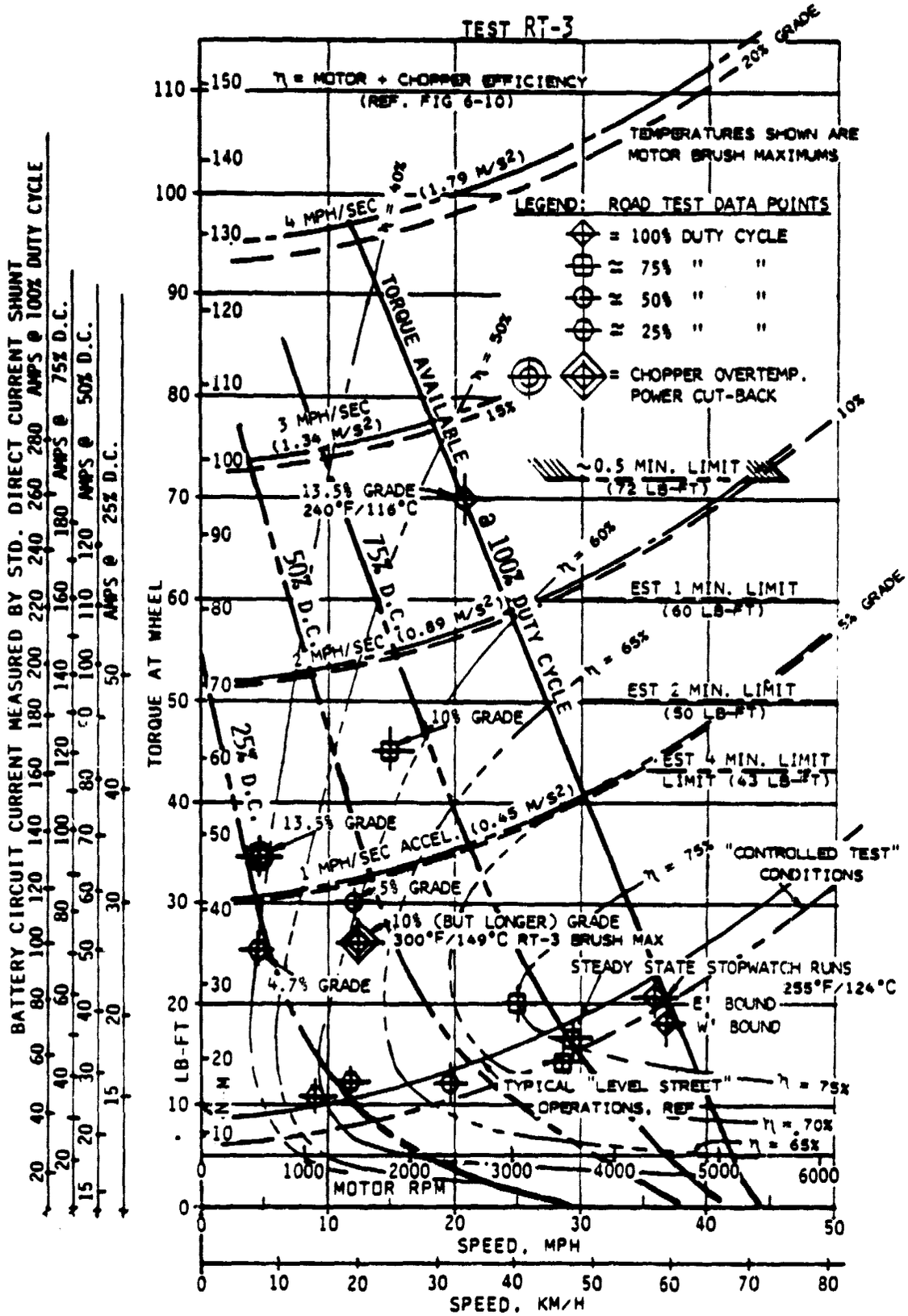

Figure 7-13 Performance Envelope Including Road Test Data Correlation – For EP-10 Vehicle with PM Motor and Chopper Control

the average state of charge was lower for this road test than for the other three and considerably below the dynamometer test state of charge. This lower state of charge was due both to calibrating (by oscilloscope) the road test duty cycle potentiometer immediately before this test and to the additional repeating of several climbing test runs.

Two of the Figure 7-13 data points, flagged by special symbols, are decidedly removed from the prediction curve of their selected duty cycle and represent quite transient data. In both of these instances, encountered during relatively steep climbs for this motor, the chopper had reached an over-temperature condition (above 150°F or 65°C) and was automatically curtailing its current output at an apparently increasing rate.

The one data point which attained a 100% duty cycle current of 260 amperes reflects a short duration 13.5% climb lasting only some 16 seconds from a standing start to crest of the hill. No chopper overheating occurred and the motor brush temperature reached only 240°F (116°C). When this same slope was tried at 50% duty cycle (the double circle symbol) the chopper controller temperature limit took over as mentioned above (the motor brushes had reached only 220°F or 104°C). The chopper installation for these road tests was in an under-hood, modestly-ventilated region, with no forced draft cooling of its heat-sink fins. Its over-temperature protection circuit curtailed current and speed on each of several climbs of intermediate duration 10% grades (data points scattered and not plotted). This current curtailment more-than-adequately protected the PM motor brushes from over-temperatures. The peak brush temperature for this road test was barely 300°F (149°C).

A final significant output of the road test program is a summary comparison of energy use rates for the four motor/controller combinations. "Bottom line" data, that is, in the consideration of either energy use or system efficiency. It should be remembered, however, that the test program performed was much more energy demanding than typical EV driving — due to its variety and concentration of relatively steep climbs. This concentration upon high torque, high current operations overemphasizes the effect of poor efficiencies in this regime (as the PM motor) as well as making the average energy rates lower than normal.

The energy use rate summary is shown in Table 7-5. Temperature corrected specific gravity of the battery electrolyte was used as the most accurate indicator of the state-of-charge of the batteries. For this battery set, carefully documented discharge tests had established the ampere-hour to acid density rate as 0,57 amp-hr per "count." (Where 1260 counts means a sp.gr. of 1.260; the rate will be similar to that for any lead-acid traction battery.)

The energy rate data of the table clearly shows that the reduced efficiencies previously shown by the dynamometer tests — with either the chopper controller (as used) or the rather poorly vehicle matched PM motor — are reflected in the energy used per mile. While the differences shown were somewhat exaggerated by the high-current test program, as

discussed above, they do indicate a need for better understanding and engineering of power circuits wnen using a chopper controller.

Table 7-5 Road Test Energy Use Summary

TEST NUMBER & POWER SYSTEM		ELECT. SP.GR.	% FULL* CHARGE	BAT'Y AMP-HR	NOM** KWH	VEH. MILES	ENERGY RATE KWH/MI	KWH/KM
RT-1	START	1.258	97%			637.5		
SERIES MOTOR	FINISH	1.188	28%			653.2		
& V-SWITCH	DIFF.	069	(69%)	39.3	1.89	15.7	.120	.075
RT-2	START	1.256	96%			657.9		
PM MOTOR	FINISH	1.166	6%			676.3		
& V-SWITCH	DIFF.	090	(90%)	51.3	2.46	18.4	.134	.083
RT-4	START	1.255	95%			696.9		
SERIES MOTOR	FINISH	1.172	12%			712.5		
& CHOPPER	DIFF.	083	(83%)	47.3	2.27	15.6	.146	.090
RT-3	START	1.248	88%			681.1		
PM MOTOR	FINISH	1.153	-7%			696.7		
& CHOPPER	DIFF.	095	(95%)	54.2	2.60	15.6	.167	.104

* ASSUMES CORRECTED SPECIFIC GRAVITY OF 1.260 = FULL CHARGE AND 1.160 = ZERO CHARGE FOR ROAD VEHICLE APPLICATIONS (THEN ΔSP.GR POINTS = Δ%CHG).

** NOMINAL KWH = NOM. BATTERY VOLTAGE (2V/CELL)X AMP-HOUR DRAIN/1000.

8/ CONCLUSIONS AND RECOMMENDATIONS

This program examined a broad range of factors influencing the performance and efficiency of the EV propulsion systems tested. A relatively large list of conclusions and recommendations resulted, as follows:

Conclusions

1. Conventional DC instruments (shunts and voltmeters), when installed in the battery side of chopper controllers of the type tested, provide adequate accuracy for EV power and energy consumption measurements. (ref. Sec. 4.6, p24)

2. Chopper controlled motor and circuit efficiencies were significantly improved, in the lower duty cycle ranges, by the addition of motor circuit inductance. The added inductance also reduced acoustic noise by reducing the chopper frequency wave amplitudes in motor circuit currents (ref. Sec. 6.1).

3. Efficiencies of the propulsion systems under chopper control, after improvements by added inductance, were still significantly lower than when under voltage-switch control. With the chopper, however, operations were simpler and smoother. (ref. Sec. 6.2, 6.3 & 7.5)

4. The series motor was found quite suitable for moderate performance EVs using a simple, single-ratio drive train. The PM motor, although it provided generally comparable efficiencies and power ranges, was less suitable due to its constant-rate speed-vs-torque characteristic. (ref. Sec. 5.3 & Sec. 7)

5. System efficiency and performance differences indicated in the dynamometer tests also occurred in actual vehicle road tests. The road test data also confirmed the adequacy of the analysis procedures described. (ref. Sec. 7)

6. A partial recharge (like a 10% charge) of a nearly discharged battery pack can result in quickly following operations with battery performance, for brief periods, as good (similar or less voltage drop) as a nearly fully charged battery. (ref. Sec. 5.2, p31)

7. Solenoid activated contactors of types often used in EV power circuits can have high resistances compared to other circuit elements, especially after a period of vehicle (vibration environment) use. (ref. Sec. 5.4)

Recommendations

1. It is recommended that an analytical and test program be defined and performed that would (a) investigate the desired impedance characteristics (i.e., inductance and capacitance needs as functions of power circuit component resistances, etc.), in conjunction with the effect of various chopper frequencies, to improve chopper system efficiency and reduce acoustic and RF noise; and (b) make these data available in parametric form readily usable by small business EV developers.

2. It is recommended that one of the several on-going or pending EV fleet test programs using chopper-controlled propulsion systems be augmented to explore the more general applicability of conclusion 1 above. Use of the much simpler and less costly instrumentation for power or energy use determination would be a significant economy for operational fleets or private vehicles even if not found adequate for some R&D testing.

3. It is recommended that EV developers using chopper controllers, especially with single-ratio drive trains, consider the potential system efficiency gain in providing one step of series-parallel voltage switching (to one-half the full battery-pack voltage), to avoid prolonged operations at low chopper duty cycles and thereby improve efficiency at or below speeds some 55 to 60% of maximum.

9/ REFERENCES

1. Shipps, Paul R., "A Development of High-Efficiency Electric Mini-Cars," Proceedings of the Fourth Intersociety Conference on Transportation, Paper No. E&F-3, 9 pages, July, 1976.

2. Shipps, Paul R., "Minimizing Electric Cars to Maximize Performance," Proceedings of the Eleventh Intersociety Energy Conversion Engineering Conference, Vol. I, p369-376, Sept. 1976.

3. Schuring, D.S., "Transient Versus Steady-State Tire Rolling Loss Testing," SAE Paper 790116, Feb. 1979.

4. Brown, C. & I. Gusakov, "A Mathematical Technique for Predicting Equilibrium Rolling Resistance of Tires from Short Duration Tests," SAE Paper 790118, Feb. 1979.

5. Hoffman, Charles T., Jr., and Douglas J. Beurmann, "Measurement and Reduction of On-Road Brake Drag," SAE Paper 790723, June, 1979.

6. Anon., "Aerodynamic Resistance Reduction of Electric and Hybrid Vehicles, A Progress Report - Sept. 1978," HCP/M5030-274, Jet Propulsion Laboratory, Pasadena, Calif., April, 1979.